

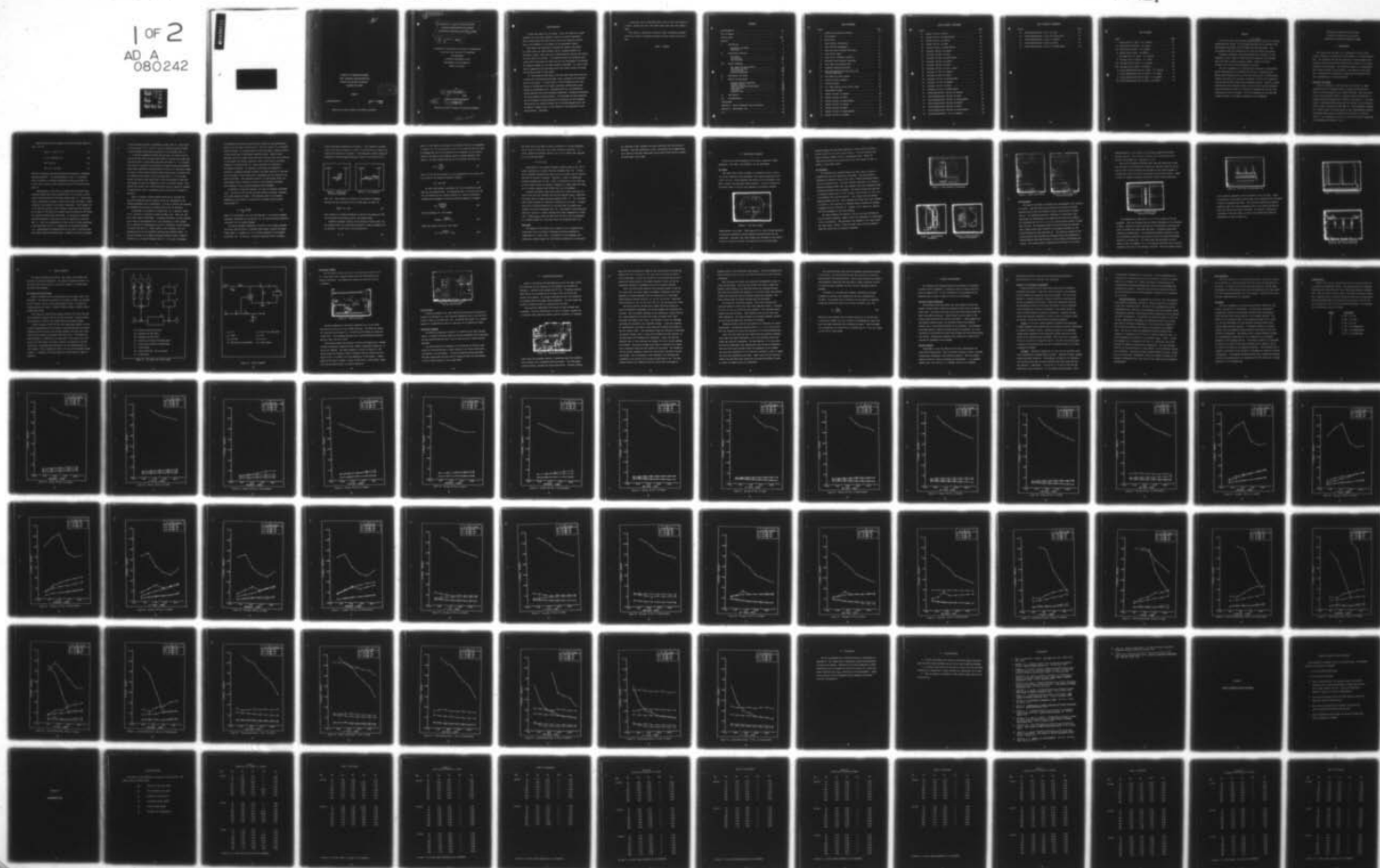
AD-A080 242

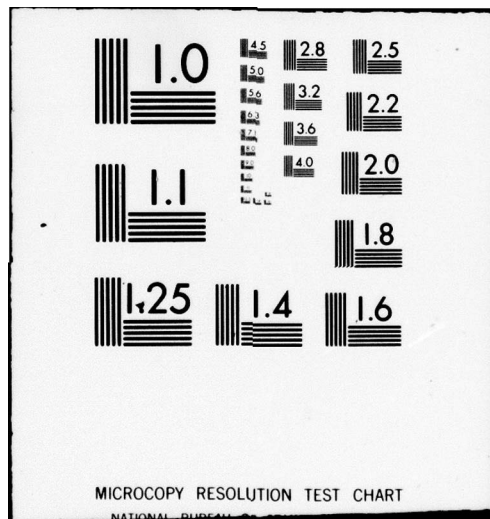
AIR FORCE INST OF TECH WRIGHT-PATTERSON AFB OH SCHOO--ETC F/6 20/5
COMPARISON OF GERMANIUM-STAINLESS STEEL ELECTRODE CONFIGURATION--ETC(U)
DEC 79 R J HOFFMAN
AFIT/6EP/PH/79D-5

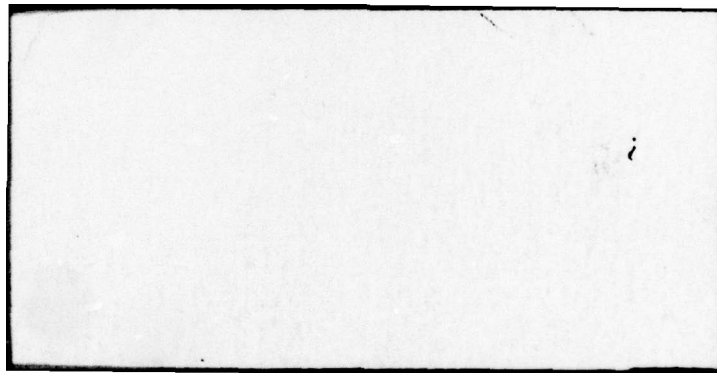
UNCLASSIFIED

NL

1 of 2
AD A
080242







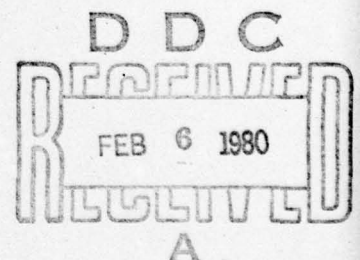
Ver

COMPARISON OF GERMANIUM-STAINLESS
STEEL ELECTRODE CONFIGURATIONS FOR
POSSIBLE UTILIZATION IN ELECTRIC
DISCHARGE HF LASERS

THESIS

AFIT/GEP/PH/79D-5

ROGER J. HOFFMAN
LT USAF



Approved for public release; distribution unlimited

14

6
COMPARISON OF GERMANIUM-STAINLESS STEEL
ELECTRODE CONFIGURATIONS FOR POSSIBLE
UTILIZATION IN ELECTRIC DISCHARGE HF LASERS.

9 Master's THESIS

Presented to the Faculty of the School of Engineering
of the Air Force Institute of Technology
Air University
in Partial Fulfillment of the
Requirements for the Degree of
Master of Science

Accession For
NTIS GPR1
DDC TAB
Unannounced
Justification

By
Distribution
Availability Codes
Date
Initials or
Signature

10 by
Roger J. Hoffman B.S.
Lt USAF

Graduate Engineering Physics

12111

11 December 1979

Approved for public release; distribution unlimited

012 225

LB

Acknowledgments

I chose this thesis for two reasons: first, HF lasers are a prime candidate for space laser systems, in which I am deeply interested; second, being spoiled by three years of bench work during my enlisted days, I was delighted at the prospect of an experimental thesis.

Many people were beneficial in helping me complete this thesis. Dr. Ernest Dorko, my thesis advisor, and Dr. Wolfgang Schuebel, my laboratory sponsor, spent many hours coordinating with various labs during the early days of the thesis. Dr. Schuebel obtained the germanium electrodes from the University of Essex and was also instrumental in obtaining the computer program for the Chang reference electrodes. Dr. Dorko's many helpful suggestions and criticisms proved most helpful during the design and writing portions of this thesis.

Mr. John Brohas and Ron Ruley of the AFIT Model Fabrication Shop did a superb job of constructing the laser cavity, diffusers and electrodes used in the project. Lt Chuck Krabec of the AF Avionics Lab was very helpful in solving many of the small procedural problems which arose during the experimental work. Discussions with Mr. Joe Brandelik of Systems Research Labs proved extremely beneficial in helping me understand the theory behind the entire project. His knowledge and past experience proved invaluable in understanding and interpreting the data obtained. Thanks goes to Mr. Dennis Grosjean, also of Systems Research Labs, who provided the computer time and tape needed for the fabrication of the Chang reference electrodes.

I would also like to thank Barb Taylor for her skill and finesse as a typist. Without her help, this thesis would never have been legibly typed.

This thesis is dedicated to Adrienne, whose friendship and warmth served as a source of inspiration during the final weeks of my stay at AFIT.

ROGER J. HOFFMAN

Contents

Acknowledgments	ii
List of Figures	v
List of Tables	viii
Abstract	ix
I Introduction	1
Background and Theory	1
Objectives	7
II Experimental Apparatus	9
The Cavity	9
The Diffusers	10
The Electrodes	12
III Support Equipment	16
Gas Supply and Vacuum System	16
Electronics Package	19
Cooling System	20
Monitoring Equipment	20
IV Experimental Procedure	21
V Results and Discussion	25
Electrode Surface Conditions	25
Diffuser Effects	25
Results of Discharge Experiments	26
Laser Operation	28
Discussion	28
Graphical Data	29
VI Conclusions	66
VII Recommendations	67
Bibliography	68
Appendix A: Support Equipment Turn-On Procedure	70
Appendix B: Experimental Data	72
Vita	98

List of Figures

Figure		Page
1	Primary and Secondary Avalanches	5
2	Arc Formation	5
3	Laser Cavity	9
4	Input Diffuser Construction	11
5	Input Diffuser Arrangement	11
6	Input and Output Diffuser Differences	11
7	Laser Cavity, Empty	12
8	Laser Cavity, Diffusers Installed	12
9	Stainless Steel Reference Electrodes	13
10	Macor Mount and Germanium Slab	14
11	Assembled Germanium Electrode	15
12	Electrode Mounting with Electrical and Cooling Connections	15
13	Gas Supply and Vacuum System	17
14	Thyratron Pulser Schematic	18
15	Thyratron Pulser	19
16	D.C. Power Supply and Gas Control Panel	20
17	Experimental System	21
18	Helium, 100 pps, Ge Cathode	30
19	Helium, 100 pps, Ge Anode	31
20	Helium, 100 pps, Ge Anode-Cathode	32
21	Helium, 200 pps, Ge Cathode	33
22	Helium, 200 pps, Ge Anode	34
23	Helium, 200 pps, Ge Anode-Cathode	35
24	Helium, 60 Torr, Ge Cathode	36

List of Figures (continued)

Figure		Page
25	Helium, 60 Torr, Ge Anode	37
26	Helium, 60 Torr, Ge Anode-Cathode	38
27	Helium, 80 Torr, Ge Cathode	39
28	Helium, 80 Torr, Ge Anode	40
29	Helium, 80 Torr, Ge Anode-Cathode	41
30	Nitrogen, 100 pps, Ge Cathode	42
31	Nitrogen, 100 pps, Ge Anode	43
32	Nitrogen, 100 pps, Ge Anode-Cathode	44
33	Nitrogen, 200 pps, Ge Cathode	45
34	Nitrogen, 200 pps, Ge Anode	46
35	Nitrogen, 200 pps, Ge Cathode-Anode	47
36	Nitrogen, 10 Torr, Ge Cathode	48
37	Nitrogen, 10 Torr, Ge Anode	49
38	Nitrogen, 10 Torr, Ge Anode-Cathode	50
39	Nitrogen, 25 Torr, Ge Cathode	51
40	Nitrogen, 25 Torr, Ge Anode	52
41	Nitrogen, 25 Torr, Ge Cathode-Anode	53
42	Sulfur-Hexafluoride, 100 pps, Ge Cathode	54
43	Sulfur-Hexafluoride, 100 pps, Ge Anode	55
44	Sulfur-Hexafluoride, 100 pps, Ge Cathode-Anode	56
45	Sulfur-Hexafluoride, 200 pps, Ge Cathode	57
46	Sulfur-Hexafluoride, 200 pps, Ge Anode	58
47	Sulfur-Hexafluoride, 200 pps, Ge Cathode-Anode	59
48	Sulfur-Hexafluoride, 7 Torr, Ge Cathode	60

List of Figures (continued)

Figure		Page
49	Sulfur-Hexafluoride, 7 Torr, Ge Anode	61
50	Sulfur-Hexafluoride, 7 Torr, Ge Cathode-Anode	62
51	Sulfur-Hexafluoride, 13 Torr, Ge Cathode	63
52	Sulfur-Hexafluoride, 13 Torr, Ge Anode	64
53	Sulfur-Hexafluoride, 13 Torr, Ge Cathode-Anode	65

List of Tables

Table	Page
I Helium with S.S. Anode - S.S. Cathode	74
II Helium with Ge Cathode - S.S. Anode	76
III Helium with Ge Anode - S.S. Cathode	78
IV Helium with Ge Anode - Ge Cathode	80
V Nitrogen with S.S. Anode - S.S. Cathode	82
VI Nitrogen with Ge Cathode - S.S. Anode	84
VII Nitrogen with Ge Anode - S.S. Cathode	86
VIII Nitrogen with Ge Anode - Ge Cathode	88
IX Sulfur-Hexafluoride with S.S. Anode - S.S. Cathode	90
X Sulfur-Hexafluoride with Ge Cathode - S.S. Anode	92
XI Sulfur-Hexafluoride with Ge Anode - S.S. Cathode	94
XII Sulfur-Hexafluoride with Ge Anode - Ge Cathode	96

Abstract

An HF laser cavity was designed and ^{Omega}constructed in which four electrode combinations were tested. The electrodes consisted of two stainless steel Chang-profiled electrodes and two 50-~~10~~ cm germanium electrodes. The four possible electrode combinations for anode and cathode were tested.

Breakdown, sustaining, and arcing voltages were recorded, for each combination, over a range of 25-200 pulses per second for the following gases with their respective pressure ranges: helium, 50-90 Torr; nitrogen, 5-30 Torr; sulfur-hexafluoride, 3-15 Torr.

The use of germanium as a cathode material resulted in substantially greater suppression of arc formation than the use of stainless steel. Helium, which sustained arcs at 60 Torr and 100 pps with a stainless steel cathode, was found to be arc-free at pressures to 90 Torr with repetition rates as high as 200 pps when using a germanium cathode. Similarly, sulfur-hexafluoride, which sustained arcing at 3 Torr and 150 pps with stainless steel electrodes was found to be arc-free at pressures over 13 Torr when germanium was used as a cathode. The use of germanium as both anode and cathode resulted in the highest suppression of arc formation.

COMPARISON OF GERMANIUM-STAINLESS STEEL
ELECTRODE CONFIGURATIONS FOR POSSIBLE
UTILIZATION IN ELECTRIC DISCHARGE HF LASERS

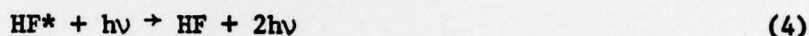
I. Introduction

This project was the result of a requirement of the Air Force Avionics Laboratory to design an HF laser capable of a 10 KHz repetition rate. The repetition rate has been achieved, but the stainless steel electrodes which have been used undergo severe corrosion due to arcing phenomena in the discharge. This corrosion results in an unacceptably short useful lifetime of the electrodes. The purpose of this thesis was to investigate the possibility of improving the discharge by the use of germanium as an electrode material.

Background and Theory

Since the invention of the ruby laser in 1960 (Ref. 1), laser physicists have been working steadily to design lasers which will operate in various regions of the infrared spectrum. The first report of laser action from HF formed in a chemical reaction initiated by a pulsed electrical discharge was by Deutsch in 1967 (Ref. 2). The first report of continuous lasing action from the reaction of F_2 with H_2 was made by Spinler and Kittle in 1969 (Ref. 3). Their apparatus consisted of a tubular reactor into which H_2 and F_2 were simultaneously injected. The ensuing flame reaction resulted in 10 μ S pulses at 2.7953 and 2.9111 μ , corresponding respectively to the $P_2(5)$ and $P_2(8)$ transitions of the generated HF molecule (Ref. 3).

Common reactions used to generate excited HF molecules (HF*) are (Ref. 4 and 5):



Reaction 3 represents spontaneous emission and Reaction 4 represents stimulated emission. To achieve Reactions 1 and 2, an electrical pulse is applied to a premixed combination of SF_6 and H_2 (Ref. 4). In the case of Deutsch, pulse repetition rates of 2-10 pps were used (Ref. 2).

Jacobson et al., found that the average power from an HF laser increased linearly with pulse repetition rate, to the limit at which arcing occurred between the electrode surfaces (Ref. 6). This arcing caused a substantial decrease in laser output power and caused a severe corrosion of the surface of the laser's electrodes. In HF lasers, due to the corrosive effects of free fluorine, usable electrode lifetimes are as short as 10^6 pulses for uncooled brass electrodes and 10^9 pulses for uncooled stainless steel electrodes. By cooling the electrodes, lifetime extensions of less than an order of magnitude are possible (Ref. 4). Since the requirements for these sorts of lasers necessitate a high repetition rate (i.e., 10,000 pps), the electrode lifetimes (i.e., approximately 28 discharge-hours in the case of uncooled stainless steel) become unacceptably short. Analysis of severe arc regions

on the electrodes indicate a contaminant buildup (Ref. 4). This buildup is postulated to be a result of reactive discharge products formed in the discharge volume near the surface of the electrodes (Ref. 7).

It has been suggested by Brown that the onset of arcing is due in part to the fact that the spent gases cannot be removed fast enough from the laser cavity at high pulse repetition rates (Ref. 7). It is thought that arcing is caused by the production of products during the discharge pulse whose conductivity characteristics are such as to facilitate arcing. In order to obtain stable operation, these products must be removed from the discharge volume prior to the next pulse (Ref. 7). In his study, using a CO_2 laser, Brown showed that a flow rate allowing at least two gas changes per pulse was necessary in order to alleviate arcing. This implies that lasers, with 10 KHz pulse rates, must be capable of extremely high gas flow rates, a capability which is difficult to realize in practice.

There is, however, another approach which may be utilized; the electrodes themselves may be tailored so that the suppression of arc forming mechanisms can be accomplished. In order to develop this approach, the phenomena which initiate a discharge must first be described.

A discharge, as introduced by Penning (Ref. 8), in general, refers to the conduction of electrical current through a gas. There are, however, three types of discharges: a breakdown discharge, in which currents on the order of microamperes flow; a glow discharge, in which current flow is measured in milliamperes; and the arc discharge, in which amperes of current flow (Ref. 8). Before either a glow discharge or an arc discharge can occur, the breakdown discharge must manifest itself. At low gas pressures, the breakdown discharge manifests itself in what is referred to as a Townsend discharge (Ref. 8). This type of discharge

is initiated by an electron freed from the cathode by some photoelectric process such as cosmic ray interaction. This free electron is accelerated toward the anode. By collision with a neutral gas atom, a second electron is freed which also is accelerated toward the anode. Each of these electrons is able to ionize other atoms which yield yet more free electrons. In this manner, one initial electron is able to give rise to an entire avalanche of electrons (Ref. 8). These avalanches are referred to as Townsend avalanches. In addition to generating an avalanche of electrons, a Townsend discharge provides a secondary emission of electrons from the surface of the cathode due to bombardment of ions created by the initial avalanche. This secondary emission, if sufficiently large, provides enough electron feedback to create a self-sustaining discharge. This discharge is the previously-mentioned glow discharge.

At moderate to high gas pressures, two types of breakdown mechanisms occur. The first is the already discussed Townsend discharge, sometimes also called Paschen discharge. This discharge leads to the Paschen breakdown law as related to the product Pd , pressure times electrode spacing (Ref. 9):

$$Pd = \frac{1}{\alpha/P} \ln(1 + \frac{1}{\gamma}) \quad (5)$$

where P is the pressure, d is the electrode gap, α is the first Townsend ionization coefficient for the gas and γ is the second Townsend ionization coefficient for the cathode surface.

The second breakdown mechanism is referred to as streamer breakdown, and occurs when the product Pd becomes large enough to permit the space-charge field of a single avalanche to become comparable to the applied field (Ref. 10). In this case, secondary avalanches tend to converge

toward the primary avalanche as in Figure 1. This summing of currents allows the primary avalanche to bridge the electrode gap in a highly conducting thin channel as in Figure 2. This phenomenon quickly brings the discharge to self-sustaining conditions usually in the form of an arc

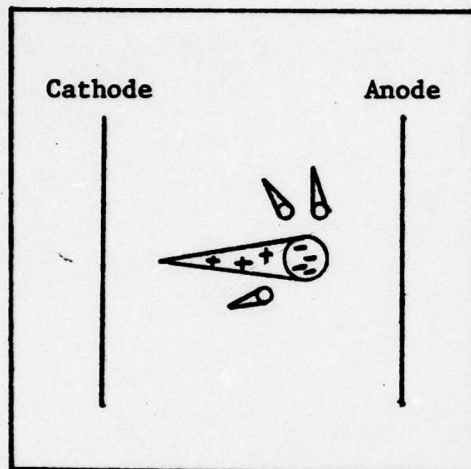


Figure 1. Primary and Secondary Avalanches

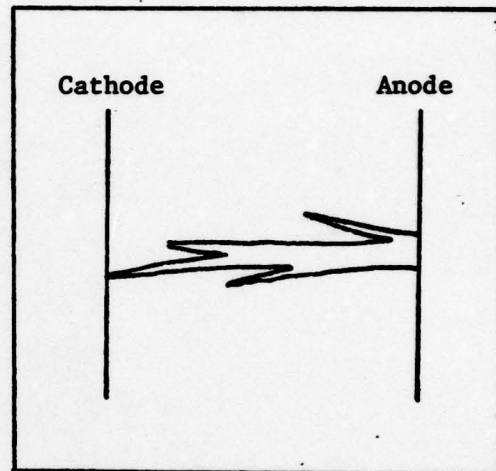


Figure 2. Arc Formation

(Ref. 10). This condition is referred to as Raether's breakdown criteria and can be written for air, in MKS units, as (Ref. 9):

$$\left(\frac{\alpha}{p}\right)Pd = 20 + \ln d \quad (6)$$

This condition of streamer breakdown is stated as the equality of the local avalanche space-charge field to the applied field.

Raether's breakdown criteria can be derived as follows (Ref. 10): The lateral extent of an individual avalanche is usually assumed to be by diffusion. In this case, it can be shown that

$$r^2 = Z\lambda \quad (7)$$

where r is the radius of the head of an avalanche after it has propagated a distance Z in the field direction, and λ is the electron mean free path. By assuming that all of the electrons in the avalanche, N_e , are concentrated in the head of the avalanche, which is assumed spherical with radius r , the space-charge field E_r can be calculated and written as

$$E_r = \frac{eN_e}{4\pi\epsilon_0 r^2} \quad (8)$$

where e is the electron charge, ϵ_0 is the permittivity of free space, and N_e is given by the Townsend avalanche condition

$$N_e = \exp(\alpha Z) \quad (9)$$

In order that Raether's condition, Eq. (6) be satisfied, E_r must equal E_0 , the applied field. By substituting Eqs. (7) and (9) into Eq. (8), the formula for the critical distance, Z_c , which an individual avalanche must propagate to initiate streamer breakdown is obtained:

$$E_0 = \frac{\exp(\alpha Z_c) e}{4\pi\epsilon_0 Z_c \lambda} \quad (10)$$

After rearranging, Eq. (10) becomes

$$\exp(\alpha Z_c) = \frac{E_0 4\pi\epsilon_0 \lambda}{e} Z_c \quad (11)$$

Taking the natural log of Eq. (11) yields

$$\alpha Z_c = \ln \frac{4\pi\epsilon_0 E_0 \lambda}{e} + \ln Z_c \quad (12)$$

The first term on the right is fairly insensitive to the gas parameters and is about 20 in MKS units for typical breakdown conditions. As a result, Raether's breakdown criteria, Eq. (6) is obtained after equating Z_c to the electrode gap d :

$$\alpha d = 20 + \ln d. \quad (13)$$

Unfortunately, the streamer breakdown condition given by Eq. (6) is easily satisfied for a typical TEA laser discharge (Ref. 10). Clearly, such a breakdown mechanism will favor an arc mode rather than the desired glow mode if allowed to progress. Therefore, a means of suppressing streamer breakdown must be used. Since, by definition, an arc discharge is one in which current is measured in amperes, it seems likely that some sort of current limiting would inhibit this type of breakdown.

Jacobson and Kimbell showed that resistively loaded electrodes produced a more arc-free discharge than did non-resistive (*i.e.*, conductive) electrodes under the same operating parameters (Ref. 11). The electrodes they studied consisted of resistively loaded pins in an array. A similar study done by Deutsch showed that an electrode made of graphite also resulted in arc-free discharges (Ref. 12). The graphite, being inherently resistive, acted as a current limiting device which suppressed arc formation. Gibson *et al.*, have also shown that the use of 50- Ω cm germanium as a cathode results in a discharge free of arc formation (Ref. 13).

Objectives

The purpose of this thesis was to compare a set of germanium electrodes with a set of reference conducting electrodes installed in combinations in a laser cavity. The behavior of the breakdown, sustaining and arcing voltages for the different combinations of electrodes

as a function of gas, pressure, and pulse repetition rate was noted and recorded. From this compilation of data, conclusions and recommendations as to types of electrode combinations and pressures which would be optimal in an HF laser, can be made.

II. Experimental Apparatus

The HF laser system designed for this thesis consisted of three components: the cavity, the diffusers, and the electrodes.

The Cavity

The laser cavity, shown in Figure 3, consisted of a 30.5 x 30.5 x 14.6 cm box, fabricated from plexiglass, with inside dimensions of 20.3 x 22.9 x 9.5 cm. Clear plexiglass was chosen as it was necessary to be able to observe the discharge during operation. The 2.54 cm thick top and bottom covers of the box were removable to facilitate internal

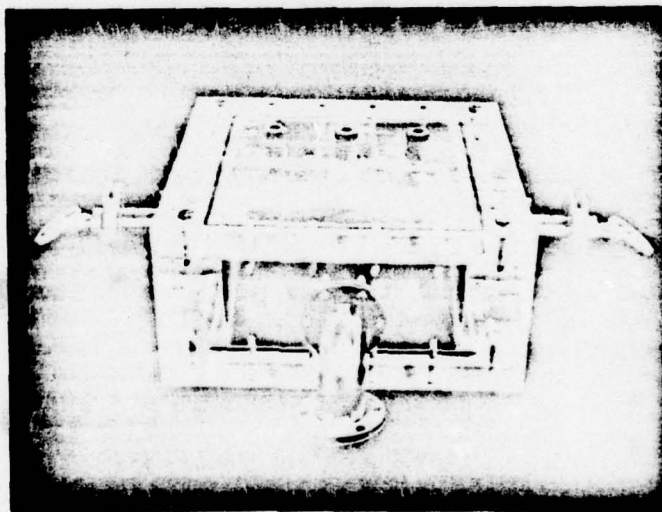


Figure 3. The Laser Cavity

modifications to the laser. Three Cajon 0.25 in. pipe fittings installed in each cover provided an easily adjustable mounting method for the electrodes. Stainless steel elbow flanges were installed on each side of the box to serve as the input and output ports for the laser gases.

Aluminum flanges were installed transverse to the gas flow in order to provide support for the laser window holders. The window holders held Calcium Fluoride windows at 58.4° , the Brewster angle. Varian "O" rings were installed in the covers and in all the fittings in order to obtain a vacuum tight cavity.

The Diffusers

Two diffusers were installed inside the laser cavity in order to streamline the gas flow between the electrodes. They also served to eliminate the unusable volume of the cavity, thereby minimizing troublesome recirculation zones. The input diffuser consisted of two pieces of machined plexiglass which, when slid together, held four plexiglass frames containing stainless steel screening. The screens allowed the input gas to uniformly expand from a 9.6 cm^2 circular cross section to a 3.8×15.3 cm rectangular cross section (Ref 14). Four screens were the minimum deemed necessary (Ref 15). The screening was 18 mesh with a wire diameter of 0.0432 cm. This resulted in a Reynolds number exceeding the minimum recommended value of 100 (Ref 15). Figures 4 and 5 depict the construction and arrangement of the input diffuser.

The output diffuser was similar to that of the input diffuser but did not contain screening. Figure 6 shows the differences in construction of the two diffusers. Both diffusers were designed to fit snugly inside the laser cavity. Figure 7 shows the empty laser cavity and Figure 8 shows the cavity with the diffusers installed.

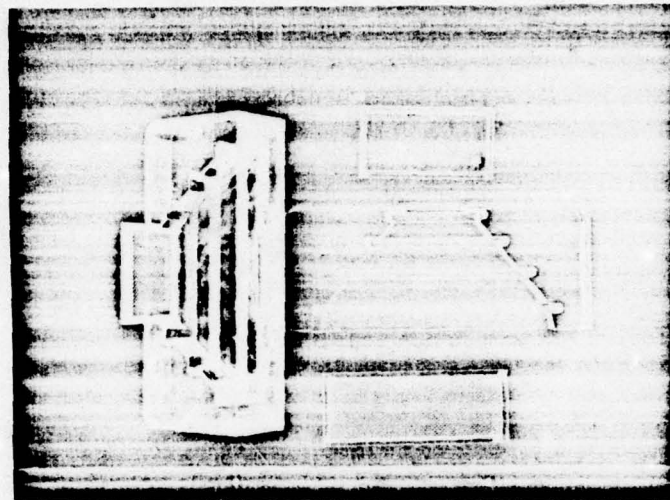


Figure 4. Input diffuser construction

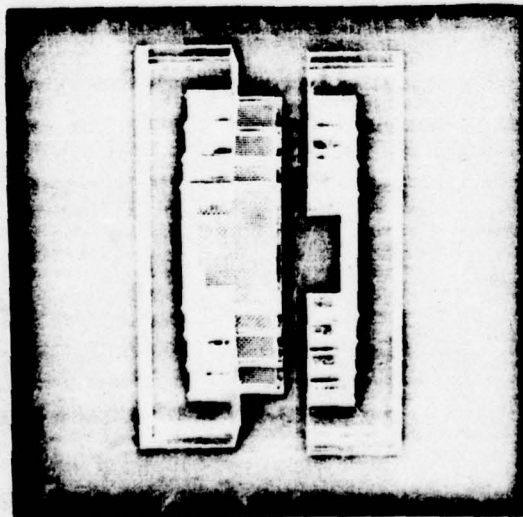


Figure 5. Input diffuser arrangement

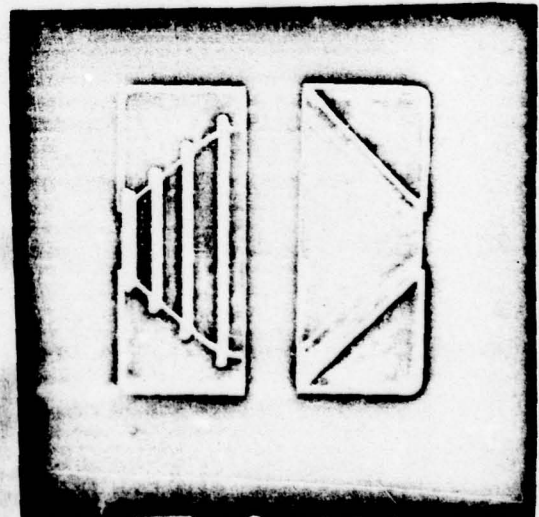


Figure 6. Input and output diffuser differences

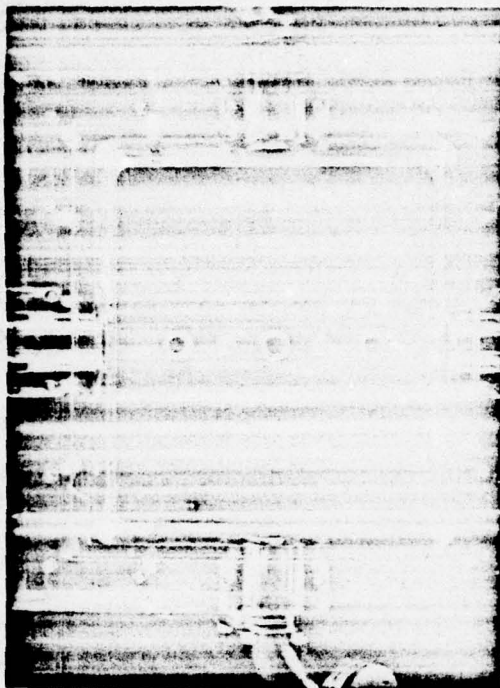


Figure 7. Empty laser cavity

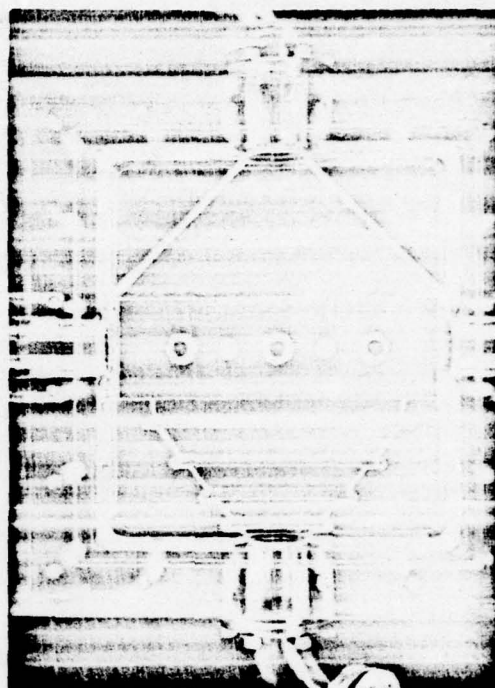


Figure 8. Laser cavity with diffusers installed

The Electrodes

Two types of electrodes, stainless steel and germanium, were tested in the cavity. Stainless steel was selected as the reference electrode material since it has been reported to give a long electrode lifetime (Ref 4). Two reference electrodes, identical in construction, were fabricated, one functioning as the anode and the other as the cathode. The electrodes were 15.2 x 2.5 x 1.9 cm in size and were hollow to permit water cooling. The discharge surface of each electrode was contoured with a Chang profile which resulted in the highest uniformity of the E-field between the electrodes (Ref 16). The numerical program for the milling machine which machined the discharge surface was generated by Systems Research Labs under contract to the AF Wright Aeronautical Laboratory. The spacing between Chang-profiled electrodes is a critical

design parameter, as the contour of the profile changes with various spacings (Ref 16). The reference stainless steel electrodes for this project were designed for a spacing of 1.2 cm.

Three 0.95 cm diameter stainless steel rods were tapped and screwed into the back of each electrode to provide for mounting inside the cavity. The end rods of each electrode were hollowed out and allowed passage of cooling water while the center rod provided the electrical contact. Figure 9 shows the completed reference electrodes in their relative positions.

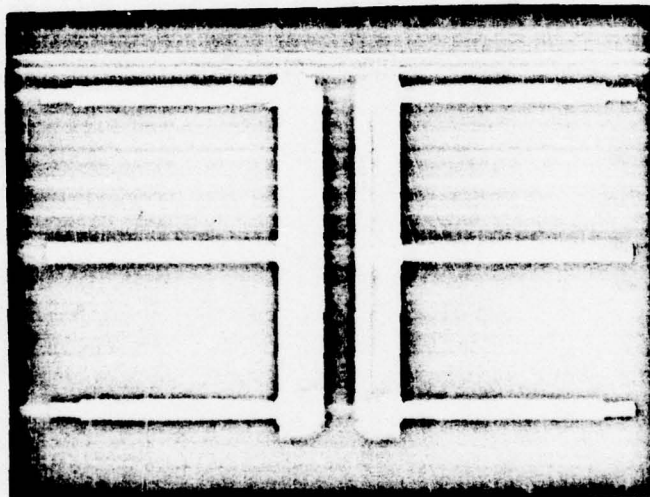


Figure 9. Stainless Steel Reference Electrodes

The germanium electrodes were 15 x 2.5 x 0.6 cm slabs of 50 Ω -cm germanium. They were obtained from the Physics Department of the University of Essex. Mounting of these electrodes was accomplished by attaching the slabs to hollowed out mounts made from Macor, a machinable glass manufactured by Corning Glass. A rod mounting arrangement identical to that of the reference electrodes was utilized in order to provide interchangeability of electrode sets. Each Macor mount was fabricated in such a manner so that the combined size of the electrode and mount was as close as possible to the size of the reference electrode. This was intended to give

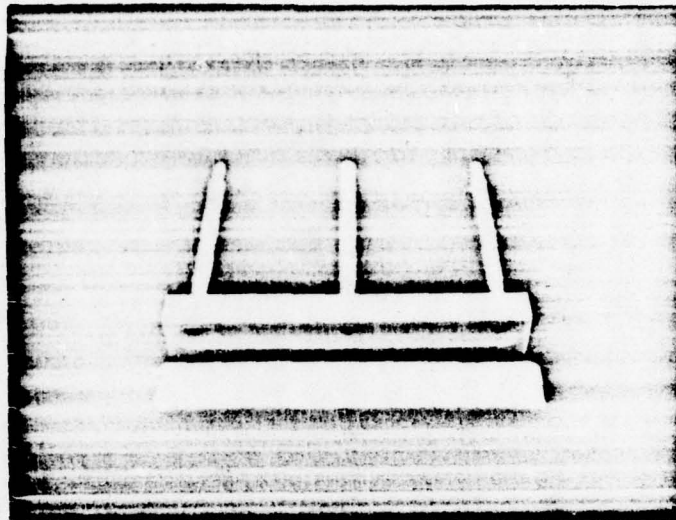


Figure 10. Macor mount and germanium slab

a more realistic comparison of the performance of the two types. Figure 10 illustrates the hollowed out Macor mount and the germanium slab and Figure 11 shows the assembled electrode. The electrical connection was made by soldering copper wire from the germanium slab to the center mounting rod before the slab was attached to the mount. The method of mounting the electrodes in the laser cavity, as well as the cooling and electrical connections, is shown in Figure 12.

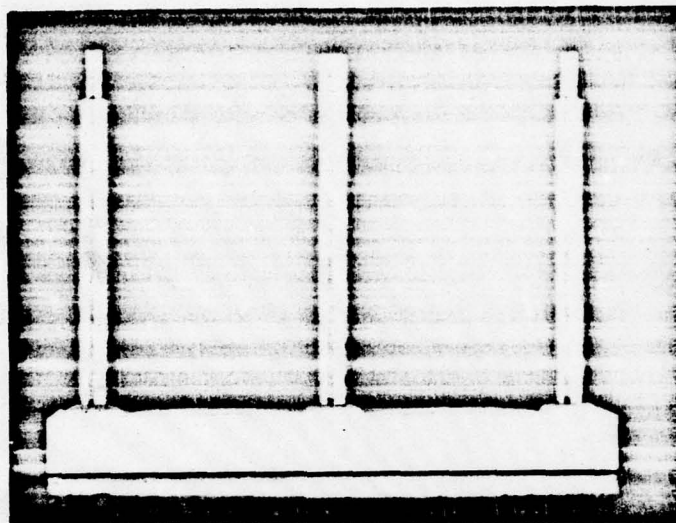


Figure 11. Assembled germanium electrode

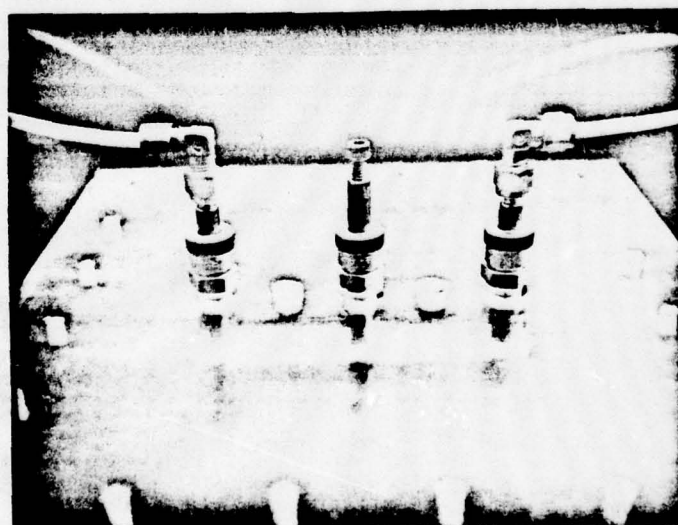


Figure 12. Electrode mounting with electrical and cooling connections

III. Support Equipment

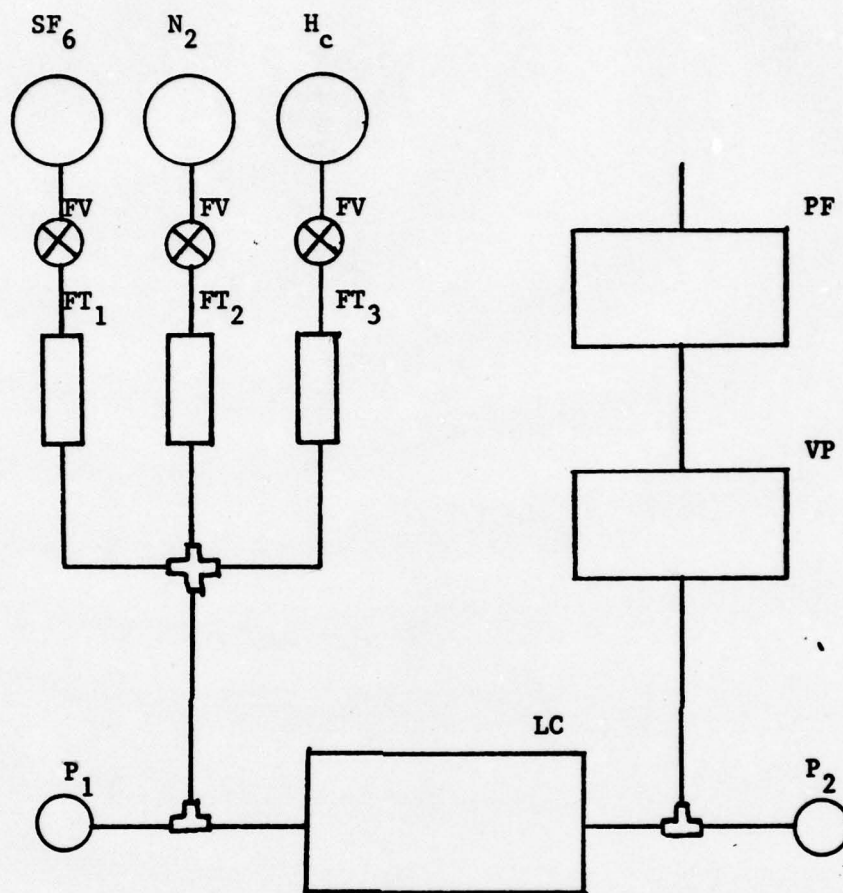
The support equipment required for this project was obtained from the Air Force Avionics Laboratory. The support equipment consisted of a gas supply and vacuum system, an electronics package, a cooling system and monitoring equipment.

Gas Supply and Vacuum System

Helium, nitrogen and sulfur-hexafluoride were the gases used in the experiment. The helium was supplied by the Bureau of Mines, the nitrogen by Air Products, and the sulfur-hexafluoride by Linde. The gases had minimum purities as follows: helium, 99.995%; nitrogen, 99.998%; sulfur-hexafluoride, 98.0%.

Flow rates were controlled by Nuclear Products flow valves and they were monitored by Matheson Gas 604 and 605 flow tubes. The gas pressure was monitored by a Wallace and Tiernan 0-200 mm Hg pressure gauge.

A Welch Scientific model 1397 Duo Seal vacuum pump capable of 18 cfm provided ample pumping for the pressures encountered during this project. Exhaust gas from the cavity was filtered through a one cubic foot stainless steel box filled with Coastal brand filter coal. Two Wallace and Tiernan gauges, a 0-100 mm Hg on the gas input of the cavity and a 0-50 mm Hg on the gas output, were used to monitor the pressure in the discharge area. The gauges were equidistant from the discharge area, so the average of the two gauges was taken to be the actual discharge volume pressure. A schematic of the gas supply and vacuum system is shown in Figure 13.



FV = Nuclear Products Flow Valve

FT₁ = Matheson 604 Flow Valve

FT₂ = Matheson 605 Flow Valve

P₁ = Wallace and Tiernan 0-100 mmHg gauge

P₂ = Wallace and Tiernan 0-50 mmHg gauge

LC = Laser Cavity

VP = Welch Scientific 1397 vacuum pump

PF = Pump Filter

Figure 13. Gas supply and vacuum system

Electronics Package

The electronics package consisted of a Hippotronics model 815-1.7A D.C. power supply and a thyration pulser which was fabricated by the Avionics Laboratory. The Hippotronics supply was rated for 15 KV at 1.7 Amperes.

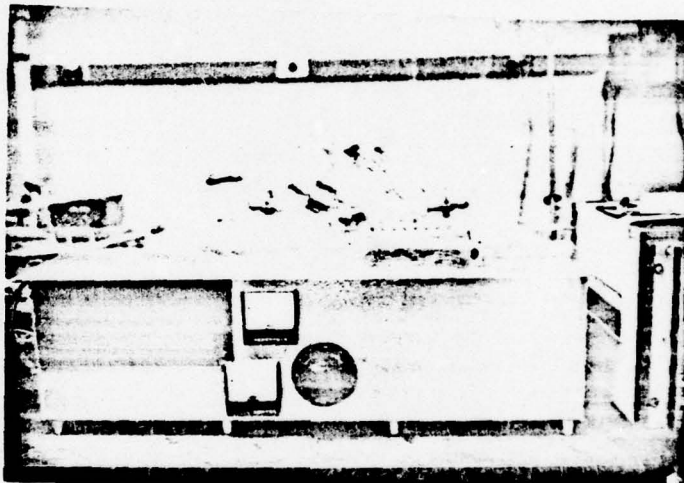


Figure 15. Thyatron Pulser

The main components of the pulser consisted of an E.G.&G. TM-30 Thyatron Driver and an E.G.&G. HY-3001 Thyatron. The TM-30 was capable of a pulse-per-second range of 1 to 10,000 and the HY-3001 was rated for 25,000 volts. The discharge capacitor was a Tobe Deutschmann Laboratory ESL-327A rated .005 μ f at 20 KV.

The thyatron heater and reservoir currents were supplied by a Chicago Standard Transformer Corporation P6457 filament transformer capable of 7.5 volts at 21 amperes. The pulser schematic is shown in Figure 14. The entire pulser was contained within a stainless steel box which acted as a shield to keep electrical noise from leaking out of the system. A photograph of the pulser is shown in Figure 15 and the D.C. power supply, along with the gas control panel, is shown in Figure 16.

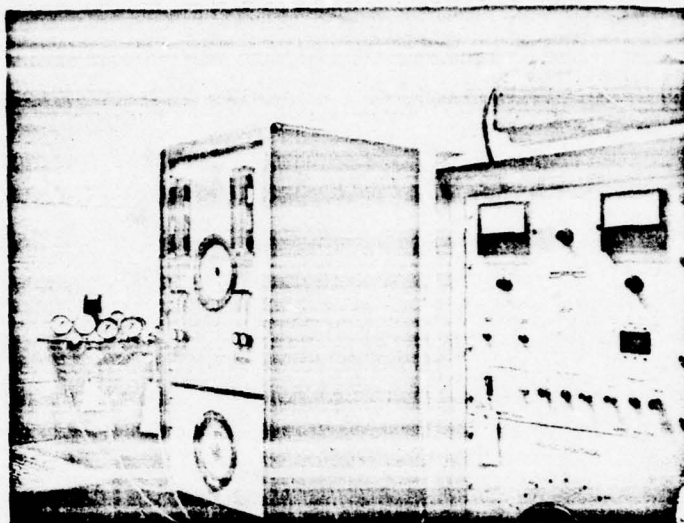


Figure 16. D.C. power supply
and gas control panel

Cooling System

A Neslab Instruments, Inc. model HX-300 cooling system was utilized to maintain the thyatron at a safe operating temperature and to cool the electrodes in order to prolong their life. The HX-300 was capable of a cooling capacity of 34,000 BTU per hour at a pump rate of 6.5 gallons per minute.

Monitoring Equipment

The monitoring equipment consisted of a Monsanto model 100A Frequency Counter, a Pearson Electronics model 410 current transformer and a Tektronics 555 Dual Beam Oscilloscope with a type 21 time base and a 53/54C Vertical Amplifier.

The 100A monitored the frequency of the TM-30 and the Pearson transformer and oscilloscope gave a visual display of the current pulse which was applied to the electrodes. A Science Accessories Corporation model 003 high voltage probe was also used in conjunction with the oscilloscope to give a visual display of the voltage pulse.

IV. Experimental Procedure

Figure 17 illustrates the experimental set-up of the laser cavity. The procedures for the operation of the equipment are contained in Appendix A. Maximum cavity pressure was 90 Torr. Discharge pressures below 50 Torr were recorded as the average of the two Wallace and Tiernan cavity gauges. As pressure approached 50 Torr, the difference in readings between the gauges became negligible. The input gauge was therefore assumed accurate for pressures above 50 Torr.

Four electrode combinations were tested in three different gas discharges. The four combinations, in order of testing, consisted of: 1) stainless steel anode and cathode, used for reference, 2) stainless

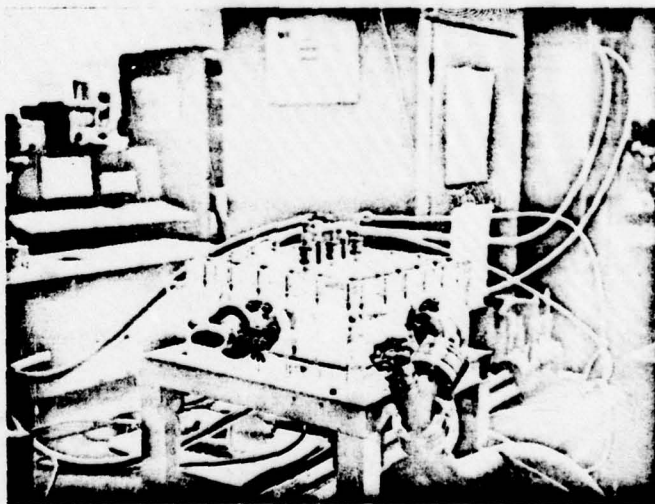


Figure 17. Experimental system

steel anode with germanium cathode, 3) germanium anode with stainless steel cathode, and 4) germanium anode and cathode. The three gases used were helium, nitrogen and sulfur-hexafluoride. Multiple pulsing,

i.e., more than one pulse per volume of gas, was insured by limiting the maximum flow rate of any gas so that less than 150 refills per second were accomplished. In this way, products of the discharge would not be swept away between pulses at the higher repetition rates, and the arc suppression qualities of germanium could be more readily observed.

Trial runs with helium indicated that pressures between 40 and 100 Torr would cover the entire range of breakdown, sustaining, and arcing phenomena of helium discharges with the reference set of electrodes. Helium pressures selected were 50, 60, 70, 80, and 90 Torr. Repetition rates used were 25, 50, 75, 100, 125, 150, 175, and 200 pulses per second.

The basic procedure followed was a simple three-step process in which the breakdown, sustaining, and arcing voltages were determined and recorded. With all support equipment on and stabilized, voltage from the D.C. supply applied to the pulser was slowly increased until a glow discharge just began in the cavity. The voltage at which the discharge just began was recorded as the breakdown voltage. A value was obtained by repeating this step three or four times and recording the average of the two closest values. The sustaining voltage was obtained by decreasing the applied voltage, after a stable glow discharge had been obtained, to the point where the discharge just disappeared. Again, the step was repeated three or four times and the average of the two closest readings was recorded. The arcing voltages were found by increasing the voltage until consistent arcing was seen between the electrodes. The average of the two closest voltages at which this occurred was recorded as the arcing voltage. For the purposes of this experiment, the discharge was considered to be arc-free if no arcing occurred below 14 KV. For each pressure tested, the repetition rate was varied from the minimum to

maximum values in the increments listed earlier. With five pressures and eight repetition rates, 40 runs were made with helium for each electrode combination.

After each gas was tested, the cavity was disassembled in order to clean the electrodes. Steel wool and acetone were used to remove any deposits which formed on the electrodes during the discharge process. Each time the electrodes were cleaned, a 1.2 cm thick spacer was inserted between the electrodes and the electrode spacing was rechecked. The spacer insured that the proper electrode gap was maintained.

The second gas tested was nitrogen. Trial runs indicated that pressures between 5 and 30 Torr would yield desirable results. Pressures of 5, 10, 15, 20, 25, and 30 Torr were selected. The repetition rates remained the same as before. This resulted in 48 runs for each electrode combination. The steps followed for obtaining breakdown, sustaining and arcing voltages were the same as for helium.

Pressures between 3 and 13 Torr proved to be sufficient for sulfur-hexafluoride. The pressures selected were 3, 5, 7, 9, 11, and 13 Torr. This also resulted in 48 runs per electrode set for sulfur-hexafluoride.

After the three gases had been tested with the reference stainless steel anode and cathode combination, one of the stainless steel electrodes was replaced by germanium. The same spacing, 1.2 cm, was used. The previous experiments were repeated with this electrode combination. After the three gases had been tested with germanium as the cathode, the electrical connections to the cavity were reversed in order to repeat the tests with germanium as the anode. Again, after each gas had been tested, the electrodes were cleaned and the spacing rechecked in order to insure the highest degree of consistency.

The final tests were made with both germanium electrodes installed in the cavity. The same procedures were used as before, as were the same pressures and repetition rates. Since arcing occurred less readily with germanium, additional runs were made at higher pressures in order to obtain the upper pressures at which arc-free discharges could be obtained.

In addition to recording the breakdown, sustaining and arcing voltages for each gas, the exchange rate was also calculated and recorded. The exchange rate is defined to be the number of discharge volume gas refills per pulse, and was found according to Eq. (14),

$$R_e = \frac{R_f}{V_D R_R} \quad (14)$$

where R_e is the exchange rate in inverse pulses, R_f is the flow rate in liters per second, V_D is the volume of the discharge in liters, and R_R is the pulse repetition rate in pulses per second. With electrodes 15.2 cm long and 2.5 cm wide with an electrode gap of 1.2 cm, V_D is equal to 45.6 cm³ or .0456 liters.

V. Results and Discussion

The numerical data obtained during this experiment is reproduced as Tables I-XII in Appendix C. Graphical results of typical runs are shown in Figures 18-53. A brief explanation of the symbology of the graphical data is given on page 29 as well as on each graph.

Electrode Surface Conditions

The stainless steel electrodes, when used together as anode and cathode, showed surface pitting and corrosion effects after the experimental runs. The effects were most severe with sulfur-hexafluoride and least noticeable with helium. These effects were the result of the arcing encountered during the initial runs (Ref 7). When germanium was used against stainless steel, the corrosion effects were markedly reduced, due to the resulting decrease in arc formation. The germanium electrodes showed no signs of pitting during the experiment, but a discoloration of the surface did result when nitrogen and sulfur-hexafluoride were tested. Cleaning with stainless steel removed the condition and restored the appearance of the surface.

Diffuser Effects

Experiments to test the effects of the input diffuser were run using sulfur-hexafluoride. With the diffuser screens in place, a uniform discharge was obtainable at all reported pressures. With the screens removed, however, a uniform discharge was unattainable. It is unknown whether this effect was due to aerodynamic effects or to possible

preionization effects caused by space charge fields generated at discontinuities of the stainless steel screening.

Results of the Discharge Experiments

Arcing occurred with all three tested gases when the reference electrodes were tested. There was a steady increase in arc formation as both pressure and repetition rate were increased. The use of germanium as a cathode resulted in a greater reduction of arcs than did the use of germanium as the anode. Greater arc suppression occurred when germanium was used as both anode and cathode, but the brilliance of the discharge was reduced, due probably to the reduced amount of current flowing through the resistive electrodes. Breakdown voltages varied with electrode combination, as well as with the different gases. The results of each gas tested will be discussed hereafter.

Helium. At the lower tested pressures, breakdown and sustaining voltages remained fairly constant with the different electrode combinations. As pressure increased, however, breakdown voltages for the germanium cathode-anode configuration were measurably greater than for the reference set of stainless steel electrodes. This can be seen in Figures 20 and 23, as well as in Figures 26 and 29. The lack of an arcing curve in Figures 18-29 indicates that the use of germanium results in arc-free discharges for helium.

Nitrogen. Sustaining voltages for all runs with the different electrode configurations remained almost the same. Breakdown voltages, however, showed noticeable variations. The breakdown voltages for the configuration containing only one germanium electrode were lower than those for the reference configurations. Figures 30, 31, 33 and 34 show that the differences tend to become small at the higher tested pressures. This

is correlated by Figures 36, 37, 39 and 40. For the configuration containing the two germanium electrodes, the breakdown voltages were higher than for the reference set. Again, the absence of arcing curves for configurations containing germanium shows that arc-free discharges were obtained with nitrogen. Additional runs made with nitrogen resulted in arc-free discharges for all three germanium configurations for pressures up to 90 Torr.

Sulfur-Hexafluoride. At pressures up to 13 Torr, only the germanium anode-cathode configuration was able to entirely eliminate arc formation at the upper repetition rates. The use of the one-germanium electrode configuration also resulted in arc suppression, with the germanium cathode configuration yielding a substantially greater suppression than the germanium anode configuration. At pressures and repetition rates of 9 Torr and 175 pps, respectively, and higher, the discharge started in the arcing mode with the reference configuration. This can be seen in Figures 45 and 51 where the reference set arcing curve intersects the breakdown curve. The use of at least one germanium electrode eliminated this condition, at pressures up to 15 Torr, at a 200 pps repetition rate. If a glow discharge was obtained at a low pressure (i.e., 7 Torr), it could be maintained up to a pressure of 30 Torr, at a repetition rate of 200 pps with the germanium cathode-anode configuration. The glow discharge could not be obtained directly at this pressure, as the breakdown resulted in arc formation. Sustaining voltages remained somewhat the same, independent of the electrode configuration, while the breakdown voltages for the reference configuration were lower than for the remaining three germanium configurations.

Laser Operation

After the completion of the discharge experiments, lasing was achieved by the addition of a 100% reflecting back mirror and a 50% reflecting output mirror. An energy of 0.5 mJ per pulse was obtained at 100 pps using the germanium cathode-stainless steel anode configuration with a gas mixture of 35 Torr sulfur-hexafluoride and 5 Torr hydrogen. Lasing with the other electrode combinations was not attempted.

Discussion

The use of germanium as an electrode consistently resulted in substantial increases in arc suppression. The germanium cathode-anode configuration resulted in the greatest increase, while the germanium anode-stainless steel cathode resulted in the smallest increase. The addition of the germanium anode to the germanium cathode did not result in a two-fold improvement over the germanium cathode-stainless steel anode as might have been expected. It actually resulted in a smaller increase than the germanium cathode-stainless steel anode did over the reference configuration. The general trend of higher breakdown voltages for the germanium configuration is to be expected due to the higher impedance of the discharge circuit. Less energy is likely to be deposited in the gas as a result of this higher impedance since energy is lost in the form of I^2R losses in the germanium electrodes. This indicates that a tradeoff is inevitable in the decision to determine the desirable electrode configuration. The germanium cathode-stainless steel configuration appears to offer the greatest gain of arc suppression with the least loss of energy deposition in the discharge gas.

Graphical Data

Figures 18-53 contain representative data for the three gases and four electrode combinations tested. Each graph contains the breakdown, sustaining and arcing curves for the corresponding reference configuration. This was done in order to yield a more easily understood comparison. Repetition rates of 100 and 200 pps are shown for the three gases, and the pressures shown are 60 and 80 Torr for helium, 10 and 25 Torr for nitrogen, and 7 and 13 Torr for sulfur-hexafluoride. The symbology for the different curves is as below:

<u>Symbol</u>	<u>Description</u>
○	E, Brk - S.S. set
△	E, Sust - S.S. set
+	E, Arc - S.S. set
×	E, Brk - Ge configuration
◇	E, Sust - Ge configuration
⤴	E, Arc - Ge configuration

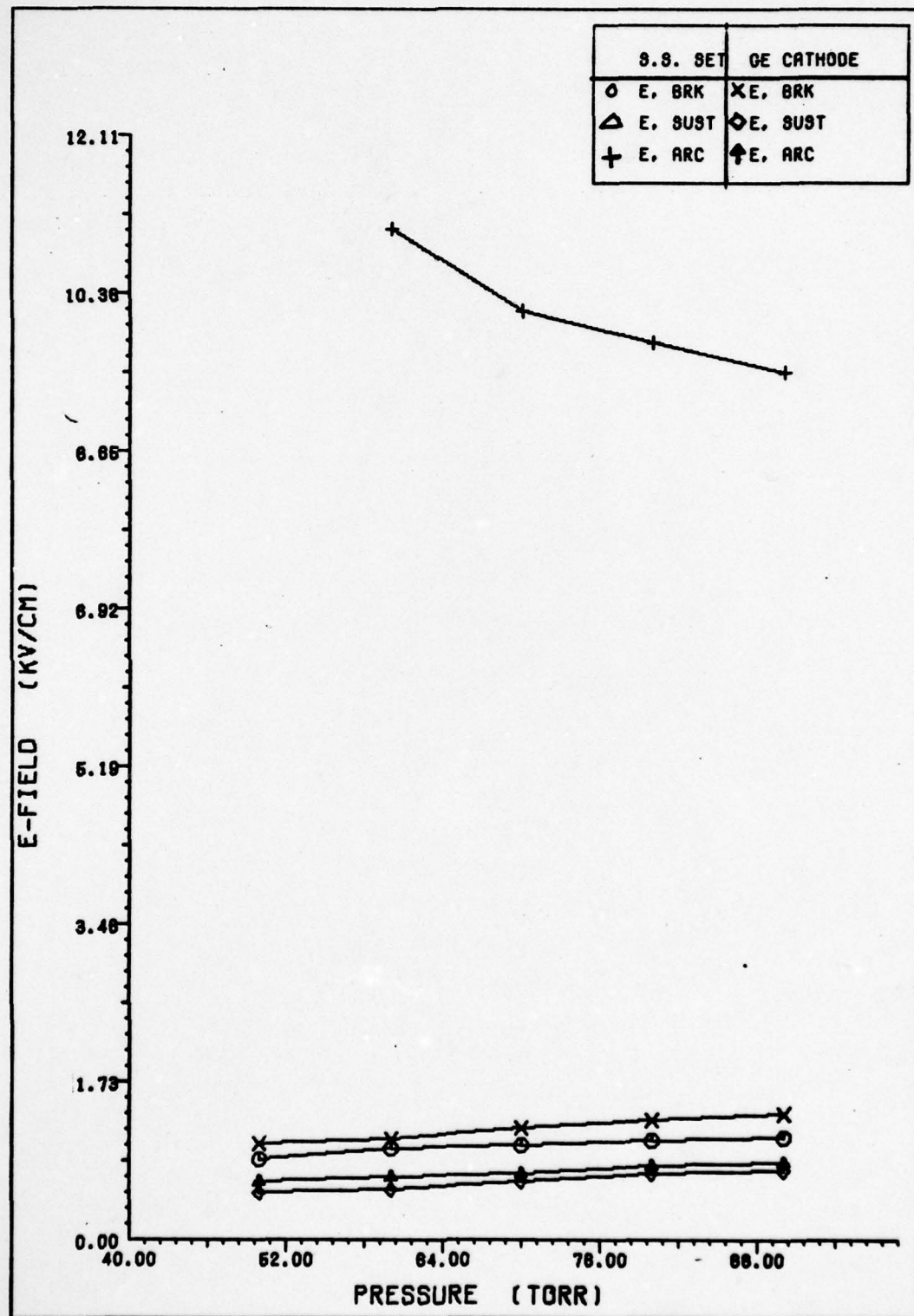


Figure 18. Helium, 100 pps, Ge Cathode

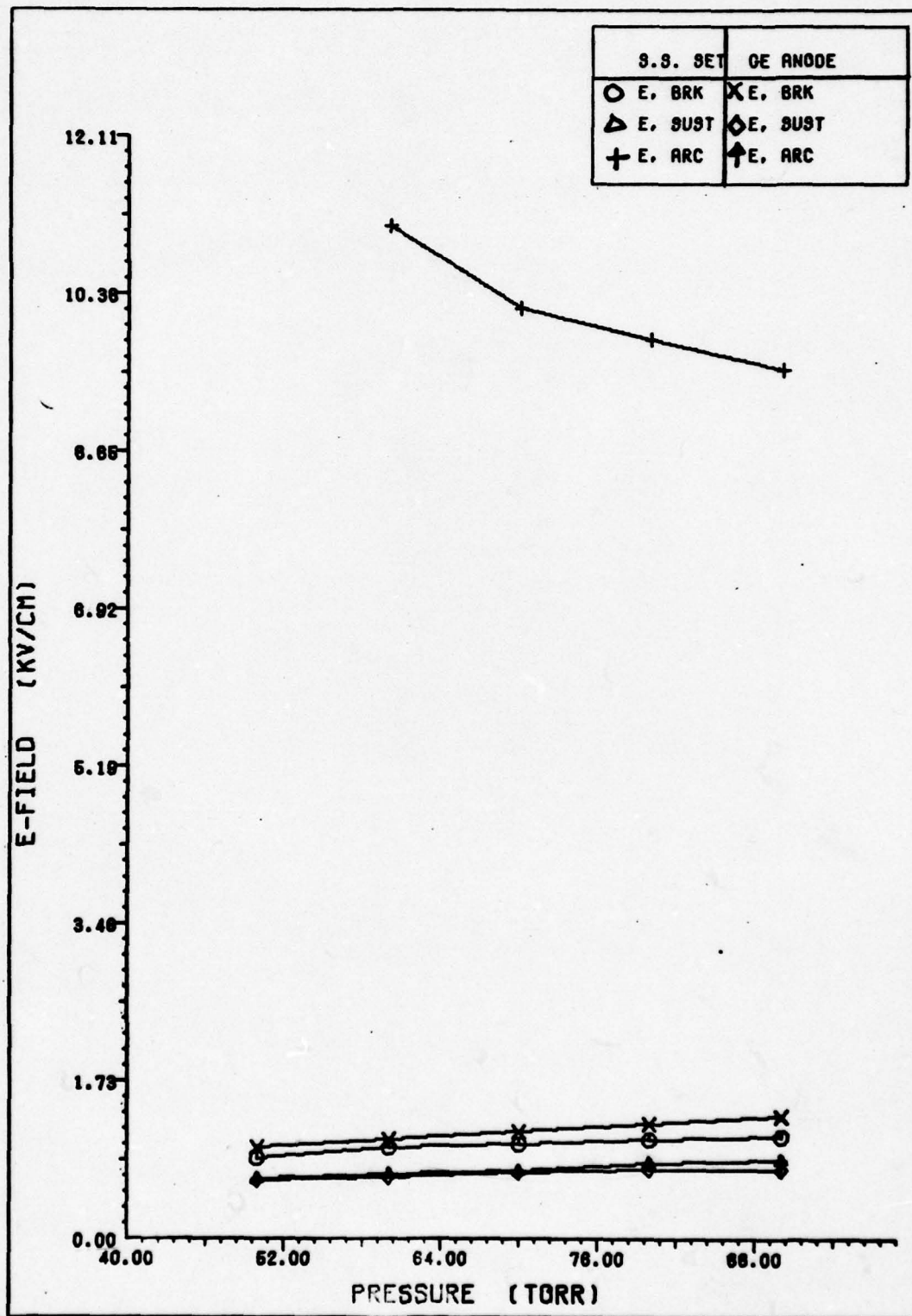


Figure 19. Helium, 100 pps, Ge Anode

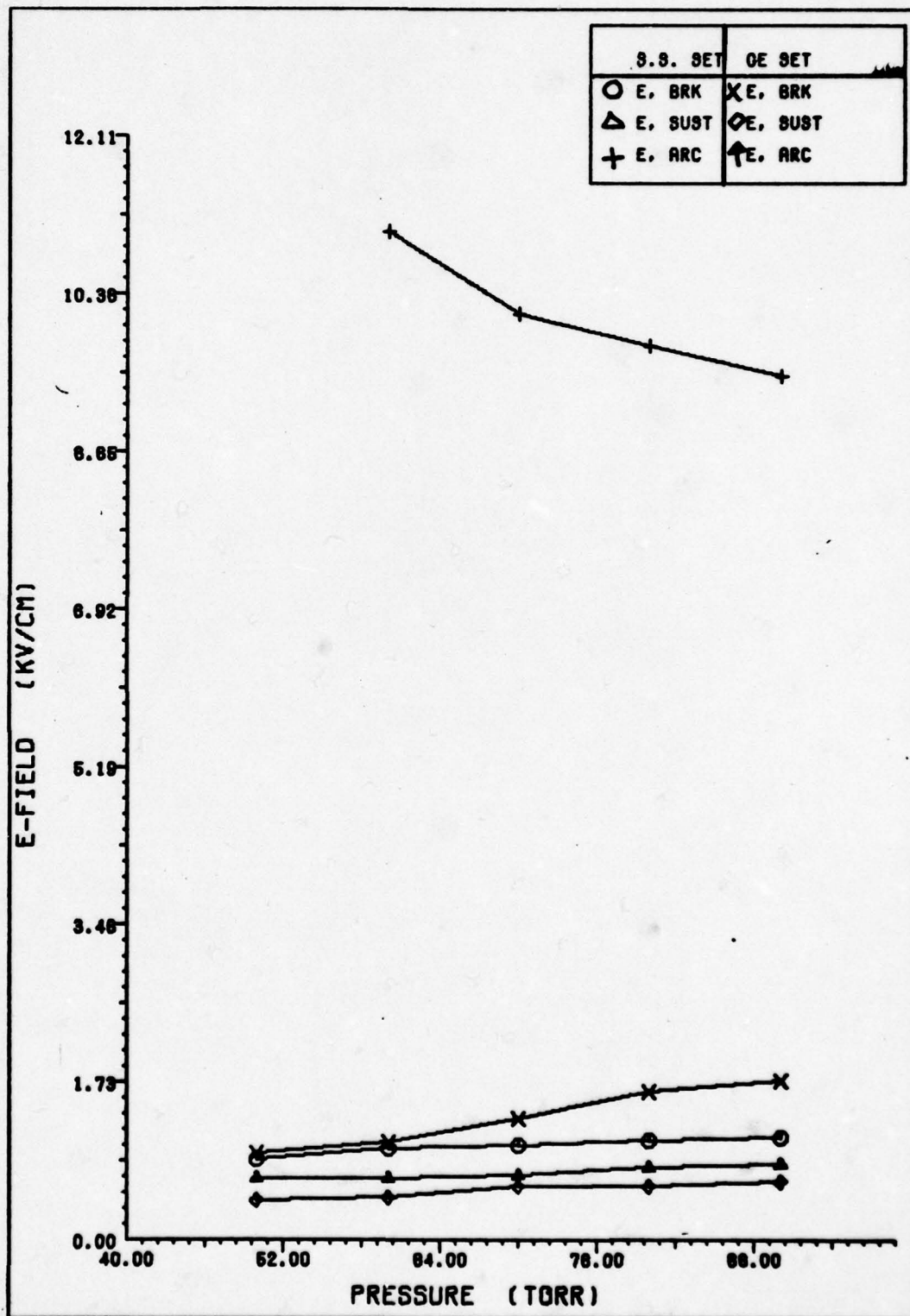


Figure 20. Helium, 100 pps, Ge Anode-Cathode

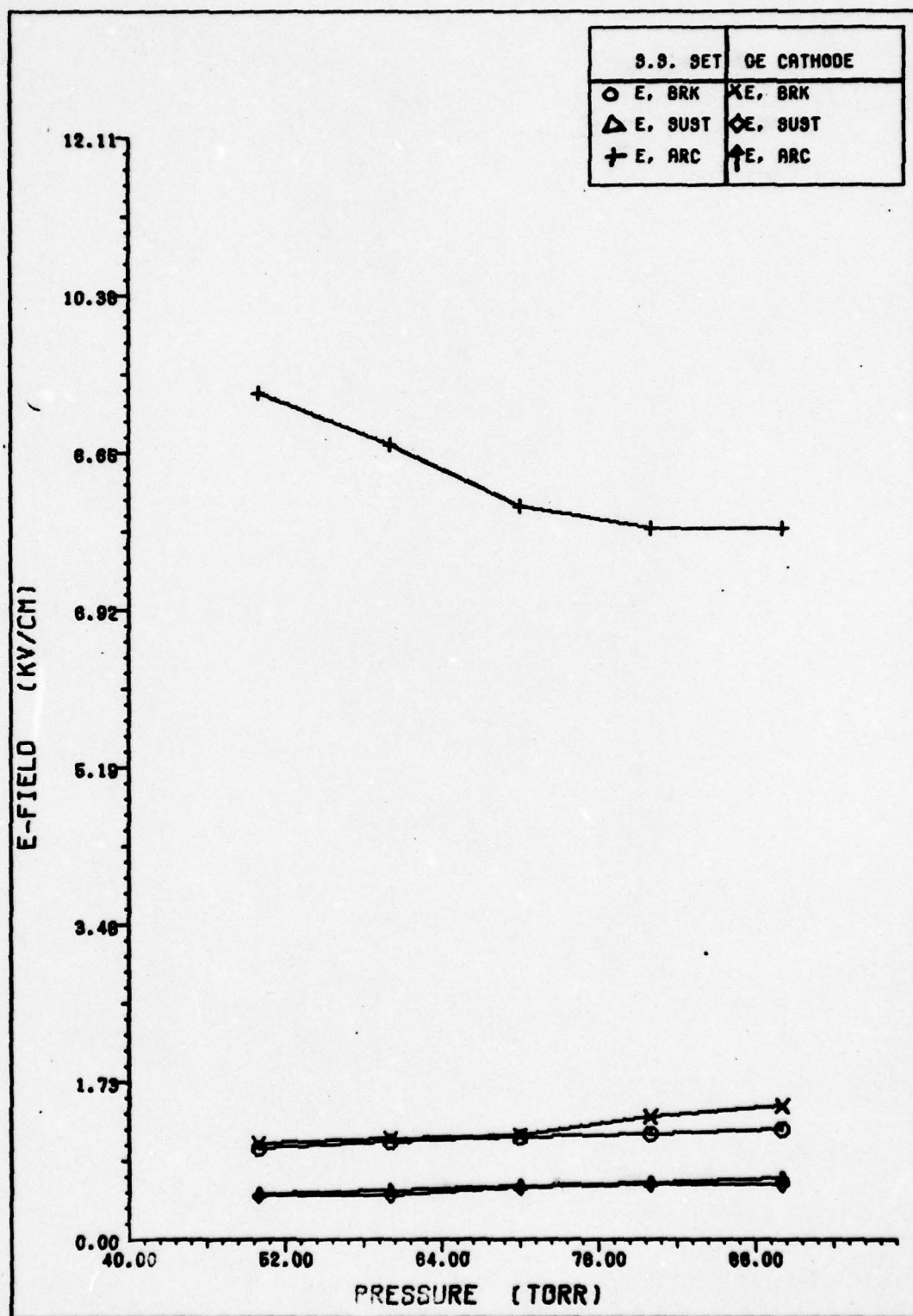


Figure 21. Helium, 200 pps, Ge Cathode

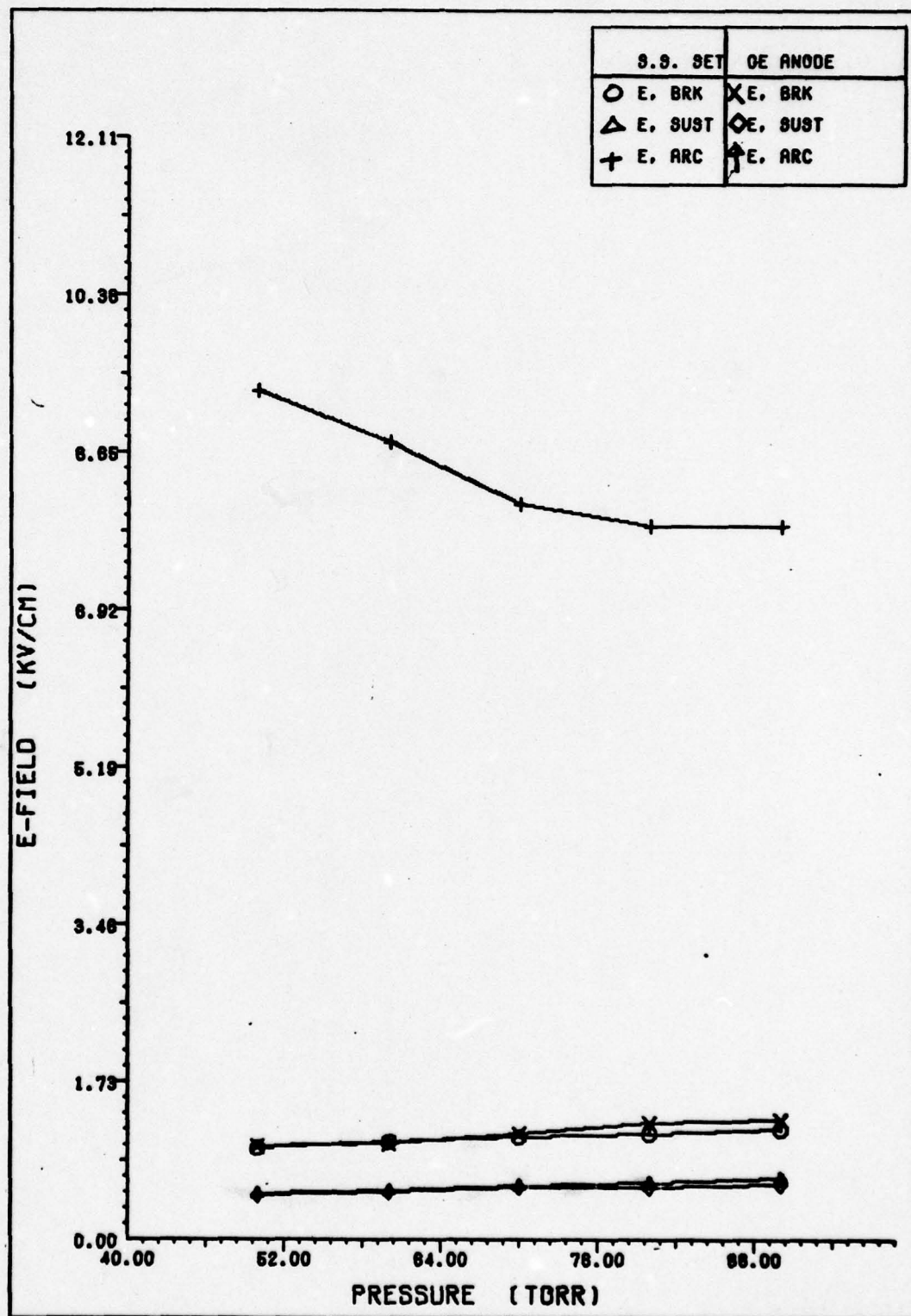


Figure 22. Helium, 200 pps, Ge Anode

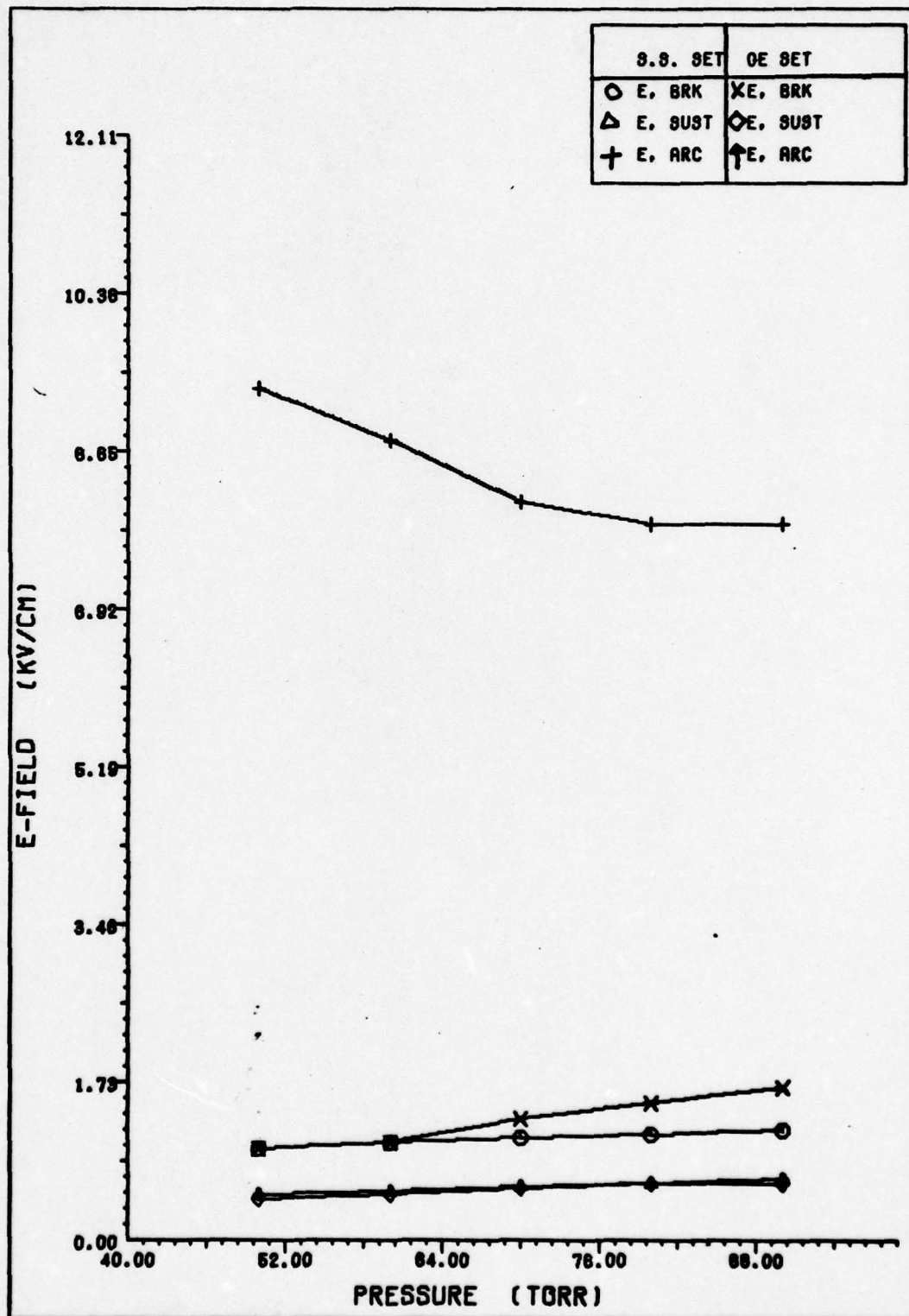


Figure 23. Helium, 200 pps, Ge Anode-Cathode

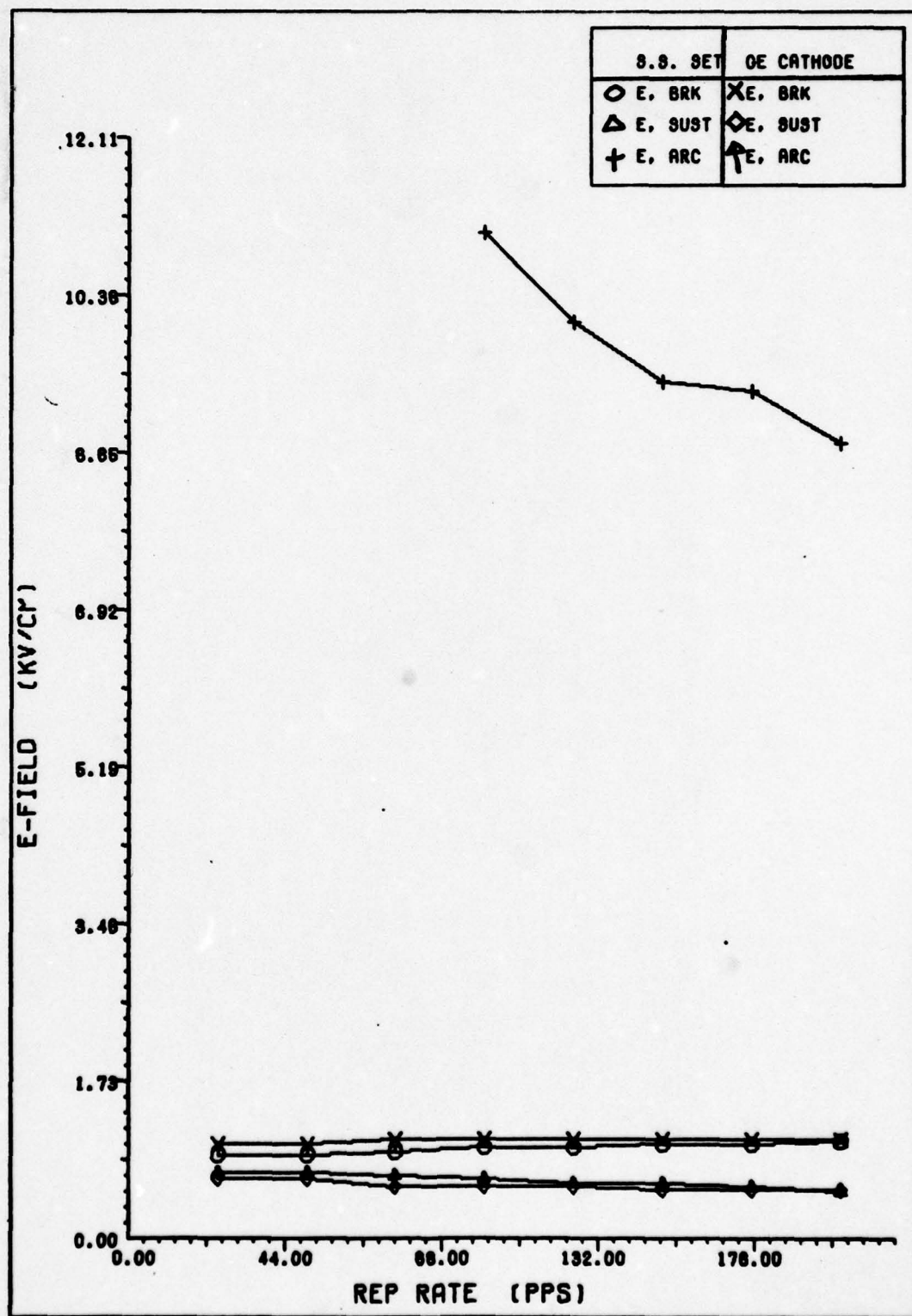


Figure 24. Helium, 60 Torr, Ge Cathode

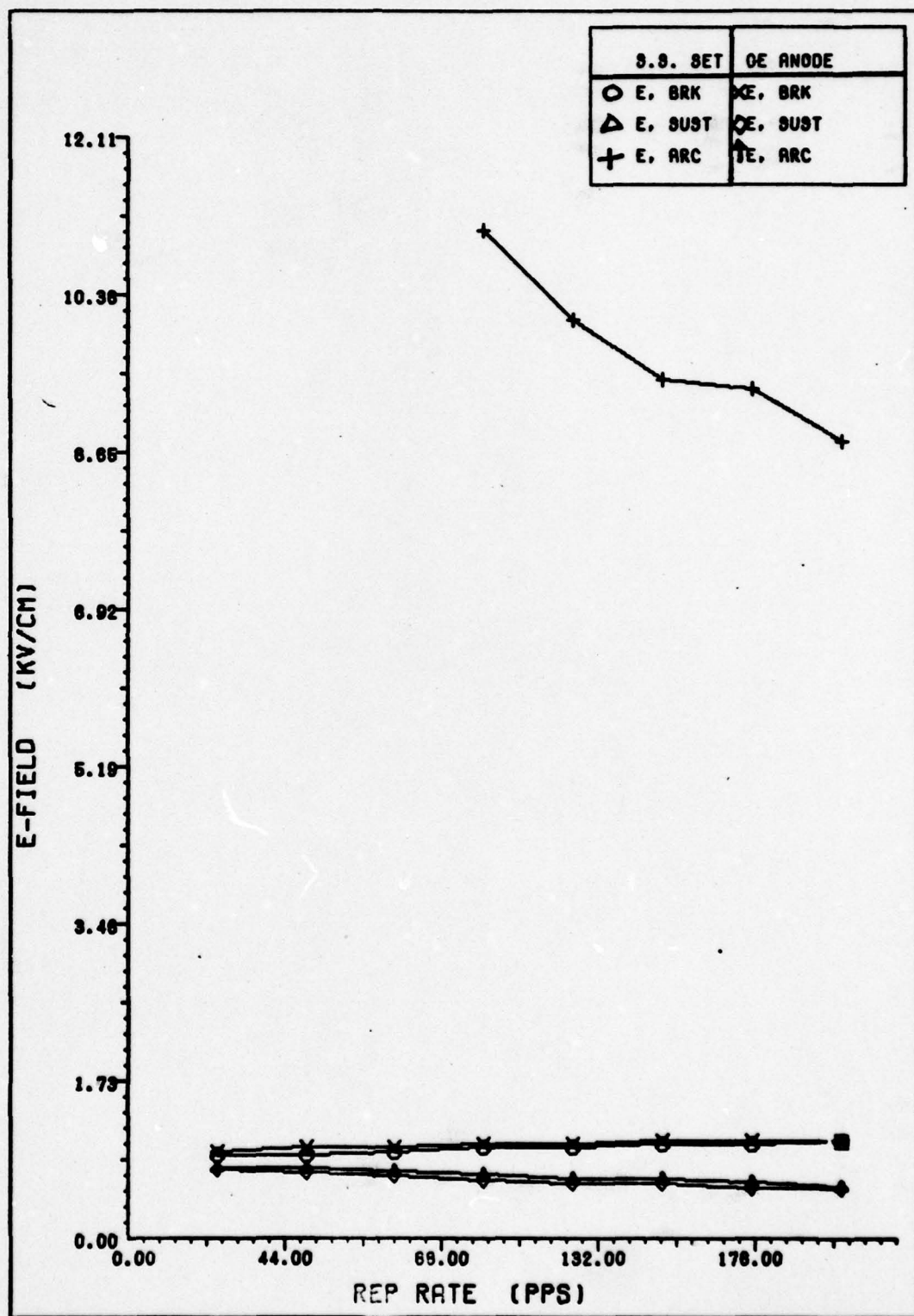


Figure 25. Helium, 60 Torr, Ge Anode

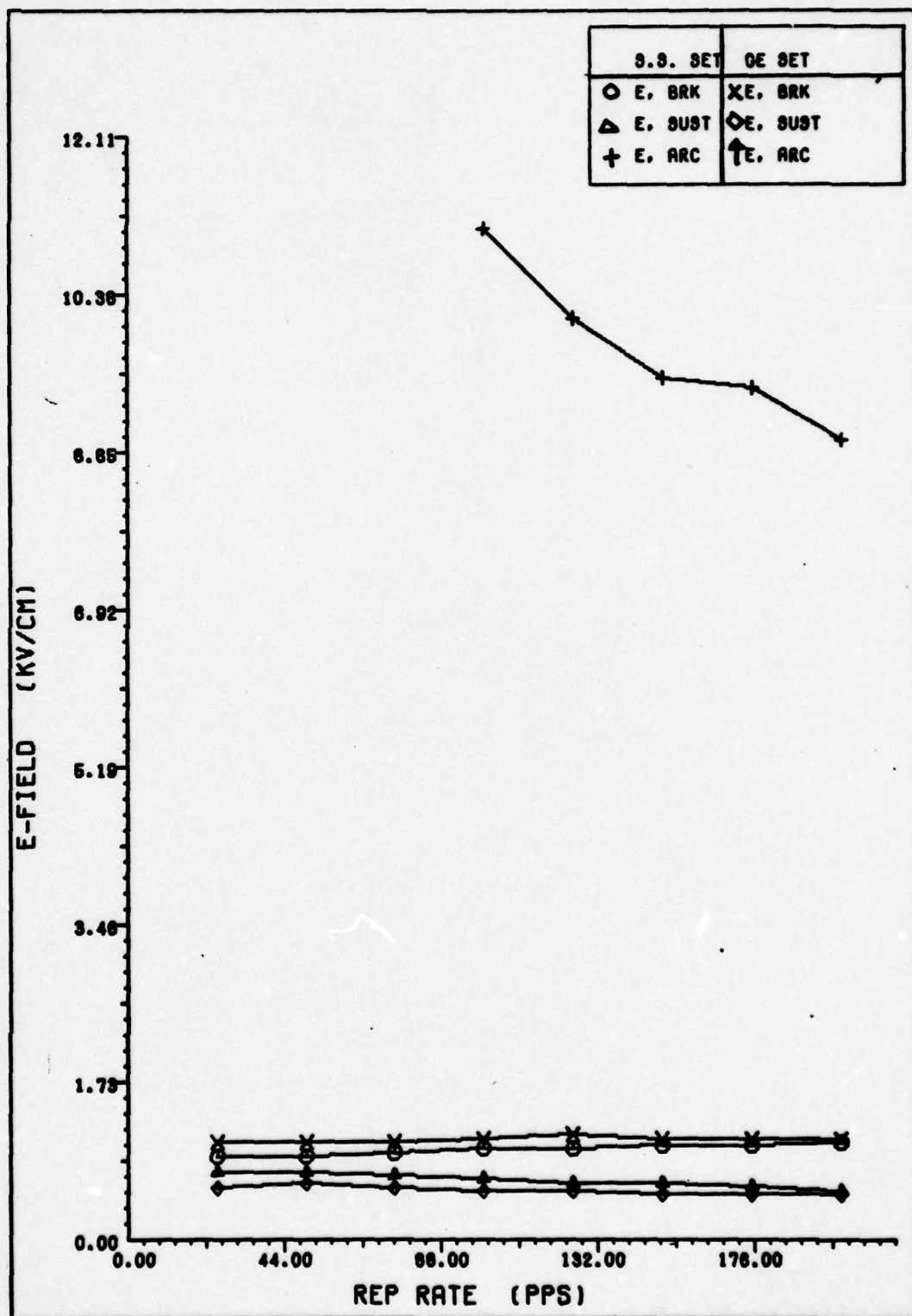


Figure 26. Helium, 60 Torr, Ge Anode-Cathode

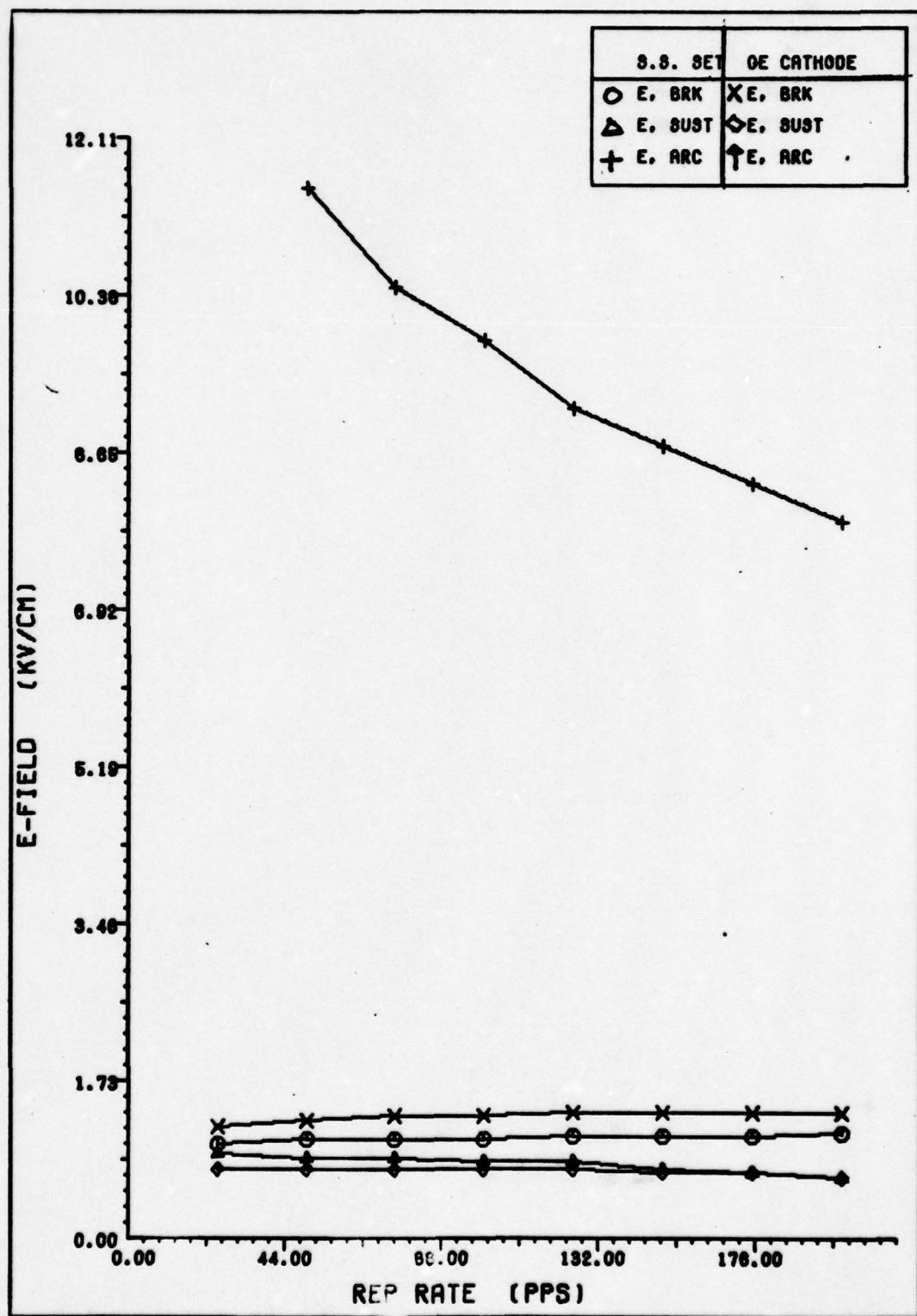


Figure 27. Helium, 80 Torr, Ge Cathode

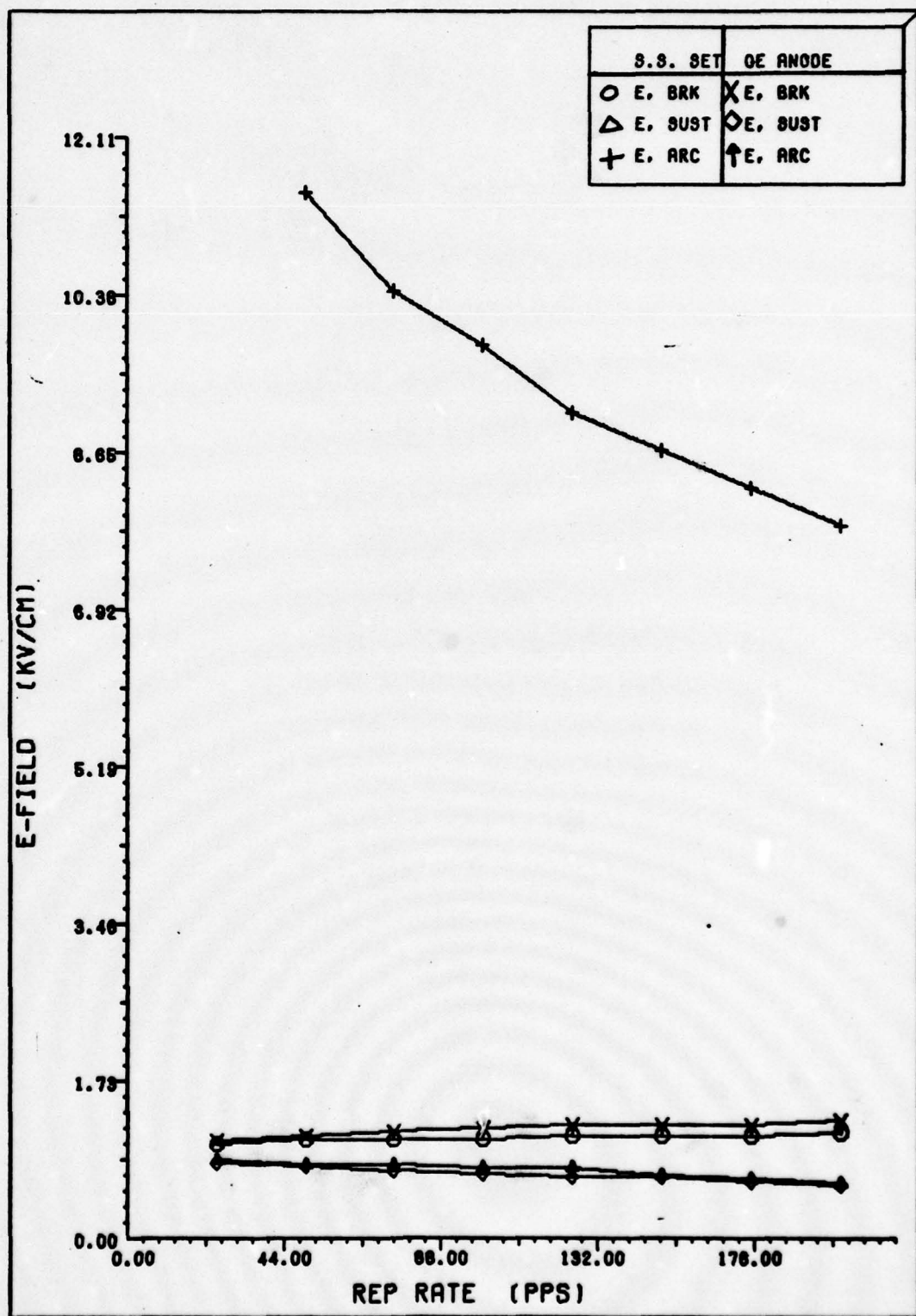


Figure 28. Helium, 80 Torr, Ge Anode

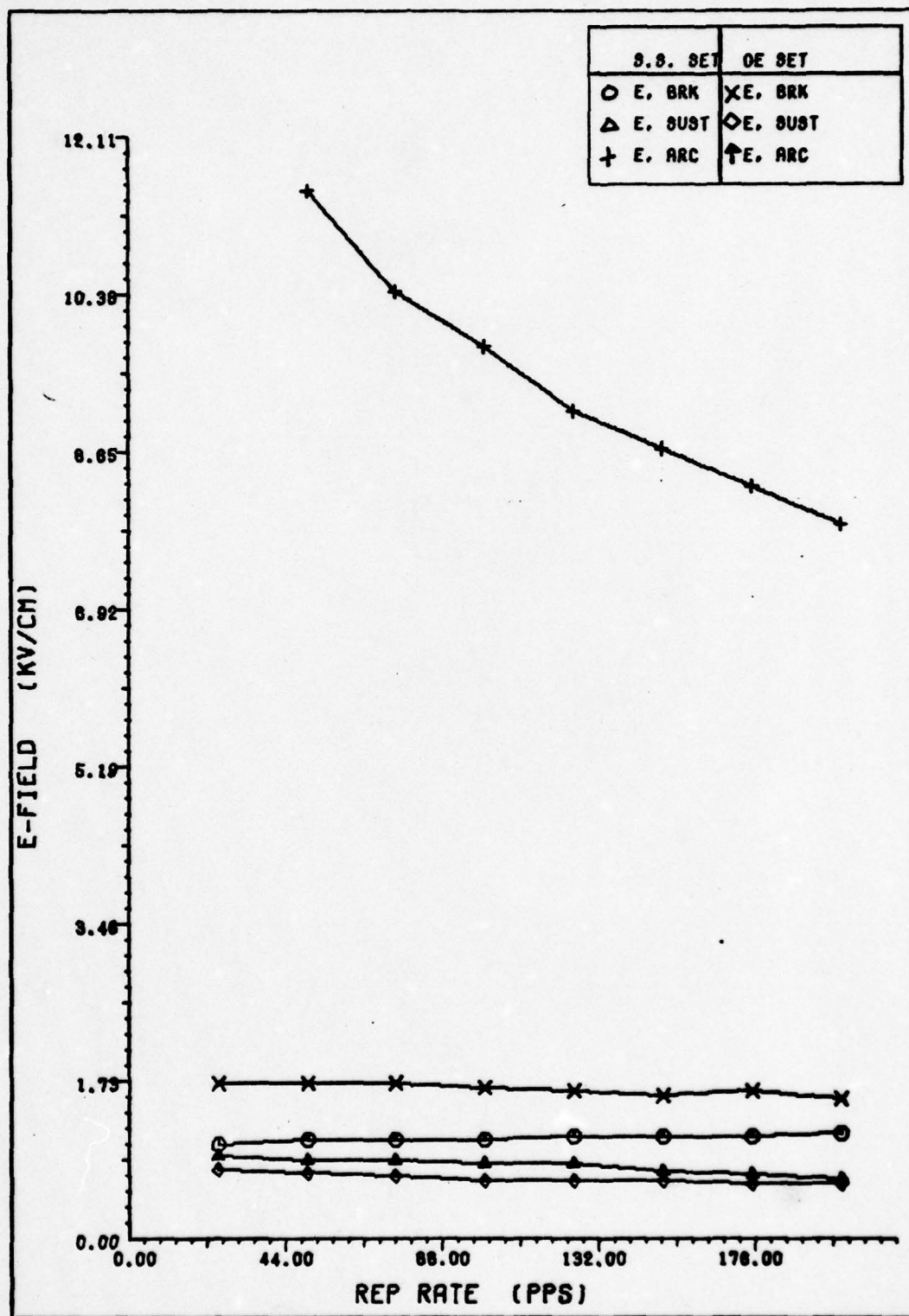


Figure 29. Helium, 80 Torr, Ge Anode-Cathode

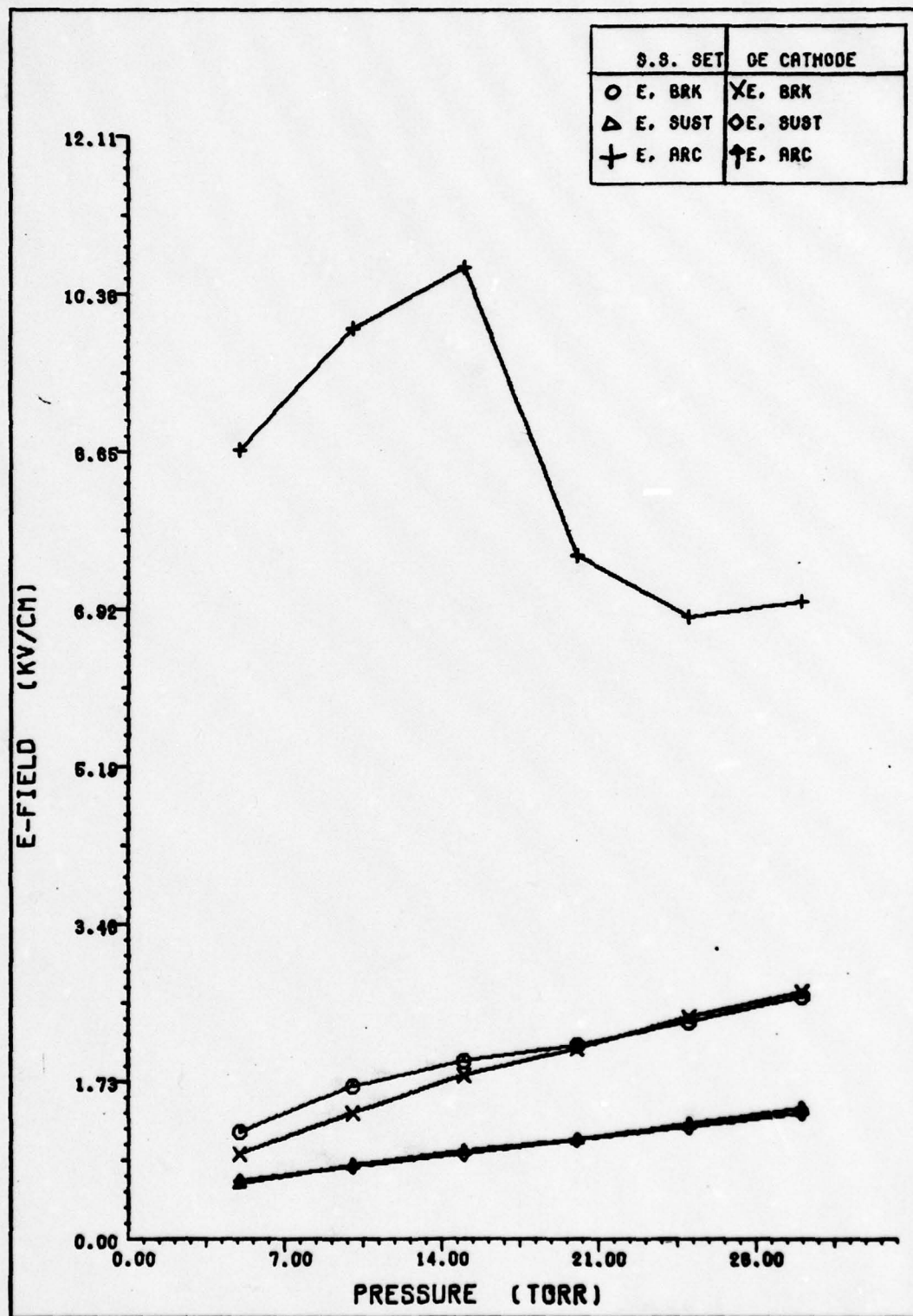


Figure 30. Nitrogen, 100 pps, Ge Cathode

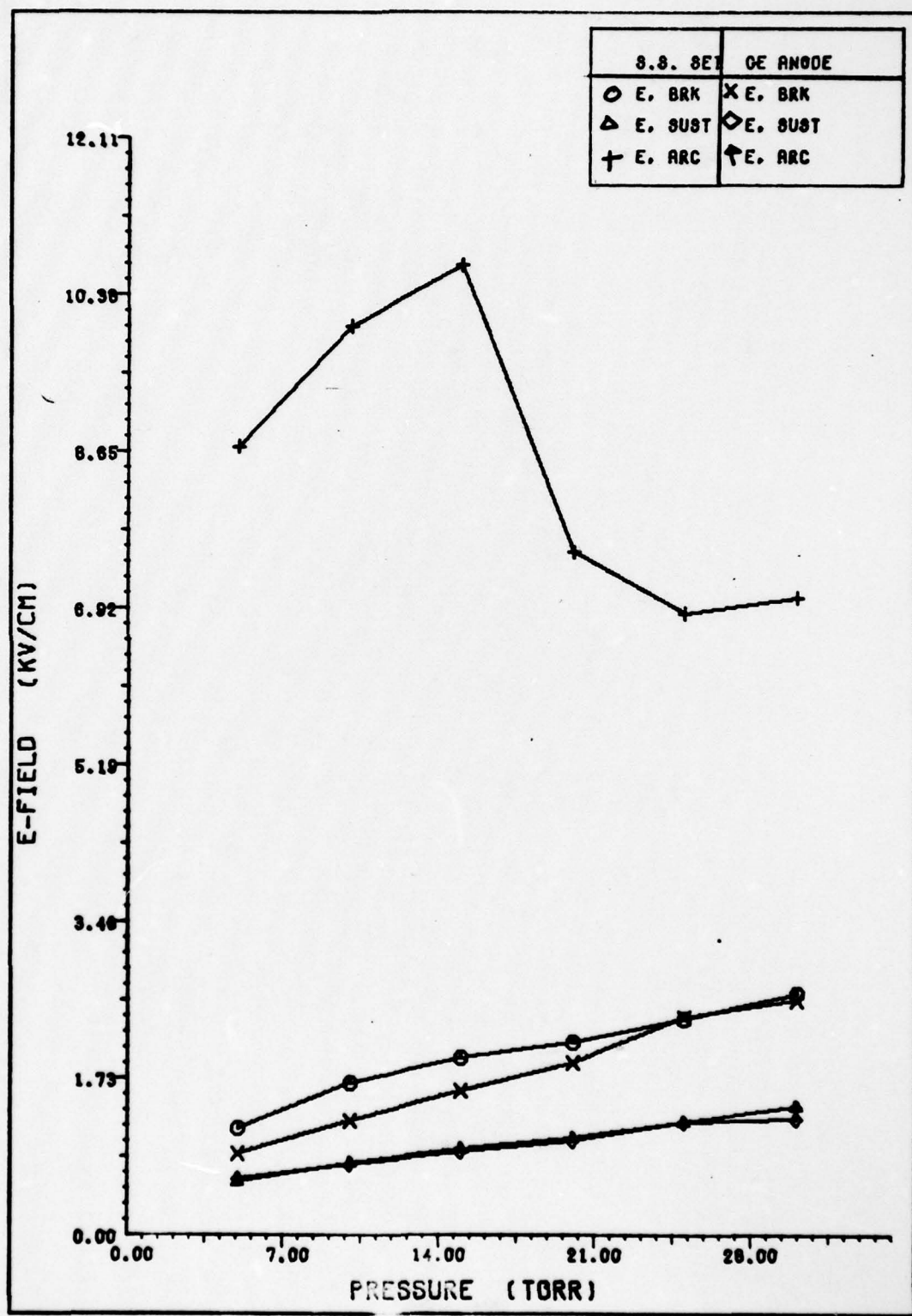


Figure 31. Nitrogen, 100 pps, Ge Anode

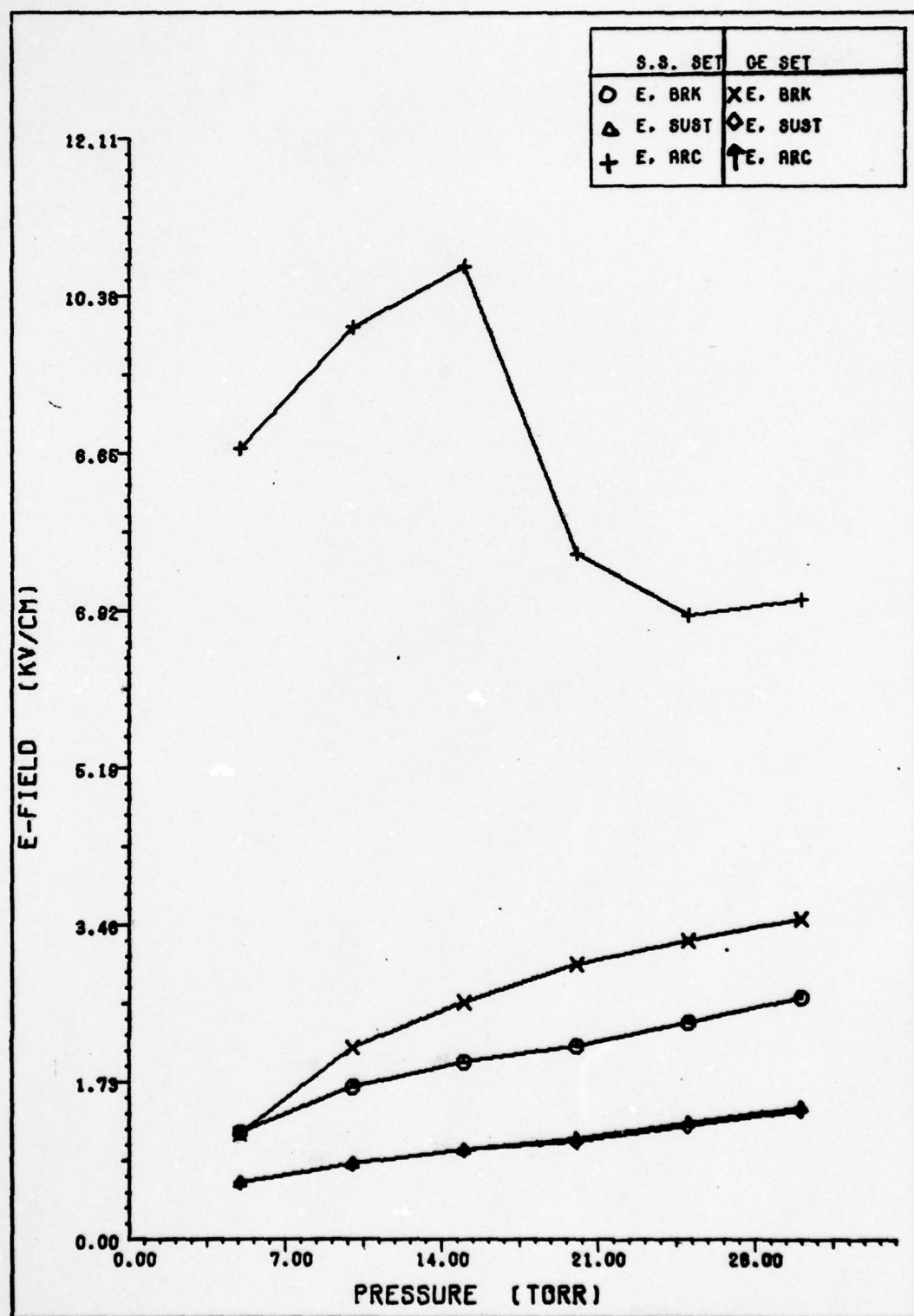


Figure 32. Nitrogen, 100 pps, Ge Anode-Cathode

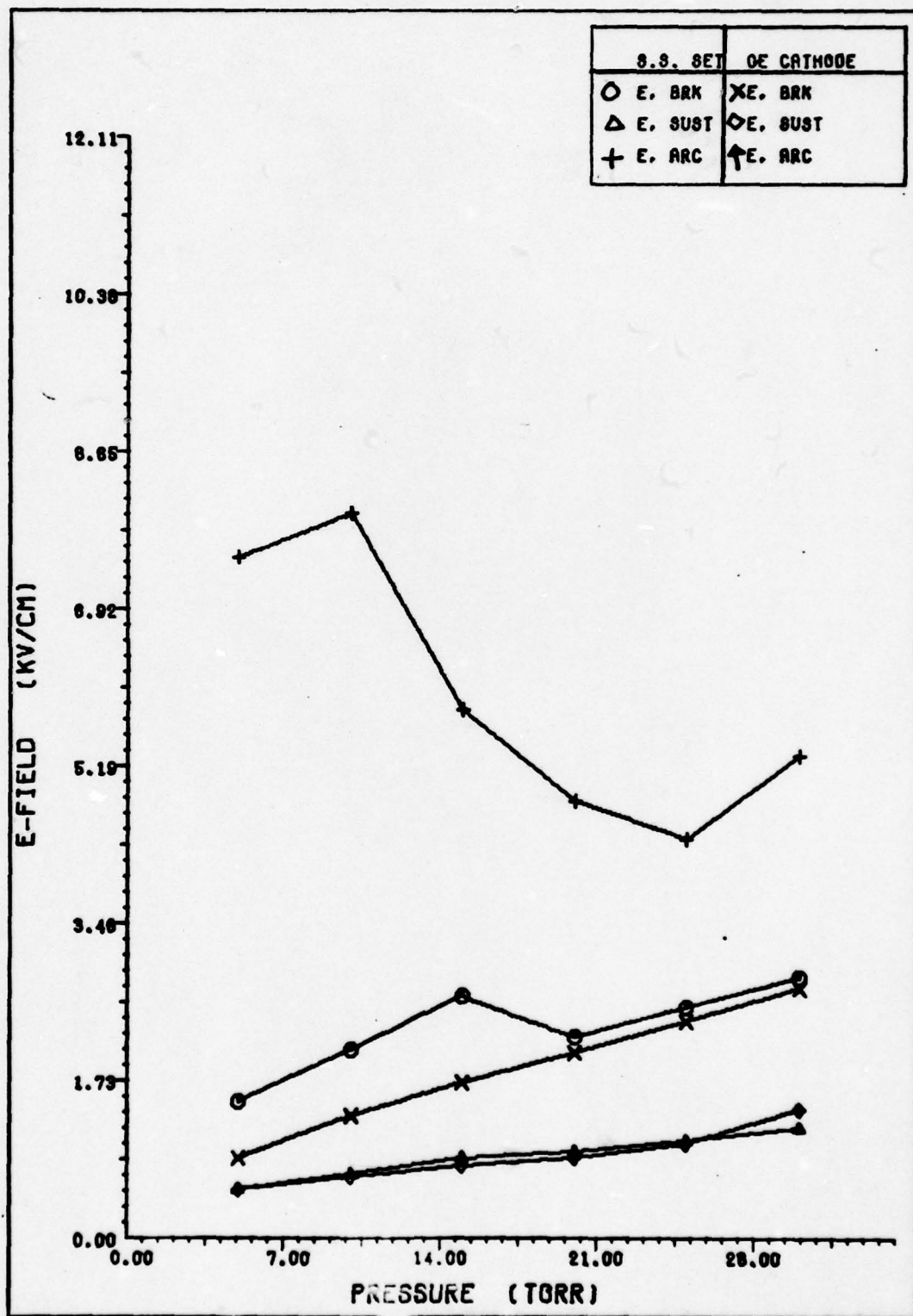


Figure 33. Nitrogen, 200 pps, Ge Cathode

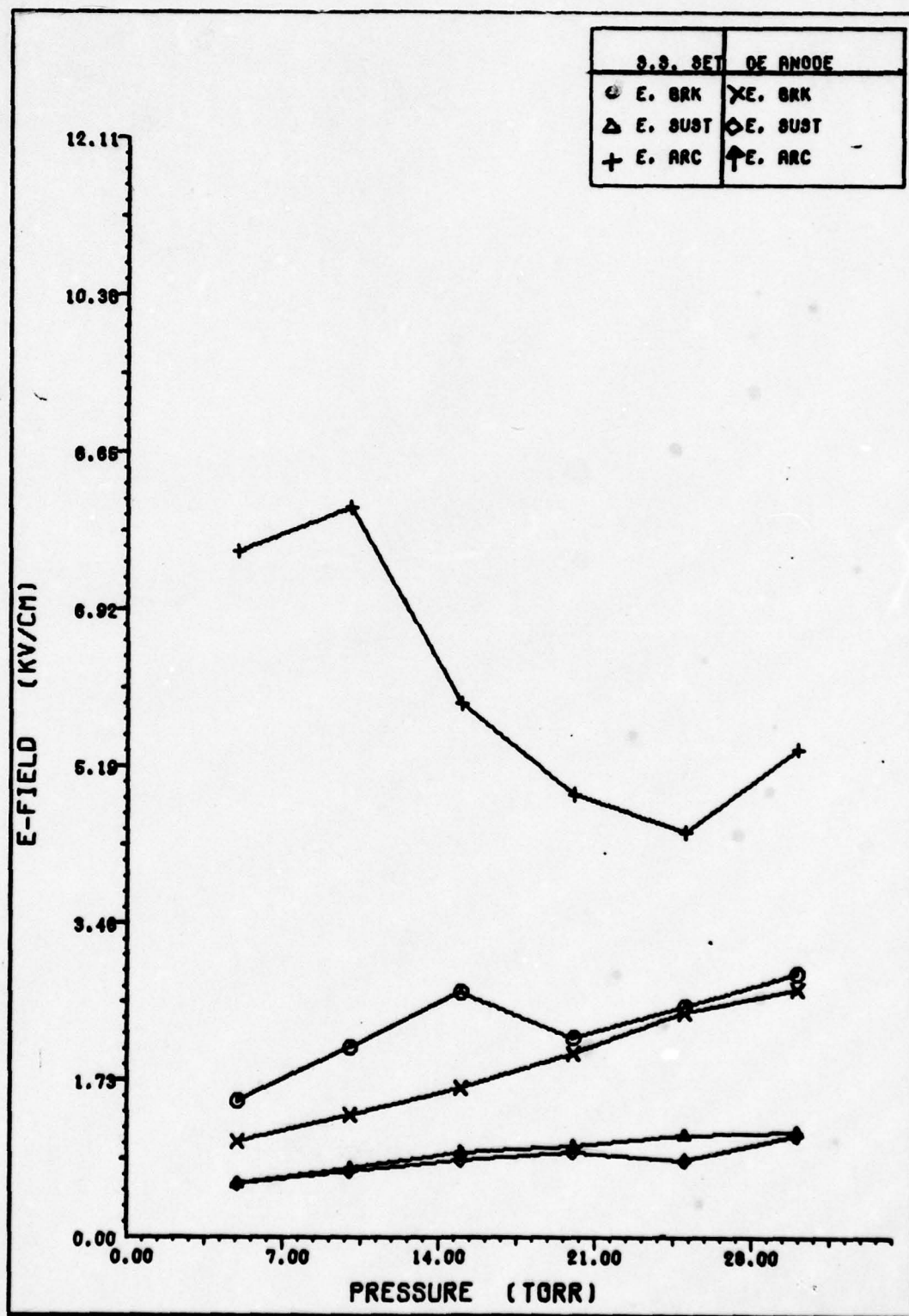


Figure 34. Nitrogen, 200 pps, Ge Anode

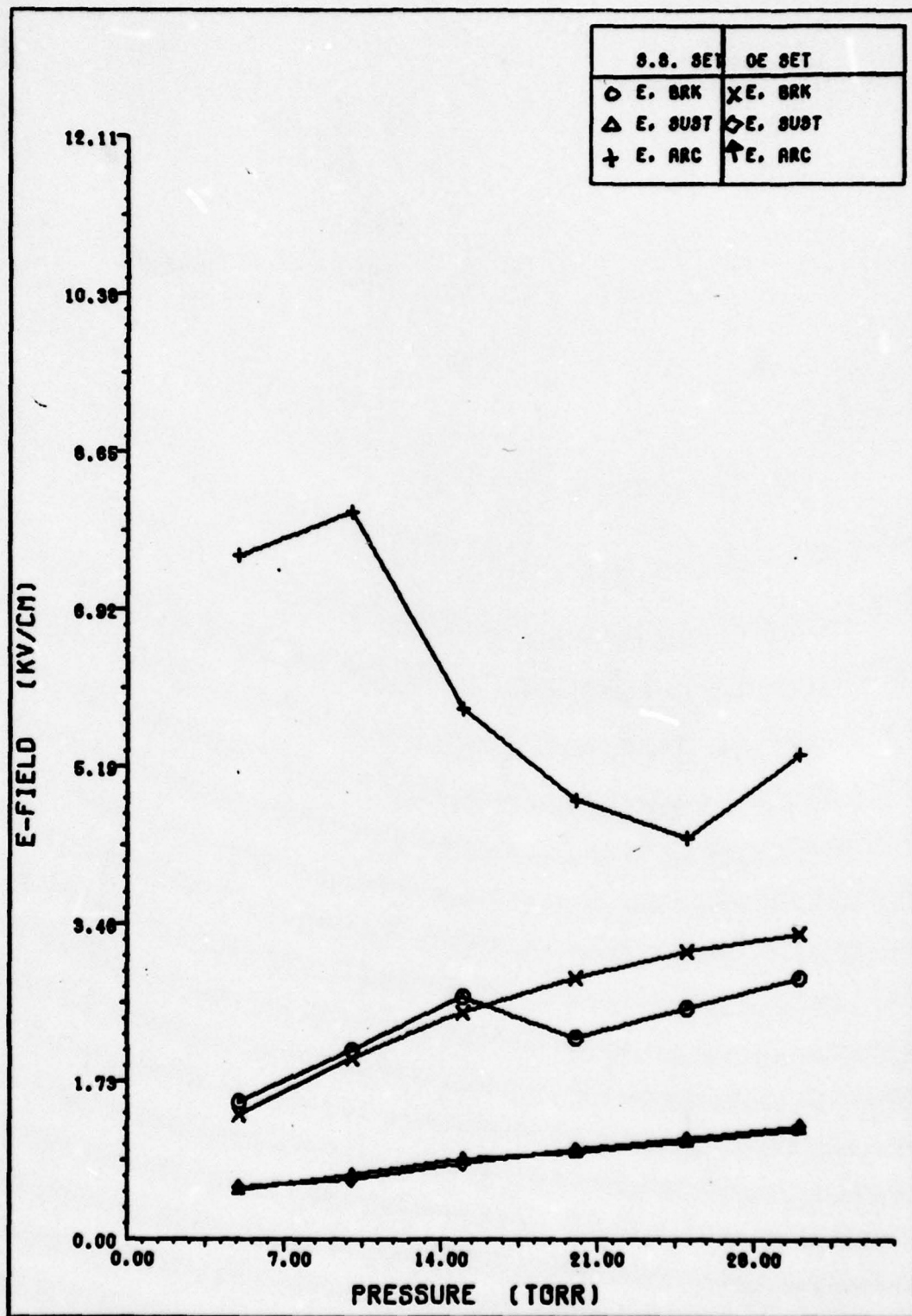


Figure 35. Nitrogen, 200 pps, Ge Cathode-Anode

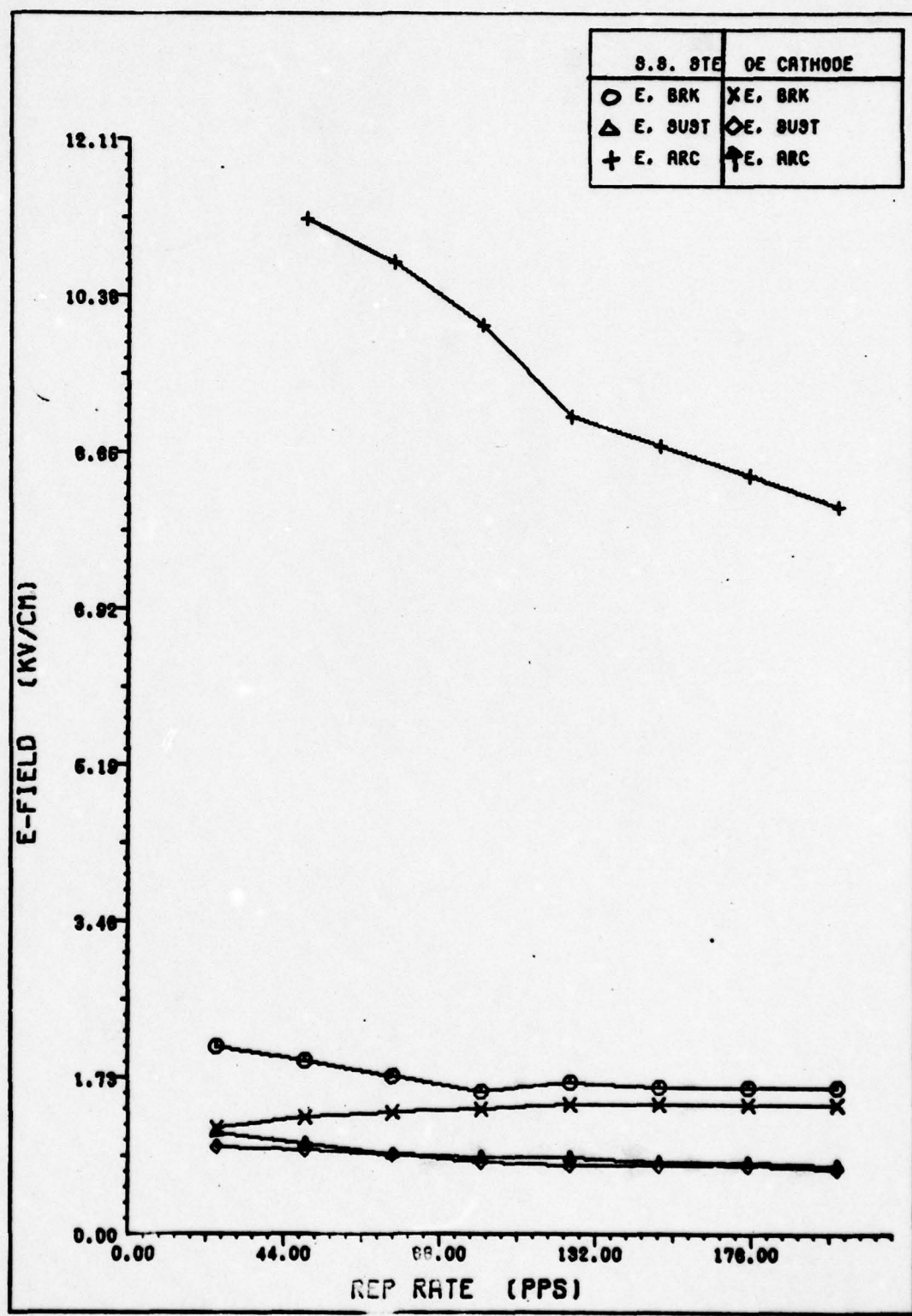


Figure 36. Nitrogen, 10 Torr, Ge Cathode

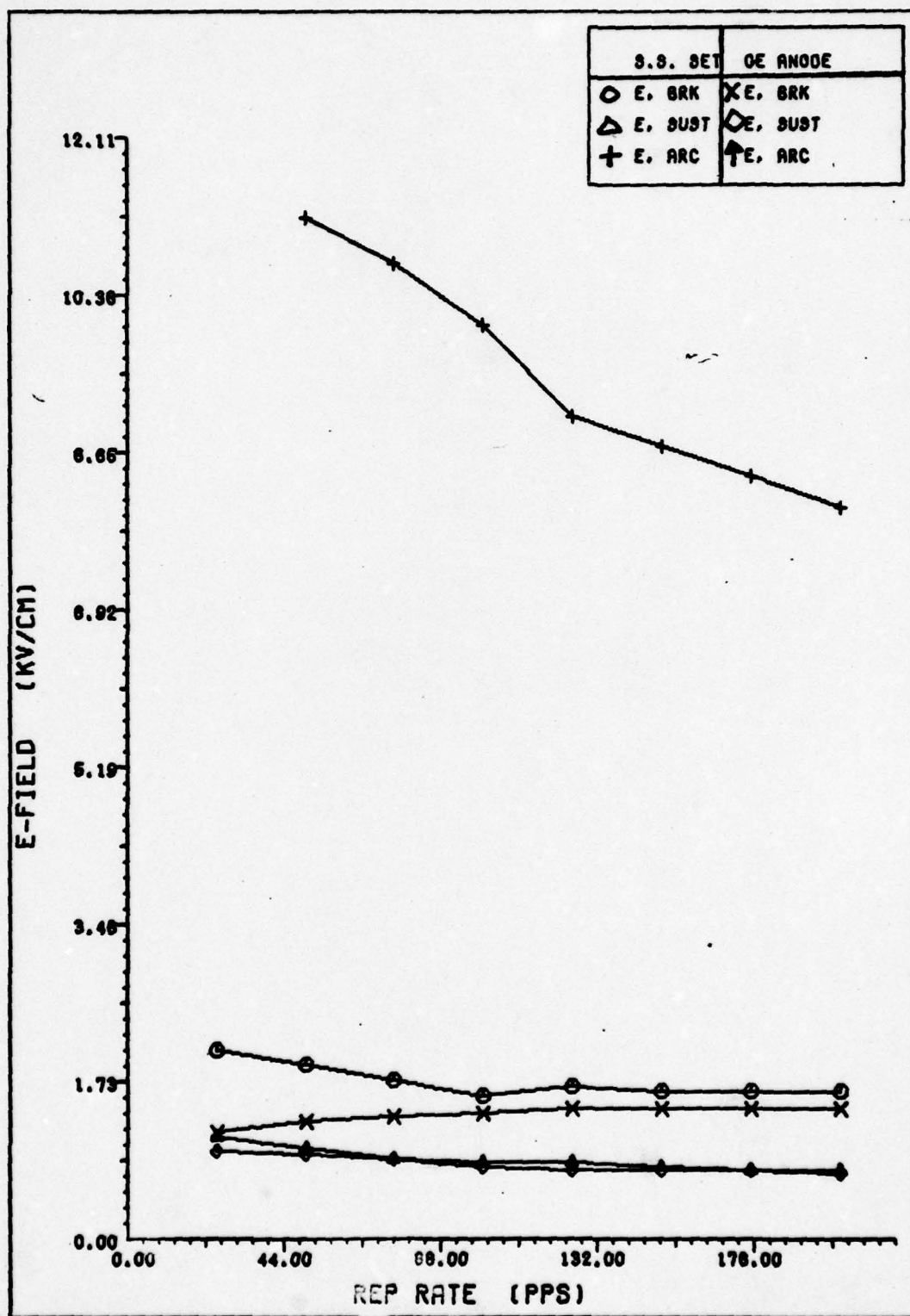


Figure 37. Nitrogen, 10 Torr, Ga Anode

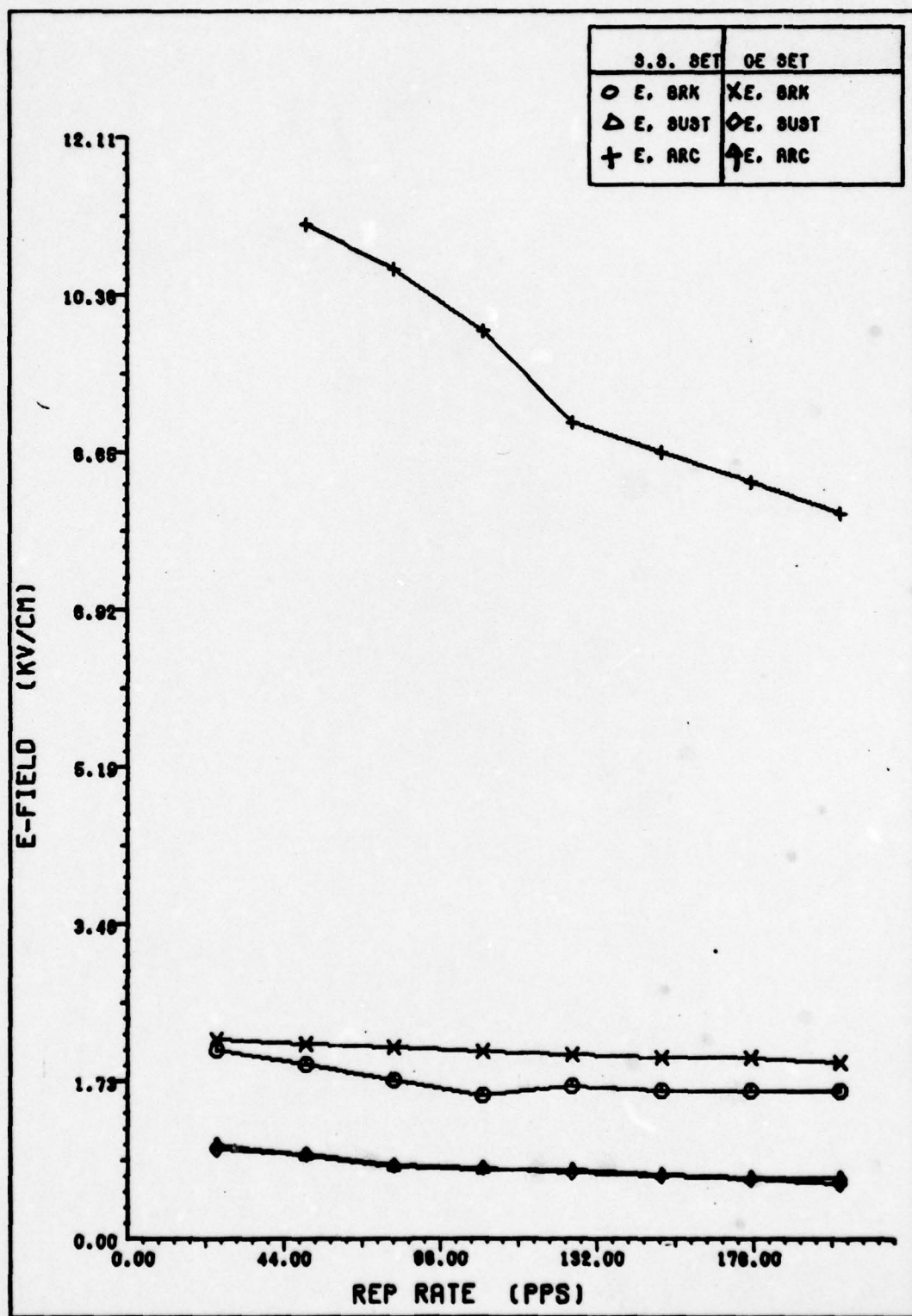


Figure 38. Nitrogen, 10 Torr, Ge Anode-Cathode

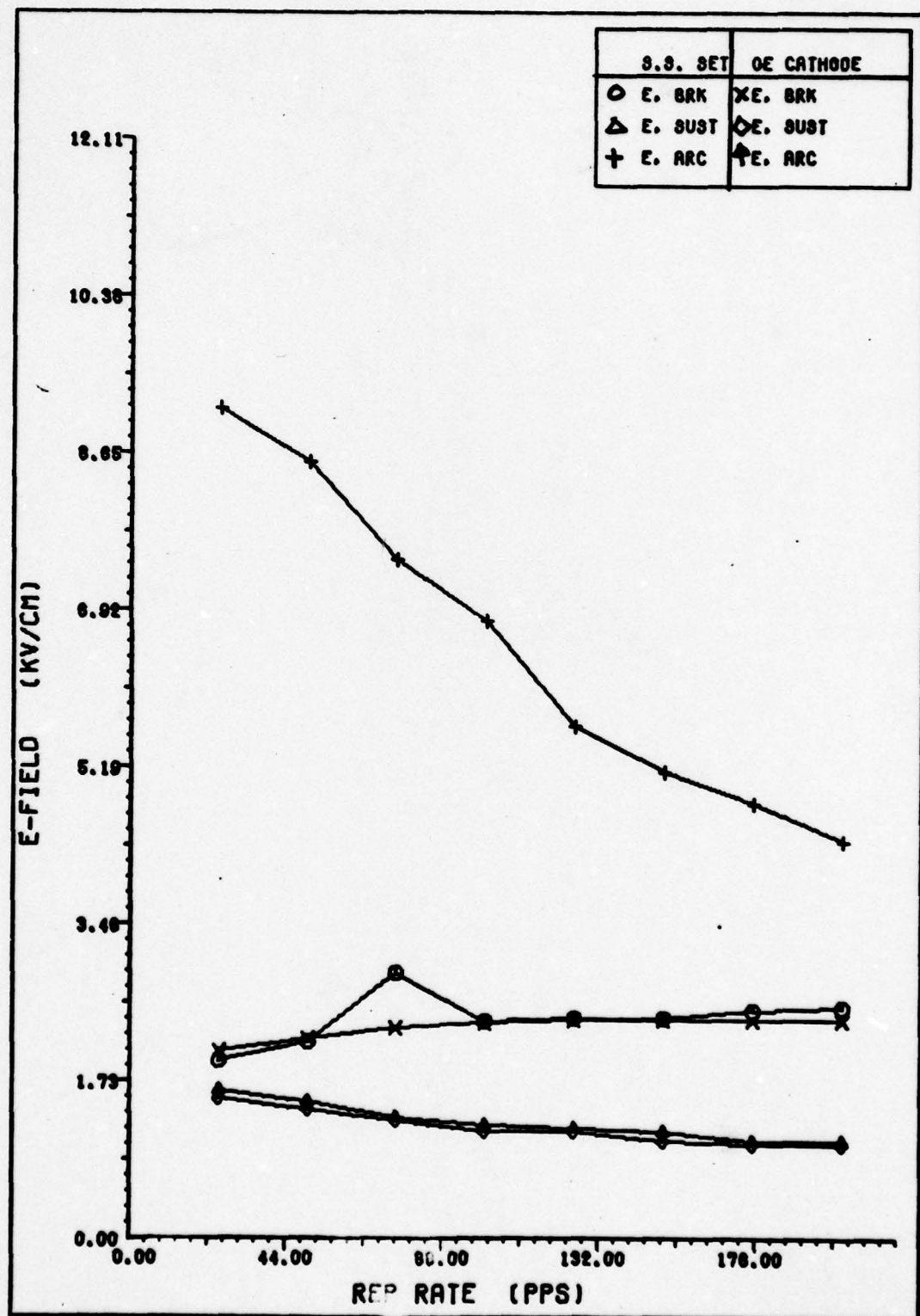


Figure 39. Nitrogen, 25 Torr, Ge Cathode

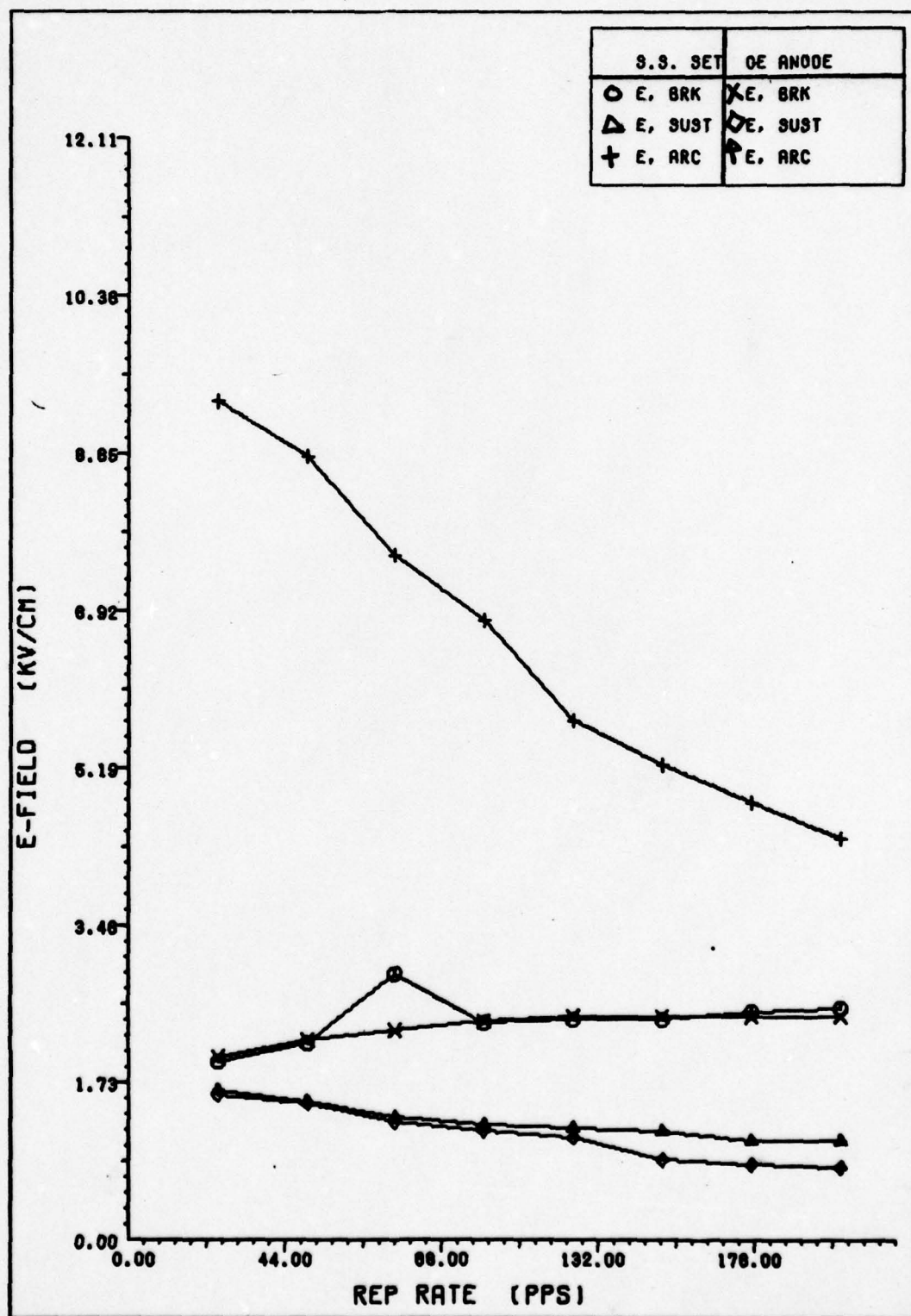


Figure 40. Nitrogen, 25 Torr, Ge Anode

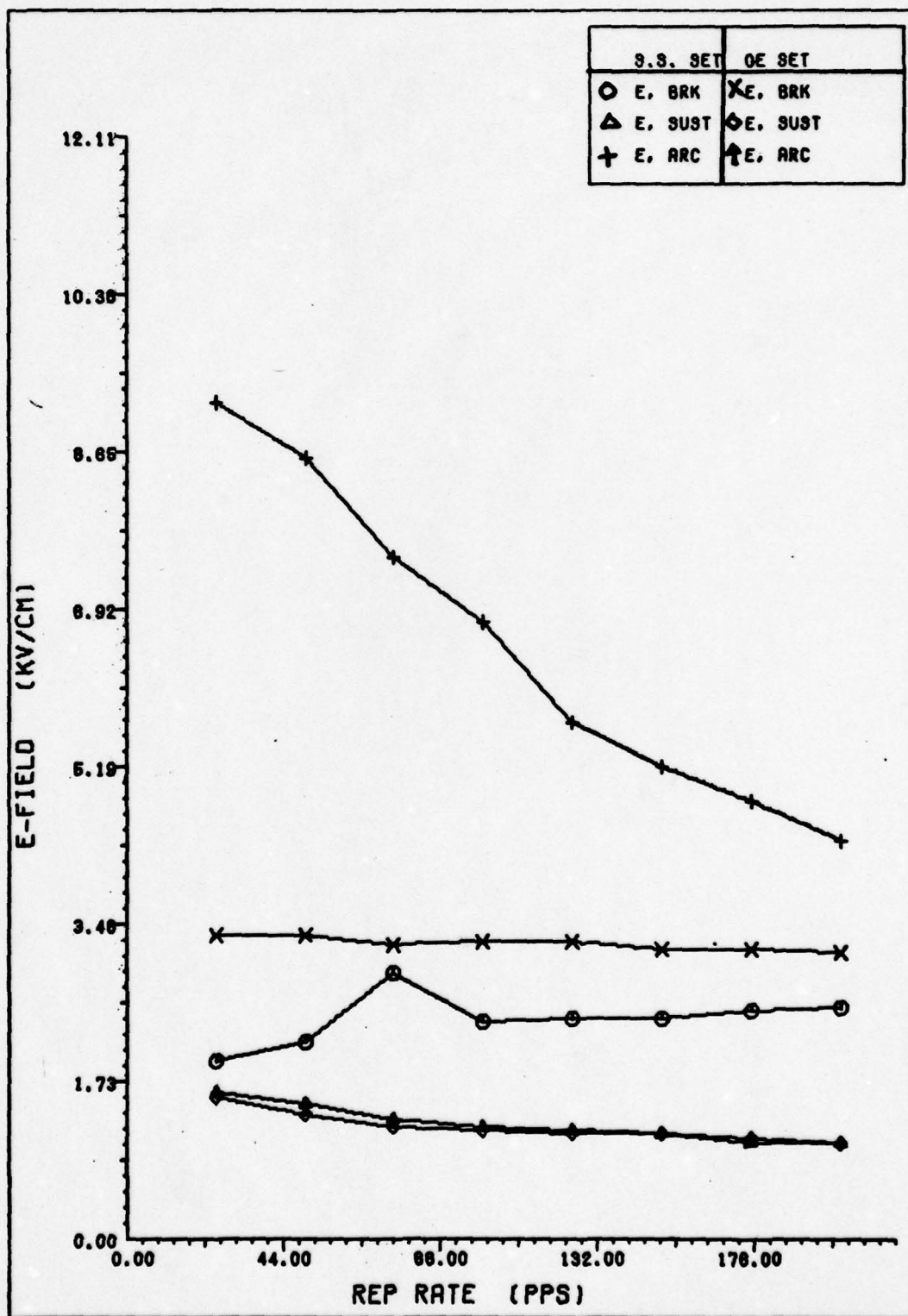


Figure 41. Nitrogen, 25 Torr, Ge Cathode-Anode

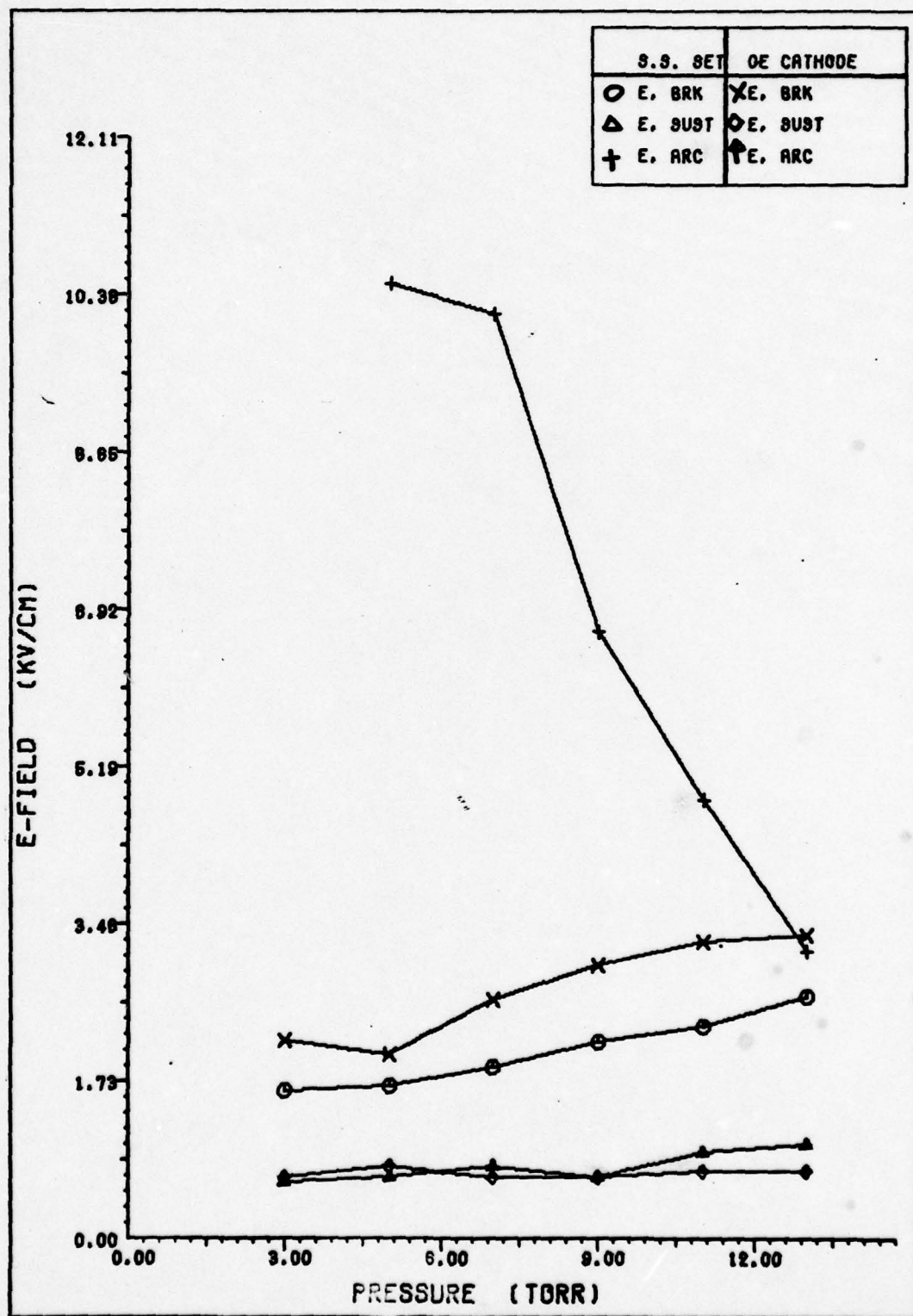


Figure 42. Sulfur-Hexafluoride, 100 pps, Ge Cathode

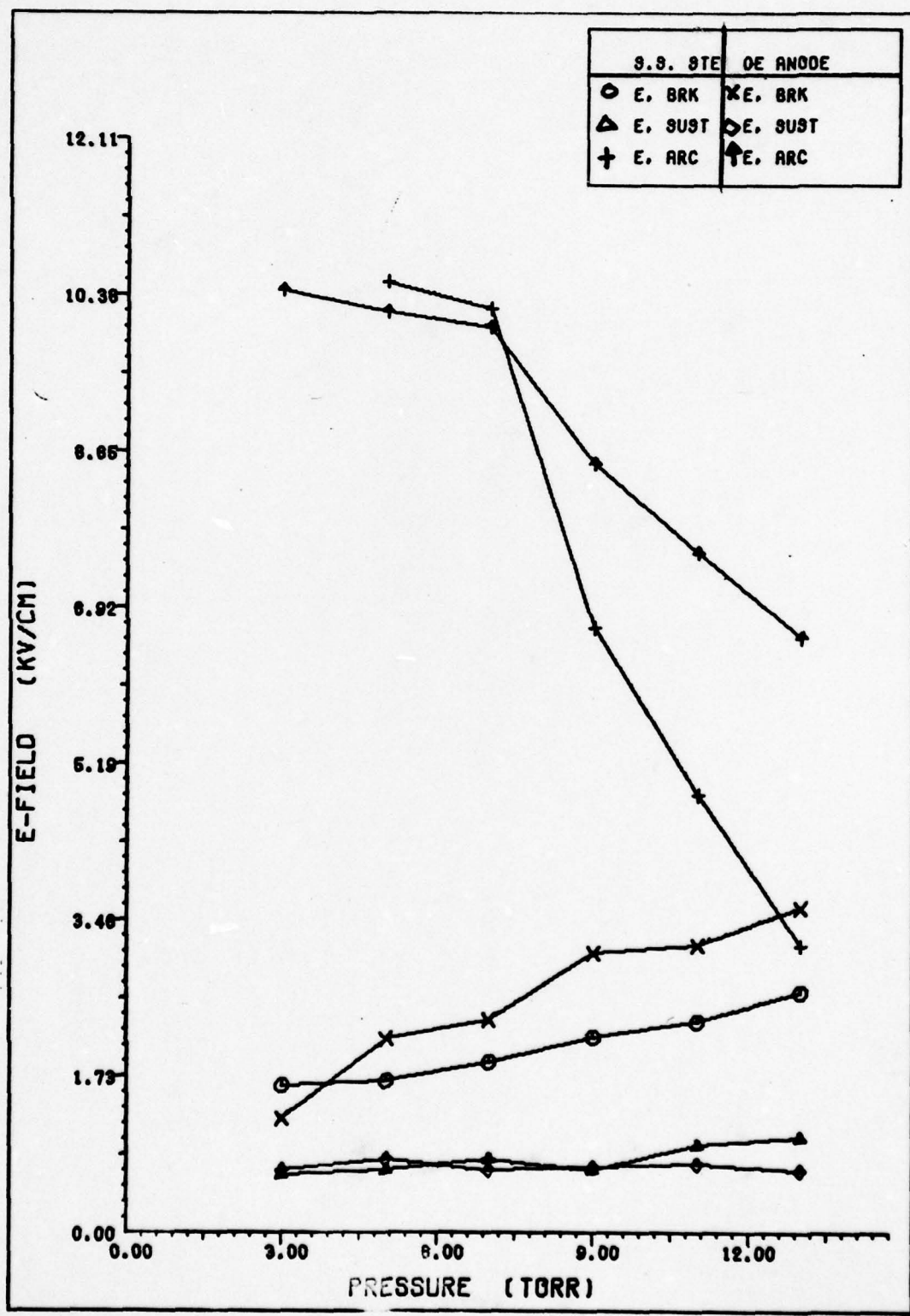


Figure 43. Sulfur-Hexafluoride, 100 pps, Ge Anode

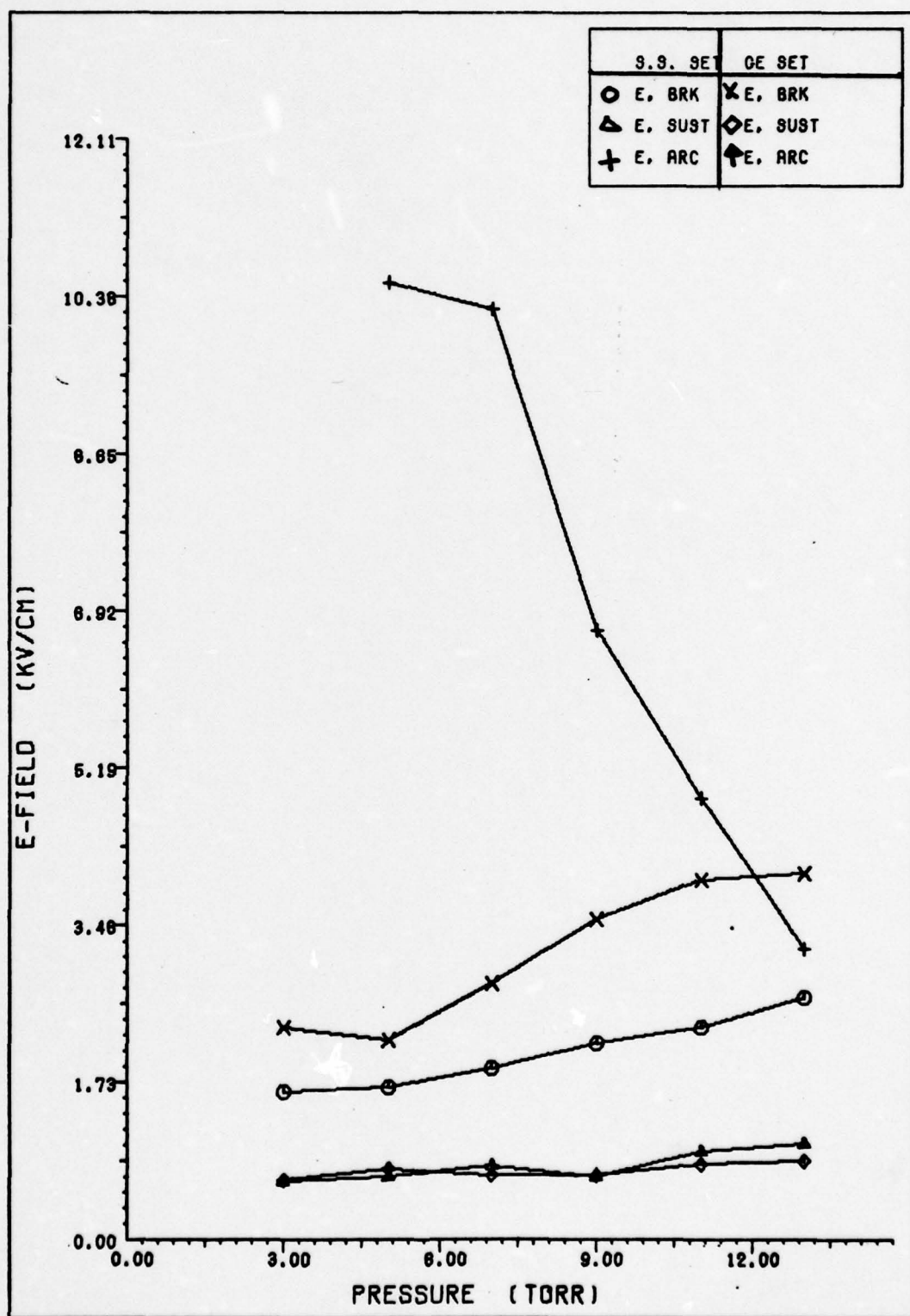


Figure 44. Sulfur-Hexafluoride, 100 pps, Ge Cathode-Anode

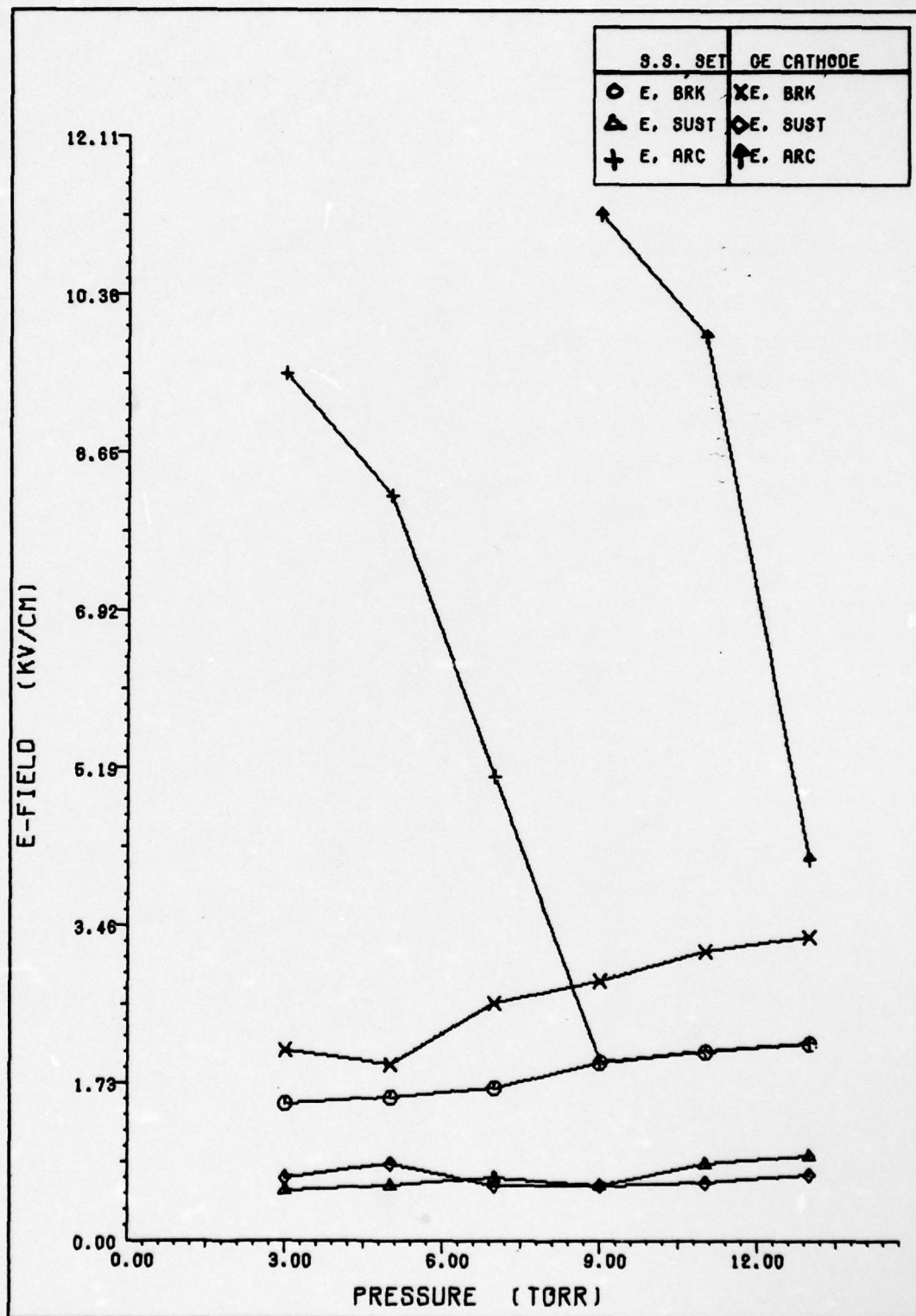


Figure 45. Sulfur-Hexafluoride, 200 pps, Ge Cathode

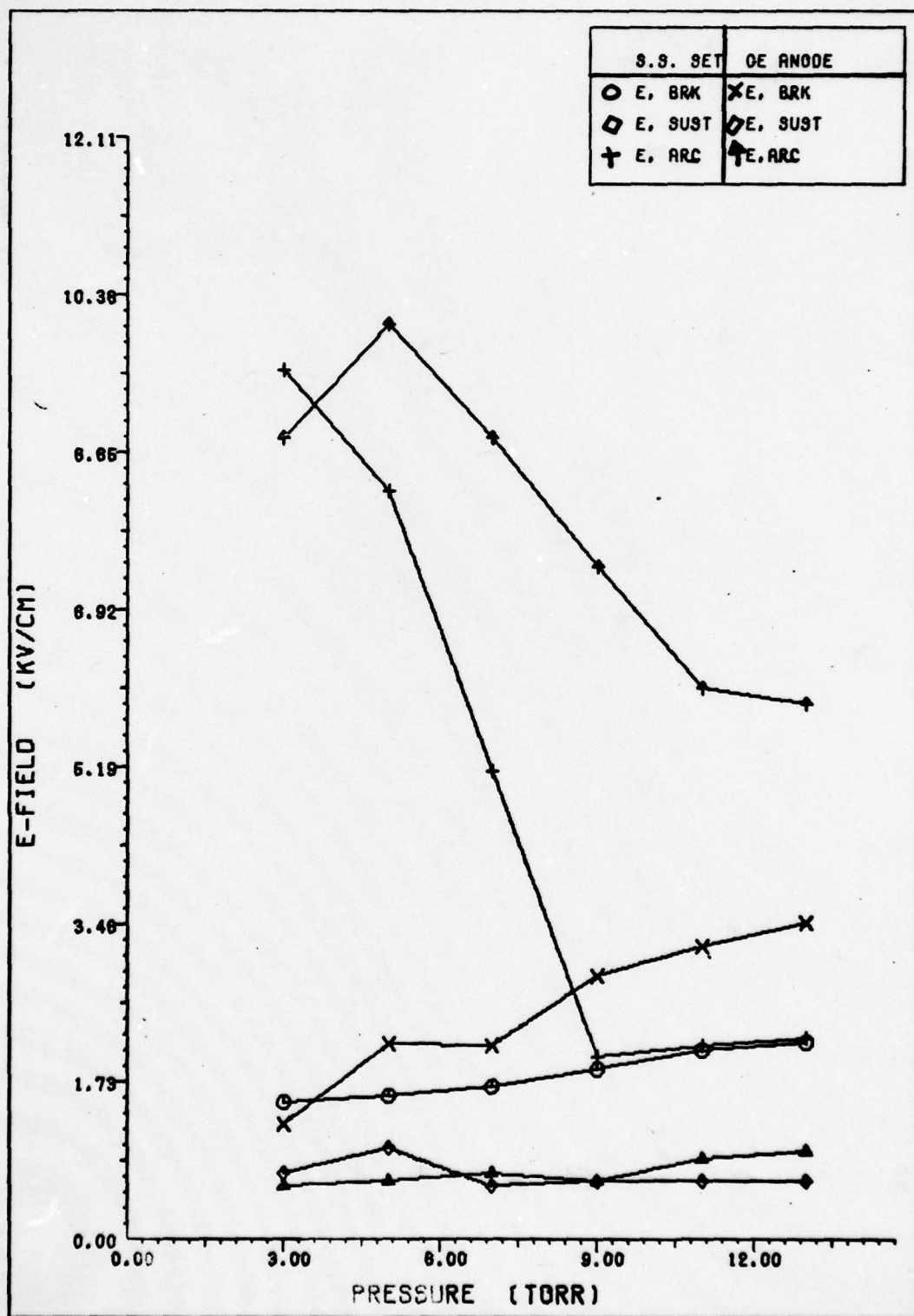


Figure 46. Sulfur-Hexafluoride, 200 pps, Ge Anode

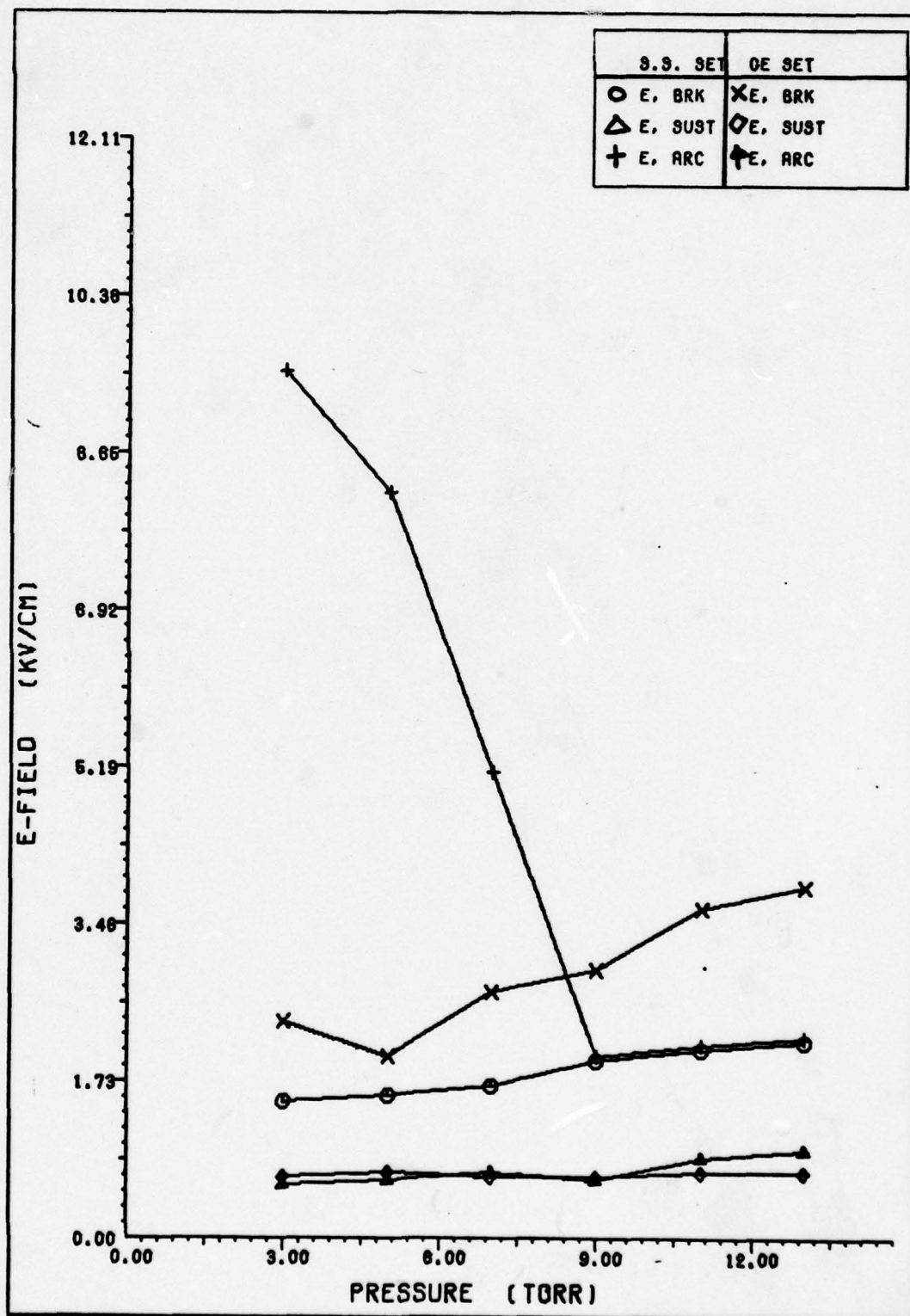


Figure 47. Sulfur-Hexafluoride, 200 pps, Ge Cathode-Anode

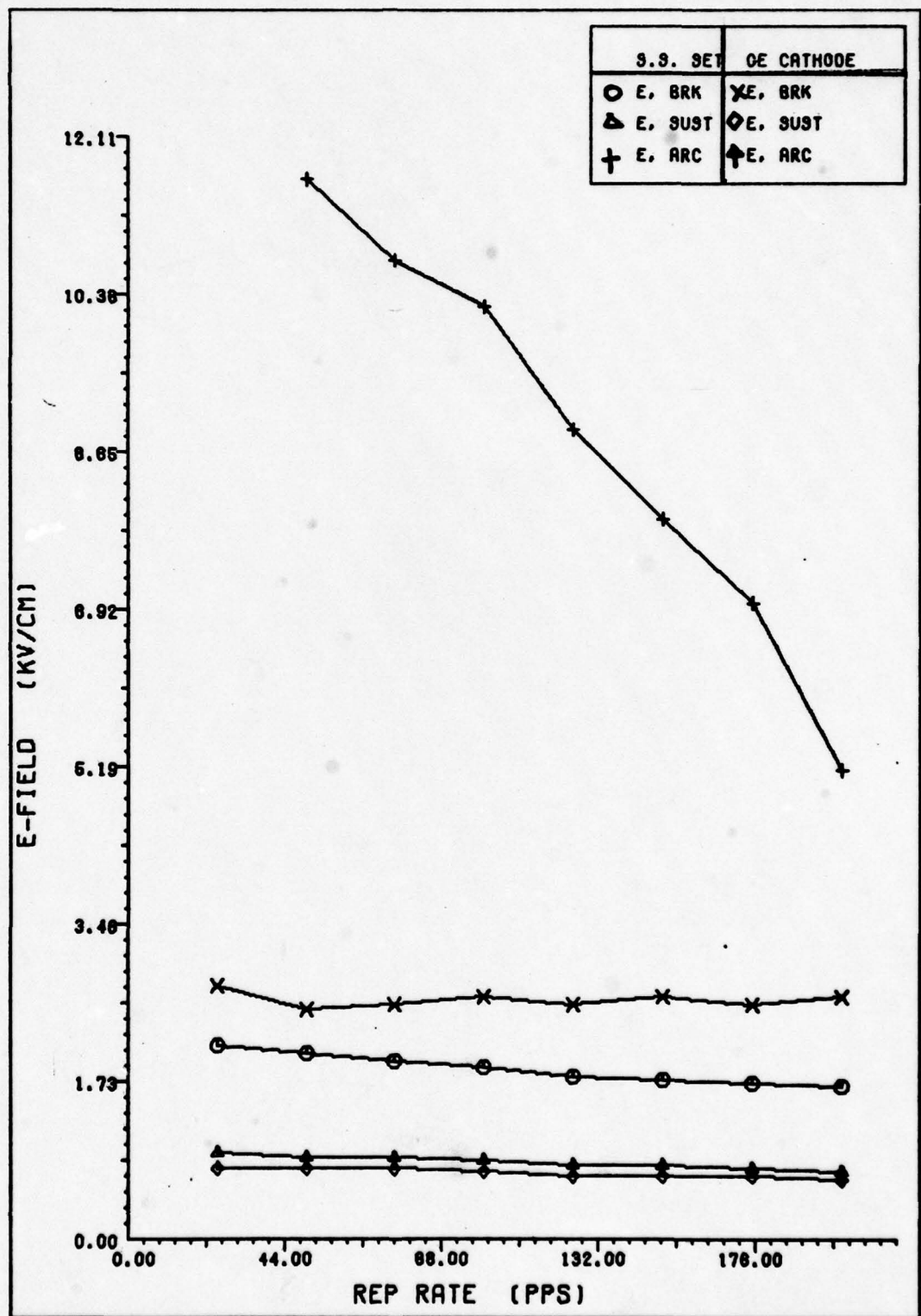


Figure 48. Sulfur-Hexafluoride, 7 Torr, Ge Cathode

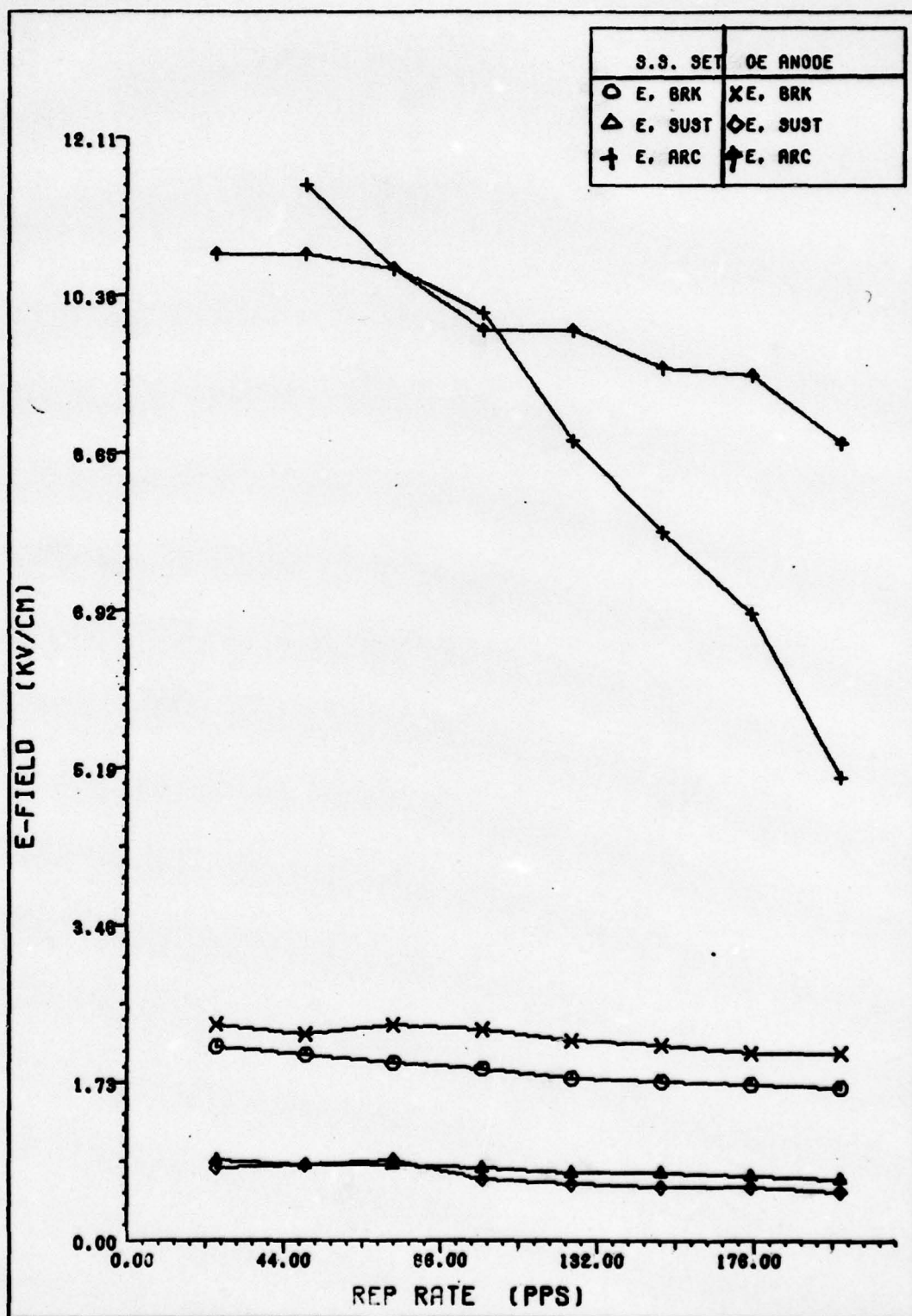


Figure 49. Sulfur-hexafluoride, 7 Torr, Ge Anode

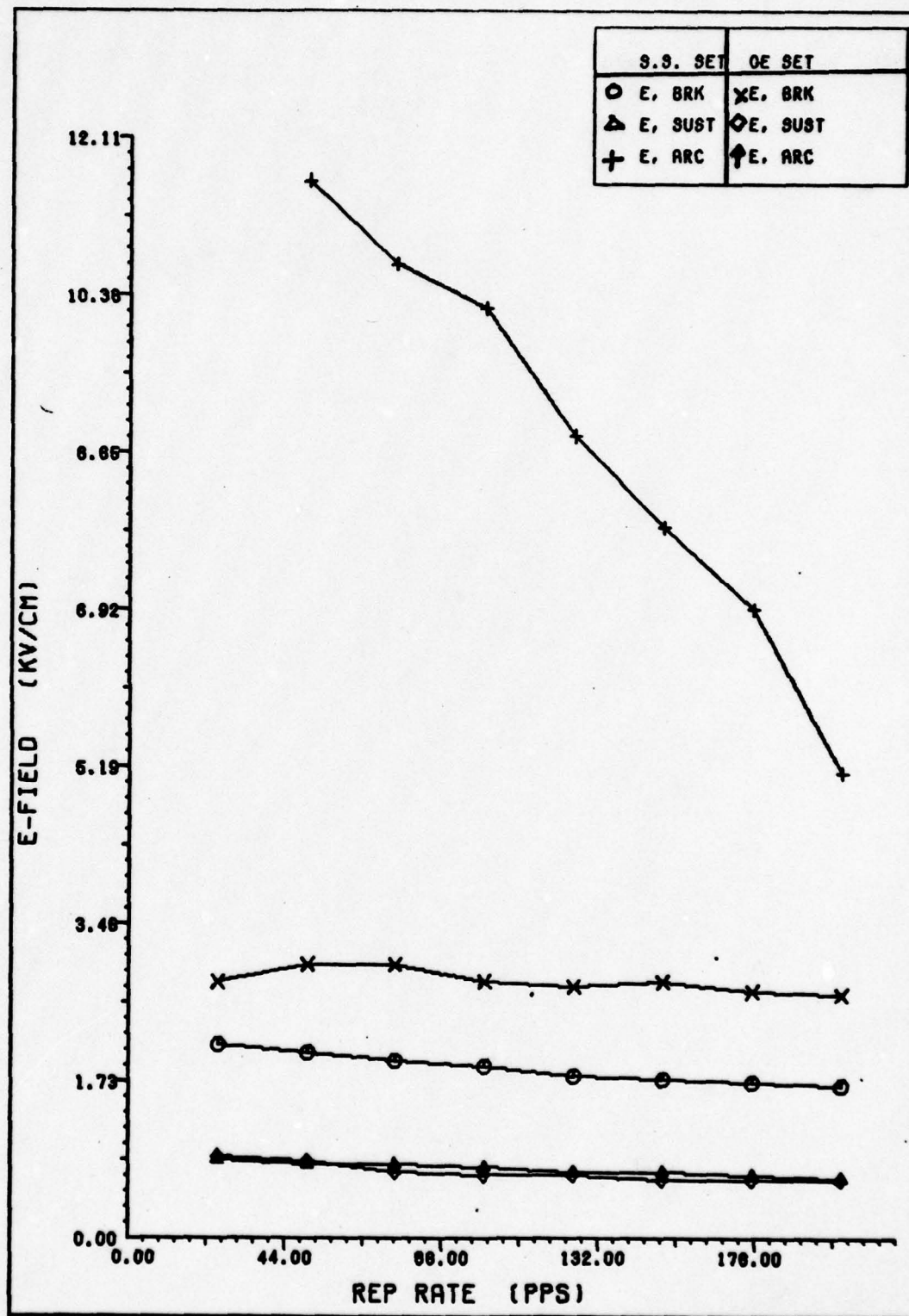


Figure 50. Sulfur-Hexafluoride, 7 Torr, Ge Cathode-Anode

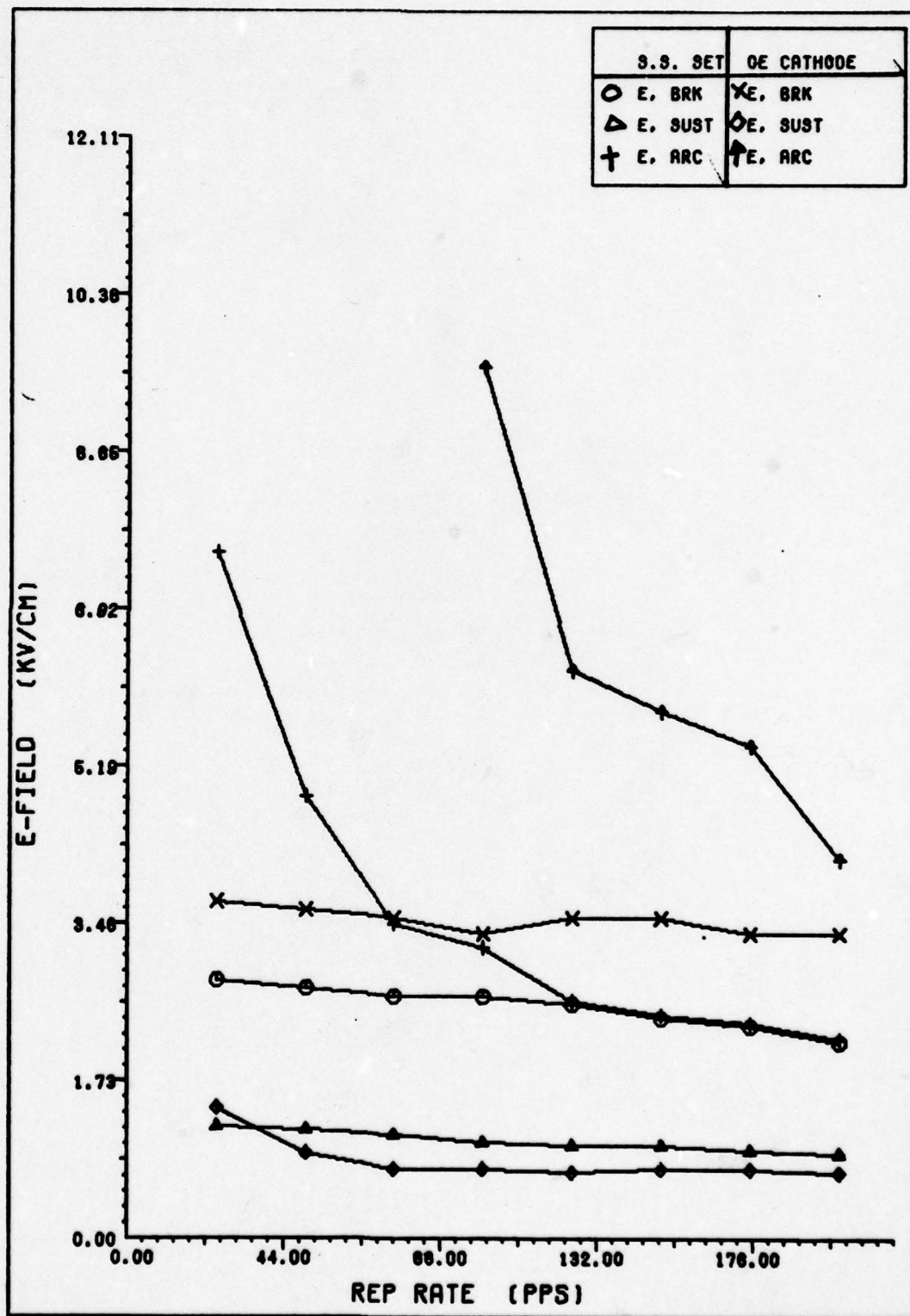


Figure 51. Sulfur-Hexafluoride, 13 Torr, Ge Cathode

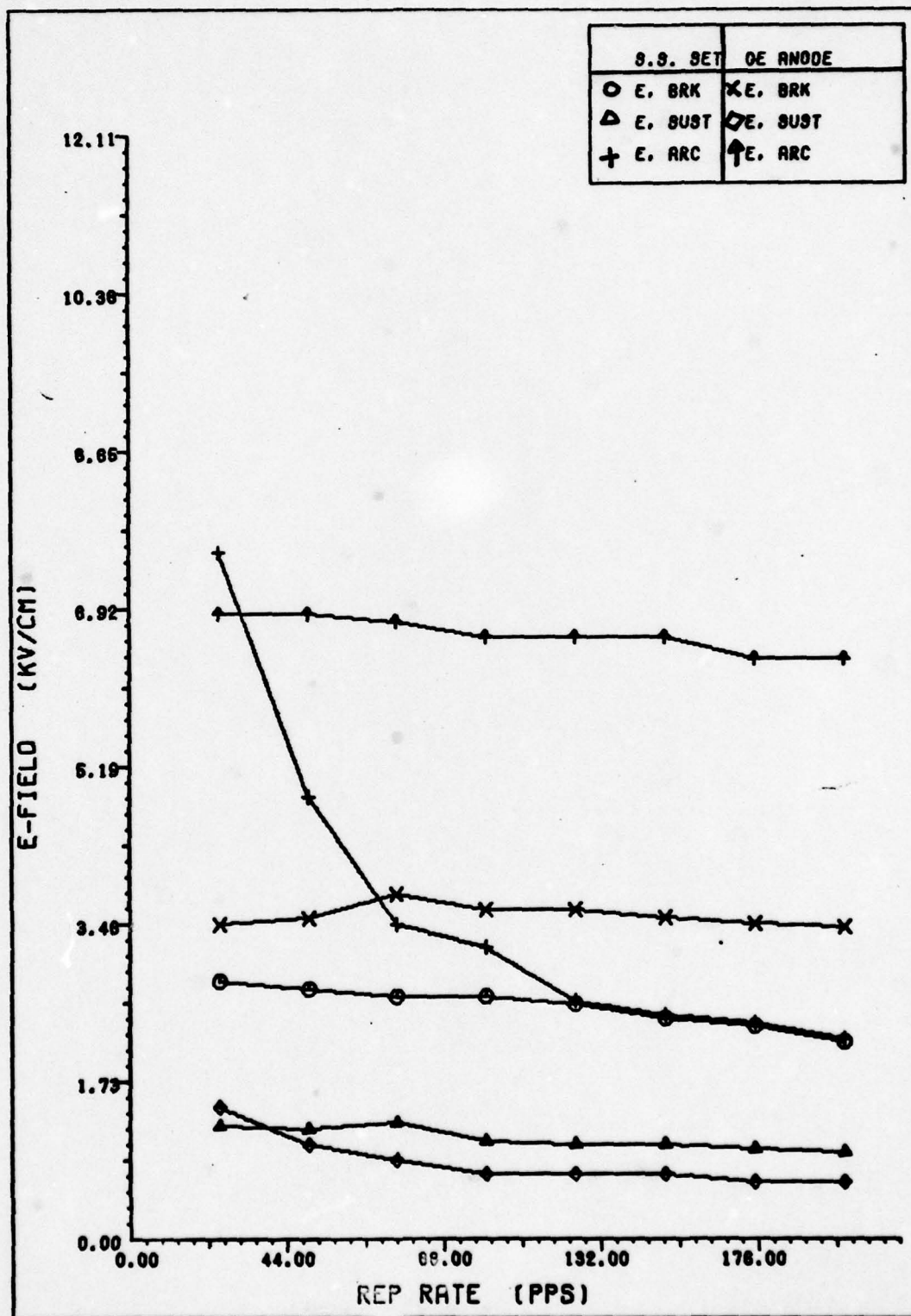


Figure 52. Sulfur-Hexafluoride, 13 Torr, Ge Anode

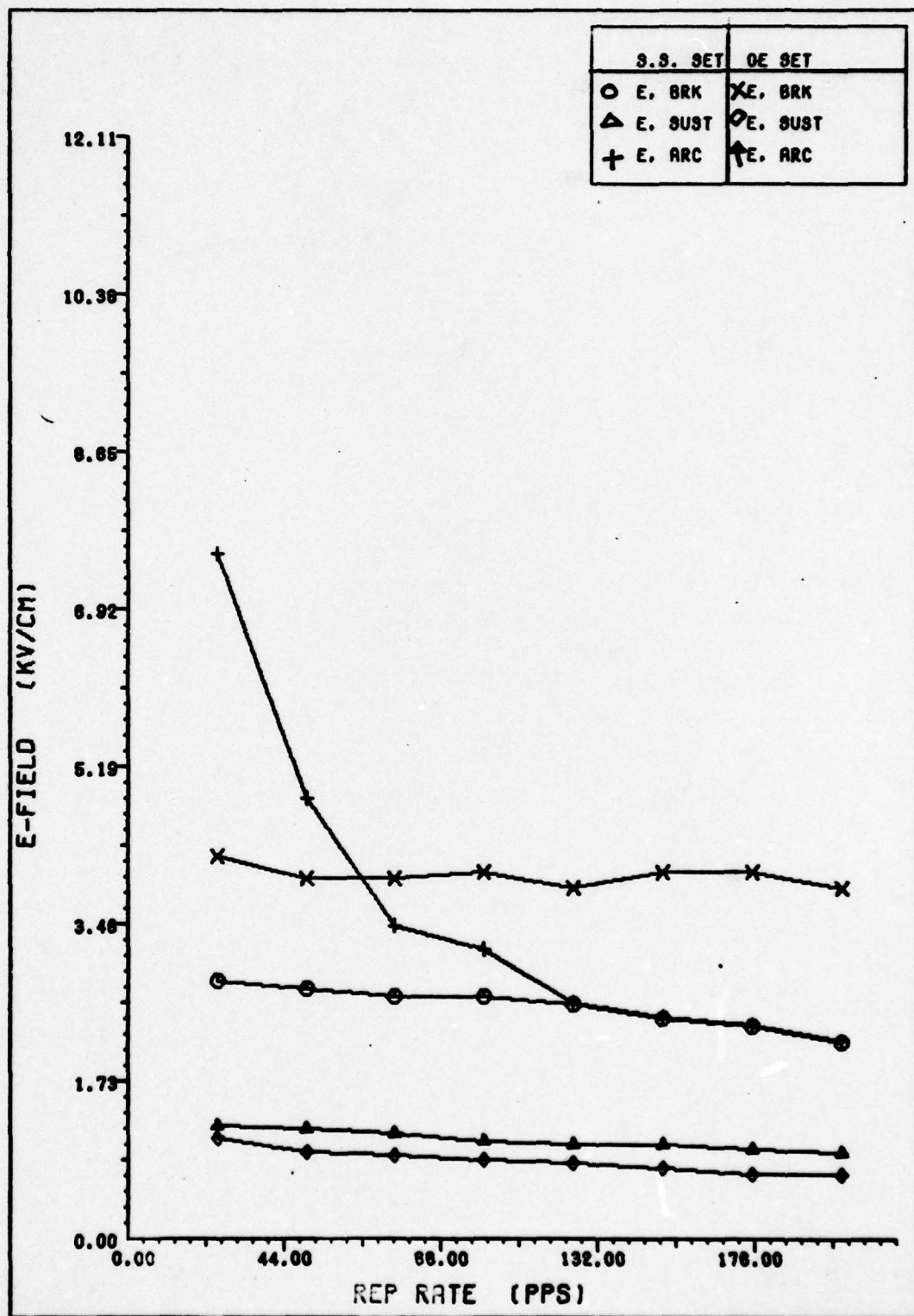


Figure 53. Sulfur-Hexafluoride, 13 Torr, Ge Cathode-Anode

VI. Conclusions

The use of germanium as an electrode results in substantial arc suppression. The largest gain in suppression results when germanium is used as the cathode. Pressures for arc-free discharges in sulfur-hexafluoride can be increased by as much as a factor of 2, given the proper repetition rate (i.e., 200 pps as in this experiment). Lasing can be achieved with the germanium cathode-stainless steel anode electrode configuration.

VII. Recommendations

1. Further experimental work should be done using higher repetition rates and other laser ingredient gases, such as those containing hydrogen.
2. The laser cavity should be operated as a laser with each electrode combination so comparisons of output energies and efficiencies can be made.
3. This work should be extended to other chemical lasers such as the CO and the CO₂.

Bibliography

1. Smith, W. and Peter P. Sarakin. The Laser, New York: McGraw Hill, Inc., 1966.
2. Deutsch, T. F. "Molecular Laser Action in Hydrogen and Deuterium Halides," Applied Physics Letters, 10: 234-236 (April 1967).
3. Spinnler, J. F. and P. A. Kittle, "Hydrogen Fluoride Chemical Laser - A Demonstration of Pure Chemical Pumping," presented at Second Conference on Chemical and Molecular Lasers, St. Louis, May 1969.
4. Brandelik, J. E. and R. F. Paulson, "Operation of an $\text{HF}(\text{SF}_6+\text{H}_2)$ TE Laser at 10-kHz Pulse Repetition Rates," IEEE Journal of Quantum Electronics, QE-13: 933-935 (December 1977).
5. Pearson, R. K., et al. "Pressure Dependency of the $\text{NF}_3\text{-H}_2$ Transverse-Discharge Pulse Initiated HF Chemical Laser," IEEE Journal of Quantum Electronics, QE-9: 723-730 (July 1973).
6. Jacobson, T. V., et al. "A High-Repetition-Rate Chemical HF Laser," IEEE Journal of Quantum Electronics, QE-9: 496-497 (April 1973).
7. Brown, R. T. "High Repetition-Rate Effects in TEA Lasers," IEEE Journal of Quantum Electronics, QE-9: 1120-1122 (November 1973).
8. Penning, F. M. Electrical Discharges in Gases. New York: Gordon and Breach, 1965.
9. Nasser, E. Fundamentals of Gaseous Ionization and Plasma Electronics. New York: Wiley-Interscience, 1971.
10. Palmer, A. J. "A Physical Model on the Initiation of Atmospheric-Pressure Glow Discharges," Applied Physics Letters, 25: 138-140 (August 1974).
11. Jacobson, T. V. and G. H. Kimbell. "WE8-Parametric Studies of Pulses HF Lasers Using Transverse Excitation," IEEE Journal of Quantum Electronics, QE-9: 173-181 (January 1973).
12. Deutsch, T. F. "Gain Measurements on Uniformly Excited HF/DF TEA Lasers," IEEE Journal of Quantum Electronics, QE-10: 84-86 (January 1974).
13. Gibson, A. F., et al. "Discharge Stabilization in HF Lasers Using Resistive Electrodes," IEEE Journal of Quantum Electronics, QE-13: 801-803 (October 1977).
14. Shepherd, D. G. Elements of Fluid Mechanics. New York: Harcourt, Brace and World, Inc. 1965.

15. River, R. Personal communication. Air Force Propulsion Laboratory, Wright-Patterson Air Force Base, Dayton, Ohio.
16. Chang, T. Y. "Improved Uniform-Field Electrode Profiles for TEA Laser and High Voltage Applications," Review of Scientific Instruments, 44: (405-407) (April 1973).

Appendix A

Support Equipment Turn-On Procedures

Support Equipment Turn-On Procedures

The procedure for equipment turn-on is detailed below. For equipment turn-off, the procedure is reversed.

1. Turn on HX-300 cooling system.
2. Turn on 1397 vacuum pump.
3. Turn on Thyratron heater and reservoir supply and increase rheostat slowly to obtain approximately 12 Amps heater current and 5.5 Amps reservoir current. (This step takes about 3 minutes to perform to allow for stabilization.)
4. Turn on TM-30 Thyratron driver and 100A frequency counter and adjust for desired repetition rate.
5. Open valves on appropriate gas canister, and adjust flow valve for desired gas pressure and flow rate.
6. Turn on Hippotronics power supply and increase voltage until desired discharge is obtained.

Appendix B

Experimental Data

Experimental Data

The results of the experiment are tabulated in Tables I-XII. The symbols used are defined below:

P_{DV}	Pressure in discharge volume
R_R	Pulse repetition rate (pps)
E_B	Breakdown voltage (KV/cm)
E_S	Sustaining voltage (KV/cm)
E_A	Arcing voltage (KV/cm)
R_E	Exchange rate (fills/pulse)

Table I
Helium with S.S. Anode-S.S. Cathode

P_{DV}	R_R	E_B	E_S	E_A^*	R_E
50 Torr	25	0.83	0.71	--	4.68
	50	0.83	0.71	--	2.34
	75	0.88	0.67	--	1.56
	100	0.88	0.63	--	1.17
	125	0.88	0.58	--	0.94
	150	0.92	0.58	10.83	0.78
	175	0.96	0.54	9.92	0.67
	200	1.00	0.50	9.33	0.59
60 Torr	25	0.92	0.75	--	4.08
	50	0.92	0.75	--	2.04
	75	0.96	0.71	--	1.36
	100	1.00	0.67	11.08	1.02
	125	1.00	0.63	10.08	0.82
	150	1.04	0.63	9.42	0.68
	175	1.04	0.58	9.33	0.58
	200	1.08	0.54	8.75	0.51
70 Torr	25	1.00	0.79	--	4.25
	50	1.00	0.79	--	2.12
	75	1.00	0.75	11.33	1.42
	100	1.04	0.71	10.17	1.06
	125	1.04	0.67	9.58	0.85
	150	1.08	0.63	9.17	0.71
	175	1.13	0.63	8.75	0.61
	200	1.13	0.58	8.08	0.53

*A dash (--) in this column represents no arc formation.

Table I (continued)

P_{DV}	R_R	E_B	E_S	E_A^*	R_E
80 Torr	25	1.04	0.88	--	4.42
	50	1.08	0.83	11.50	2.21
	75	1.08	0.83	10.42	1.48
	100	1.08	0.79	9.83	1.11
	125	1.13	0.79	9.08	0.88
	150	1.13	0.71	8.67	0.74
	175	1.13	0.67	8.25	0.63
	200	1.17	0.63	7.83	0.55
90 Torr	25	1.08	1.00	11.50	4.59
	50	1.08	0.96	10.50	2.29
	75	1.08	0.88	9.92	1.53
	100	1.13	0.83	9.50	1.15
	125	1.13	0.83	8.58	0.92
	150	1.17	0.79	8.42	0.77
	175	1.21	0.75	8.08	0.66
	200	1.21	0.67	7.83	0.57

*A dash (--) in this column represents no arc formation.

Table II
Helium with Ge Cathode-S.S. Anode

P_{DV}	R_R	E_B	E_S	E_A^*	R_E
50 Torr	25	1.00	0.58	--	4.51
	50	1.00	0.54	--	2.26
	75	1.00	0.54	--	1.50
	100	1.04	0.50	---	1.13
	125	1.04	0.50	--	0.90
	150	1.04	0.50	--	0.75
	175	1.04	0.50	--	0.64
	200	1.04	0.50	--	0.56
60 Torr	25	1.04	0.63	--	4.09
	50	1.04	0.63	--	2.04
	75	1.08	0.54	--	1.36
	100	1.08	0.54	--	1.02
	125	1.08	0.54	--	0.82
	150	1.08	0.50	--	0.68
	175	1.08	0.50	--	0.58
	200	1.08	0.50	--	0.51
70 Torr	25	1.04	0.67	--	4.18
	50	1.13	0.63	--	2.09
	75	1.17	0.63	--	1.39
	100	1.21	0.63	--	1.04
	125	1.25	0.63	--	0.83
	150	1.25	0.63	--	0.69
	175	1.25	0.63	--	0.59
	200	1.25	0.58	--	0.52

*A dash (—) in this column represents no arc formation.

Table II (continued)

P_{DV}	R_R	E_B	E_S	E_A^*	R_E
80 Torr	25	1.17	0.71	—	4.68
	50	1.25	0.71	—	2.34
	75	1.29	0.71	—	1.56
	100	1.29	0.71	—	1.17
	125	1.33	0.71	—	0.94
	150	1.33	0.67	—	0.78
	175	1.33	0.67	—	0.67
	200	1.33	0.63	—	0.59
90 Torr	25	1.29	0.79	—	4.85
	50	1.33	0.79	—	1.43
	75	1.37	0.79	—	1.62
	100	1.37	0.75	—	1.21
	125	1.42	0.71	—	0.97
	150	1.42	0.67	—	0.81
	175	1.46	0.625	—	0.69
	200	1.46	0.625	—	0.61

*A dash (—) in this column represents no arc formation.

Table III
Helium with Ge Anode-S.S. Cathode

P_{DV}	R_R	E_B	E_S	E_A^*	R_E
50 Torr	25	0.83	0.67	--	4.77
	50	0.92	0.63	--	2.38
	75	0.96	0.58	--	1.59
	100	0.96	0.58	--	1.19
	125	1.00	0.54	--	0.95
	150	1.00	0.54	--	0.95
	175	1.04	0.54	--	0.68
	200	1.04	0.50	--	0.59
60 Torr	25	0.96	0.75	--	4.25
	50	1.00	0.71	--	2.13
	75	1.00	0.67	--	1.42
	100	1.04	0.63	--	1.06
	125	1.04	0.58	--	0.85
	150	1.08	0.58	--	0.71
	175	1.08	0.54	--	0.61
	200	1.08	0.54	--	0.53
70 Torr	25	1.04	0.83	--	4.43
	50	1.08	0.75	--	2.21
	75	1.13	0.71	--	1.48
	100	1.13	0.67	--	1.11
	125	1.17	0.63	--	0.89
	150	1.17	0.58	--	0.34
	175	1.17	0.58	--	0.63
	200	1.17	0.58	--	0.55

*A dash (--) in this column represents no arc formation.

Table III (continued)

P_{DV}	R_R	E_B	E_S	E_A^*	R_E
80 Torr	25	1.08	0.83	--	4.51
	50	1.13	0.79	--	2.25
	75	1.17	0.75	--	1.50
	100	1.21	0.71	--	1.13
	125	1.25	0.67	--	0.90
	150	1.25	0.67	--	0.75
	175	1.25	0.63	--	0.64
	200	1.29	0.58	--	0.56
90 Torr	25	1.21	0.88	--	4.76
	50	1.25	0.19	--	2.38
	75	1.29	0.75	--	1.59
	100	1.29	0.71	--	1.19
	125	1.29	0.71	--	0.95
	150	1.29	0.67	--	0.79
	175	1.29	0.67	--	0.68
	200	1.33	0.63	--	0.59

*A dash (—) in this column represents no arc formation.

Table IV
Helium with Ge Anode-Ge Cathode

P_{DV}	R_R	E_B	E_S	E_A^*	R_E
50 Torr	25	1.04	0.58	--	4.08
	50	0.96	0.50	--	2.34
	75	1.00	0.46	--	1.56
	100	0.96	0.46	--	1.17
	125	1.08	0.42	--	0.94
	150	1.04	0.42	--	0.78
	175	1.00	0.42	--	0.67
	200	1.00	0.42	--	0.59
60 Torr	25	1.04	0.54	--	4.18
	50	1.04	0.58	--	2.09
	75	1.04	0.54	--	1.39
	100	1.08	0.50	--	1.04
	125	1.13	0.50	--	0.83
	150	1.08	0.46	--	0.69
	175	1.08	0.46	--	0.59
	200	1.08	0.46	--	0.52
70 Torr	25	1.38	0.67	--	4.77
	50	1.38	0.63	--	2.38
	75	1.38	0.63	--	1.59
	100	1.33	0.63	--	1.19
	125	1.38	0.58	--	0.95
	150	1.33	0.58	--	0.79
	175	1.38	0.58	--	0.68
	200	1.33	0.54	--	0.59

*A dash (--) in this column represents no arc formation.

Table IV (continued)

P_{DV}	R_R	E_B	E_S	E_A^*	R_E
80 Torr	25	1.67	0.75	--	4.51
	50	1.67	0.71	--	2.25
	75	1.67	0.67	--	1.50
	100	1.63	0.63	--	1.13
	125	1.60	0.63	--	0.90
	150	1.54	0.63	--	0.75
	175	1.60	0.58	--	0.64
	200	1.50	0.58	--	0.56
90 Torr	25	1.92	0.79	--	4.68
	50	1.88	0.79	--	2.34
	75	1.79	0.75	--	1.56
	100	1.75	0.67	--	1.17
	125	1.75	0.63	--	0.94
	150	1.71	0.63	--	0.78
	175	1.71	0.58	--	0.67
	200	1.67	0.58	--	0.59

*A dash (—) in this column represents no arc formation.

Table V
Nitrogen with S.S. Anode-S.S. Cathode

P_{DV}	R_R	E_B	E_S	E_A^*	R_E
5 Torr	25	0.96	0.71	9.67	2.68
	50	1.04	0.67	9.50	1.34
	75	1.17	0.58	9.17	0.89
	100	1.21	0.58	8.67	0.67
	125	1.29	0.54	8.33	0.54
	150	1.38	0.54	8.33	0.45
	175	1.42	0.54	7.92	0.38
	200	1.50	0.54	7.50	0.34
10 Torr	25	1.63	1.08	11.50	2.02
	50	1.63	0.96	11.17	1.31
	75	1.63	0.83	10.67	0.87
	100	1.67	0.79	10.00	0.66
	125	1.58	0.79	9.00	0.52
	150	1.75	0.75	8.67	0.44
	175	1.92	0.71	8.33	0.37
	200	2.08	0.71	8.00	0.33
15 Torr	25	1.83	1.17	11.17	2.80
	50	1.87	1.13	10.83	0.93
	75	1.93	1.00	10.83	0.93
	100	1.96	0.96	10.67	0.70
	125	1.96	0.92	9.50	0.56
	150	2.21	0.92	7.92	0.47
	175	2.38	0.88	6.25	0.40
	200	2.67	0.88	5.83	0.35

Table V (continued)

P_{DV}	R_R	E_B	E_S	E_A^*	R_E
20 Torr	25	1.96	1.42	10.00	3.10
	50	1.96	1.29	9.58	1.55
	75	2.04	1.21	8.67	1.03
	100	2.13	1.08	7.50	0.75
	125	2.17	1.04	7.08	0.62
	150	2.17	1.00	6.67	0.52
	175	2.17	0.96	5.17	0.44
	200	2.21	0.96	4.83	0.39
25 Torr	25	1.96	1.63	9.17	3.29
	50	2.17	1.50	8.58	1.65
	75	2.29	1.33	7.50	1.10
	100	2.38	1.25	6.83	0.82
	125	2.42	1.21	5.67	0.66
	150	2.42	1.17	5.17	0.55
	175	2.50	1.08	4.83	0.47
	200	2.54	1.08	4.42	0.41
30 Torr	25	2.21	1.83	9.33	3.52
	50	2.50	1.71	9.00	1.76
	75	2.58	1.54	7.83	1.17
	100	2.67	1.42	7.00	0.88
	125	2.75	1.33	6.25	0.70
	150	2.79	1.29	6.17	0.59
	175	2.83	1.25	5.67	0.50
	200	2.88	1.21	5.33	0.44

Table VI
Nitrogen with Ge Cathode-S.S. Anode

P_{DV}	R_R	E_B	E_S	E_A^*	R_E
5 Torr	25	0.83	0.67	--	2.67
	50	0.83	0.67	--	1.33
	75	0.83	0.63	--	0.89
	100	0.88	0.58	--	0.67
	125	0.88	0.58	--	0.53
	150	0.88	0.54	--	0.44
	175	0.92	0.54	--	0.38
	200	0.92	0.54	--	0.33
10 Torr	25	1.13	0.92	--	2.59
	50	1.25	0.88	--	1.29
	75	1.29	0.83	--	0.86
	100	1.33	0.75	--	0.65
	125	1.38	0.72	--	0.52
	150	1.38	0.71	--	0.43
	175	1.38	0.71	--	0.37
	200	1.38	0.67	--	0.32
15 Torr	25	1.50	1.13	--	2.81
	50	1.58	1.04	--	1.40
	75	1.71	0.92	--	0.94
	100	1.75	0.88	--	0.70
	125	1.75	0.88	--	0.56
	150	1.75	0.83	--	0.47
	175	1.75	0.79	--	0.40
	200	1.75	0.79	--	0.35

*A dash (—) in this column represents no arc formation.

Table VI (continued)

P_{DV}	R_R	E_B	E_S	E_A^*	R_E
20 Torr	25	1.75	1.38	—	3.12
	50	1.92	1.25	—	1.56
	75	2.00	1.13	—	1.04
	100	2.04	1.04	—	0.78
	125	2.04	0.96	—	0.62
	150	2.04	0.96	—	0.52
	175	2.08	0.92	—	0.45
	200	2.08	0.88	—	0.39
25 Torr	25	2.08	1.54	—	3.32
	50	2.21	1.42	—	1.66
	75	2.33	1.29	—	1.11
	100	2.38	1.17	—	0.83
	125	2.42	1.17	—	0.66
	150	2.42	1.08	—	0.55
	175	2.42	1.04	—	0.47
	200	2.42	1.04	—	0.41
30 Torr	25	2.25	1.79	—	3.49
	50	2.46	1.67	—	1.74
	75	2.54	1.46	—	1.16
	100	2.67	1.33	—	0.87
	125	2.75	1.29	—	0.70
	150	2.79	1.25	—	0.58
	175	2.79	1.21	—	0.49
	200	2.79	1.17	—	0.44

*A dash (—) in this column represents no arc formation.

AD-A080 242

AIR FORCE INST OF TECH WRIGHT-PATTERSON AFB OH SCHOO--ETC F/6 20/5
COMPARISON OF GERMANIUM-STAINLESS STEEL ELECTRODE CONFIGURATION--ETC(U)
DEC 79 R J HOFFMAN
AFIT/6EP/PH/79D-5

UNCLASSIFIED

NL

2 OF 2

AD A
080242

SI
MI



END
DATE
FILMED
3-80
DDC

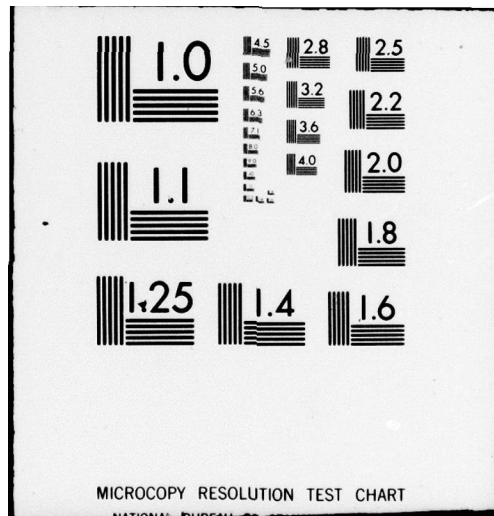


Table VII
Nitrogen with Ge Anode-S.S. Cathode

P_{DV}	R_R	E_B	E_S	E_A^*	R_E
5 Torr	25	0.83	0.71	—	2.65
	50	0.83	0.67	—	1.33
	75	0.88	0.58	—	0.88
	100	0.88	0.58	—	0.66
	125	0.92	0.54	—	0.53
	150	1.00	0.54	—	0.44
	175	1.00	0.50	—	0.38
	200	1.04	0.46	—	0.33
10 Torr	25	1.08	0.92	—	2.59
	50	1.21	0.88	—	1.30
	75	1.25	0.83	—	0.86
	100	1.25	0.75	—	0.65
	125	1.29	0.71	—	0.65
	150	1.29	0.71	—	0.43
	175	1.29	0.67	—	0.37
	200	1.33	0.67	—	0.32
15 Torr	25	1.38	1.13	—	2.78
	50	1.46	1.04	—	1.39
	75	1.54	0.96	—	0.93
	100	1.58	0.88	—	0.69
	125	1.63	0.83	—	0.56
	150	1.63	0.83	—	0.46
	175	1.63	0.83	—	0.39
	200	1.63	0.79	—	0.35

*A dash (—) in this column represents no arc formation.

Table VII (continued)

P_{DV}	R_R	E_B	E_S	E_A^*	R_E
20 Torr	25	1.63	1.29	—	3.09
	50	1.75	1.21	—	1.55
	75	1.83	1.08	—	1.03
	100	1.88	1.00	—	0.77
	125	1.96	0.96	—	0.02
	150	2.00	0.96	—	0.02
	175	2.00	0.92	—	0.44
	200	2.00	0.88	—	0.39
25 Torr	25	2.00	1.58	—	3.30
	50	2.17	1.50	—	1.66
	75	2.29	1.29	—	1.10
	100	2.38	1.27	—	0.83
	125	2.42	1.13	—	0.66
	150	2.46	0.88	—	0.55
	175	2.46	0.83	—	0.47
	200	2.46	0.79	—	0.41
30 Torr	25	2.21	1.71	—	3.53
	50	2.33	1.54	—	1.77
	75	2.46	1.38	—	1.18
	100	2.58	1.25	—	0.88
	125	2.63	1.21	—	0.71
	150	2.67	1.17	—	0.59
	175	2.71	1.13	—	0.50
	200	2.71	1.08	—	0.44

*A dash (—) in this column represents no arc formation.

Table VIII
Nitrogen with Ge Anode-Ge Cathode

P_{DV}	R_R	E_B	E_S	E_A^*	R_E
5 Torr	25	1.04	0.67	--	2.64
	50	1.08	0.63	--	1.32
	75	1.04	0.58	--	0.88
	100	1.125	0.58	--	0.66
	125	1.125	0.54	--	0.53
	150	1.17	0.54	--	0.44
	175	1.21	0.54	--	0.38
	200	1.33	0.54	--	0.33
10 Torr	25	2.21	1.00	--	2.58
	50	2.17	0.96	--	1.29
	75	2.13	0.83	--	0.86
	100	2.08	0.79	--	0.65
	125	2.04	0.75	--	0.52
	150	2.00	0.71	--	0.43
	175	2.00	0.67	--	0.37
	200	1.96	0.63	--	0.69
15 Torr	25	2.71	1.21	--	2.79
	50	2.67	1.13	--	1.40
	75	2.67	1.04	--	0.93
	100	2.58	0.96	--	0.70
	125	2.58	0.83	--	0.56
	150	2.54	0.83	--	0.47
	175	2.50	0.79	--	0.40
	200	2.46	0.79	--	0.35

*A dash (—) in this column represents no arc formation.

Table VIII (continued)

P_{DV}	R_R	E_B	E_S	E_A^*	R_E
20 Torr	25	3.00	1.38	--	3.06
	50	3.04	1.25	--	1.53
	75	3.00	1.13	--	1.02
	100	3.00	1.04	--	0.77
	125	2.96	1.00	--	0.61
	150	2.88	0.96	--	0.51
	175	2.83	0.96	--	0.44
	200	2.83	0.96	--	0.38
25 Torr	25	3.33	1.58	--	3.33
	50	3.33	1.38	--	1.67
	75	3.21	1.25	--	1.11
	100	3.25	1.21	--	0.83
	125	3.25	1.17	--	0.58
	150	3.17	1.17	--	0.56
	175	3.17	1.13	--	0.48
	200	3.13	1.08	--	0.42
30 Torr	25	3.58	1.54	--	3.50
	50	3.50	1.46	--	1.75
	75	3.50	1.42	--	1.17
	100	3.50	1.38	--	0.88
	125	3.42	1.33	--	0.70
	150	3.42	1.25	--	0.58
	175	3.33	1.25	--	0.50
	200	3.33	1.21	--	0.44

*A dash (—) in this column represents no arc formation.

Table IX
Sulfur-Hexafluoride with S.S. Anode-S.S. Cathode

P_{DV}	R_R	E_B	E_S	E_A^*	R_E
3 Torr	25	1.75	0.71	--	1.06
	50	1.71	0.71	--	0.53
	75	1.67	0.67	--	0.35
	100	1.63	0.63	--	0.27
	125	1.58	0.63	--	0.21
	150	1.58	0.58	11.33	0.18
	175	1.54	0.58	10.42	0.15
	200	1.50	0.54	9.50	0.13
5 Torr	25	1.79	0.75	--	1.18
	50	1.75	0.71	--	0.54
	75	1.75	0.67	--	0.36
	100	1.67	0.07	10.50	0.27
	125	1.67	0.63	11.58	0.22
	150	1.63	0.63	9.83	0.18
	175	1.58	0.58	8.50	0.15
	200	1.58	0.58	8.17	0.14
7 Torr	25	2.13	0.88	--	1.11
	50	2.04	0.83	11.58	0.56
	75	1.96	0.83	10.67	0.37
	100	1.88	0.79	10.17	0.28
	125	1.79	0.75	8.83	0.22
	150	1.75	0.75	7.83	0.19
	175	1.71	0.71	6.92	0.16
	200	1.67	0.67	5.08	0.14

*A dash (--) in this column represents no arc formation.

Table IX (continued)

P_{DV}	R_R	E_B	E_S	E_A^*	R_E
9 Torr	25	2.33	0.88	10.92	1.15
	50	2.92	0.75	10.00	0.57
	75	2.25	0.71	7.42	0.38
	100	2.17	0.67	6.67	0.29
	125	2.13	0.67	4.92	0.23
	150	2.13	0.63	3.17	0.19
	175	2.04	0.58	2.04	0.16
	200	1.96	0.58	1.96	0.14
11 Torr	25	2.75	1.13	10.08	1.20
	50	2.58	1.08	7.50	0.60
	75	2.42	1.04	5.83	0.40
	100	2.33	0.95	4.83	0.30
	125	2.29	0.92	3.17	0.24
	150	2.50	0.88	2.25	0.20
	175	2.17	0.88	2.17	0.17
	200	2.08	0.83	2.08	0.15
13 Torr	25	2.83	1.21	7.50	1.25
	50	2.75	1.17	4.83	0.63
	75	2.67	1.13	3.42	0.42
	100	2.67	1.04	3.17	0.31
	125	2.58	1.00	2.58	0.25
	150	2.42	1.00	2.42	0.21
	175	2.33	0.96	2.33	0.18
	200	2.17	0.92	2.17	0.16

Table X
Sulfur-Hexafluoride with Ge Cathode-S.S. Anode

P_{DV}	R_R	E_B	E_S	E_A^*	R_E
3 Torr	25	1.96	0.67	--	1.02
	50	1.92	0.67	--	0.51
	75	2.00	0.63	--	0.34
	100	2.17	0.67	--	0.26
	125	2.04	0.67	--	0.20
	150	2.13	0.67	--	0.17
	175	2.04	0.67	--	0.15
	200	2.08	0.67	--	0.13
5 Torr	25	2.13	0.71	--	1.06
	50	2.04	0.79	--	0.52
	75	2.13	0.79	--	0.35
	100	2.00	0.79	--	0.27
	125	2.04	0.83	--	0.21
	150	1.92	0.79	--	0.18
	175	1.96	0.88	--	0.15
	200	1.92	0.83	--	0.13
7 Torr	25	2.71	0.71	--	1.09
	50	2.46	0.71	--	0.55
	75	2.50	0.71	--	0.36
	100	2.62	0.67	--	0.27
	125	2.50	0.63	--	0.22
	150	2.60	0.63	--	0.18
	175	2.50	0.63	--	0.16
	200	2.60	0.58	--	0.14

*A dash (--) in this column represents no arc formation.

Table X (continued)

P_{DV}	R_R	E_B	E_S	E_A^*	R_E
9 Torr	25	3.17	0.83	--	1.13
	50	3.08	0.71	--	0.57
	75	2.92	0.71	--	0.38
	100	3.00	0.67	--	0.28
	125	2.92	0.67	--	0.23
	150	2.83	0.63	--	0.19
	175	2.92	0.63	--	0.16
	200	2.83	0.58	11.25	0.14
11 Torr	25	3.33	1.25	--	1.18
	50	3.33	0.92	--	0.59
	75	3.33	0.79	--	0.39
	100	3.25	0.75	--	0.29
	125	3.17	0.71	11.42	0.24
	150	3.08	0.67	10.80	0.20
	175	3.17	0.63	10.42	0.17
	200	3.17	0.63	9.92	0.15
13 Torr	25	3.67	1.42	--	1.22
	50	3.58	0.92	--	0.61
	75	3.50	0.75	--	0.41
	100	3.33	0.75	9.58	0.30
	125	3.50	0.71	6.25	0.24
	150	3.50	0.75	5.80	0.20
	175	3.33	0.71	5.42	0.17
	200	3.33	0.71	4.17	0.15

*A dash (--) in this column represents no arc formation.

Table XI
Sulfur-Hexafluoride with Ge Anode-S.S. Cathode

P_{DV}	R_R	E_B	E_S	E_A^*	R_E
3 Torr	25	1.92	0.63	--	1.06
	50	1.96	0.67	--	0.53
	75	2.04	0.67	--	0.35
	100	2.00	0.67	10.42	0.27
	125	1.96	0.71	10.00	0.21
	150	1.92	0.67	9.17	0.18
	175	1.92	0.67	9.17	0.15
	200	1.96	0.67	8.75	0.13
5 Torr	25	2.00	0.71	11.58	1.11
	50	2.10	0.71	10.83	0.55
	75	2.13	0.71	10.83	0.37
	100	2.13	0.79	10.17	0.28
	125	2.18	0.79	10.50	0.22
	150	2.18	0.83	10.42	0.18
	175	2.17	0.92	10.25	0.16
	200	2.10	0.96	10.00	0.14
7 Torr	25	2.38	0.79	10.83	1.13
	50	2.29	0.83	10.83	0.57
	75	2.38	0.88	10.67	0.38
	100	2.33	0.67	10.00	0.28
	125	2.21	0.63	10.00	0.23
	150	2.17	0.58	9.58	0.19
	175	2.08	0.58	9.50	0.16
	200	2.08	0.54	8.75	0.14

*A dash (—) in this column represents no arc formation.

Table XI (continued)

P_{DV}	R_R	E_B	E_S	E_A^*	R_E
9 Torr	25	2.92	1.25	10.17	1.16
	50	3.08	1.04	10.17	0.58
	75	3.00	0.75	9.00	0.39
	100	3.08	0.71	8.50	0.29
	125	3.00	0.67	8.00	0.23
	150	3.00	0.67	8.00	0.19
	175	2.83	0.63	8.00	0.17
	200	2.83	0.58	7.33	0.15
11 Torr	25	3.33	1.25	9.17	1.22
	50	3.25	1.00	9.00	0.61
	75	3.25	0.83	8.83	0.41
	100	3.17	0.75	7.50	0.30
	125	3.25	0.67	6.67	0.24
	150	3.30	0.58	6.67	0.20
	175	3.17	0.67	6.50	0.17
	200	3.17	0.58	6.00	0.15
13 Torr	25	3.42	1.42	6.83	1.26
	50	3.50	1.00	6.83	0.63
	75	3.75	0.83	6.75	0.42
	100	3.58	0.67	6.58	0.32
	125	3.58	0.67	6.58	0.25
	150	3.50	0.67	6.58	0.21
	175	3.50	0.58	6.33	0.18
	200	3.42	0.58	6.83	0.16

Table XII
Sulfur-Hexafluoride with Ge Anode-Ge Cathode

P_{DV}	R_R	E_B	E_S	E_A^*	R_E
3 Torr	25	2.21	0.63	--	1.05
	50	2.33	0.63	--	0.52
	75	2.33	0.67	--	0.35
	100	2.25	0.63	--	0.26
	125	2.42	0.63	--	0.21
	150	2.25	0.63	--	0.17
	175	2.38	0.63	--	0.15
	200	2.33	0.63	--	0.13
5 Torr	25	2.46	0.83	--	1.08
	50	2.38	0.79	--	0.54
	75	2.25	0.79	--	0.37
	100	2.17	0.75	--	0.27
	125	2.08	0.75	--	0.22
	150	2.00	0.71	--	0.18
	175	1.96	0.67	--	0.16
	200	1.96	0.67	--	0.14
7 Torr	25	2.79	0.88	--	1.11
	50	3.00	0.83	--	0.55
	75	3.00	0.71	--	0.37
	100	2.79	0.67	--	0.28
	125	2.75	0.67	--	0.22
	150	2.79	0.63	--	0.18
	175	2.71	0.63	--	0.16
	200	2.67	0.63	--	0.14

*A dash (--) in this column represents no arc formation.

Table XII (continued)

P_{DV}	R_R	E_B	E_S	E_A^*	R_E
9 Torr	25	3.33	1.00	--	1.13
	50	3.42	0.83	--	0.57
	75	3.58	0.75	--	0.38
	100	3.50	0.67	--	0.28
	125	3.25	0.67	--	0.23
	150	3.08	0.63	--	0.19
	175	3.08	0.67	--	0.16
	200	2.91	0.63	--	0.14
11 Torr	25	3.83	1.17	--	1.19
	50	3.83	1.00	--	0.60
	75	3.75	0.83	--	0.40
	100	3.92	0.79	--	0.30
	125	3.75	0.75	--	0.24
	150	3.75	0.75	--	0.20
	175	3.50	0.71	--	0.17
	200	3.58	0.67	--	0.15
13 Torr	25	4.17	1.08	--	1.25
	50	3.92	0.92	--	0.62
	75	3.92	8.88	--	0.42
	100	4.00	0.83	--	0.31
	125	3.83	0.79	--	0.25
	150	4.00	0.75	--	0.21
	175	4.00	0.67	--	0.18
	200	3.83	0.67	--	0.16

*A dash (--) in this column represents no arc formation.

Vita

Roger John Hoffman was born on 21 February 1954 in Ladysmith, Wisconsin. He graduated from Ladysmith High School in 1972 and enlisted in the Air Force shortly thereafter. After working as a Precision Measuring Equipment Specialist for three years with the 4787th Materiel Squadron, Duluth I.A.P., Minnesota, he applied for and received a 3-year AFROTC scholarship. In May 1978 he was commissioned a 2nd Lieutenant in the USAF upon receipt of his Bachelor of Science degree from the University of Wisconsin. In June of the same year, he entered the Air Force Institute of Technology to pursue a Master of Science degree.

Permanent address: 505 East Tenth Street

Ladysmith, Wisconsin 54848

Unclassified

SECURITY CLASSIFICATION OF THIS PAGE (When Data Entered)

REPORT DOCUMENTATION PAGE		READ INSTRUCTIONS BEFORE COMPLETING FORM
1. REPORT NUMBER AFIT/GEP/PH/79D-5	2. GOVT ACCESSION NO.	3. RECIPIENT'S CATALOG NUMBER
4. TITLE (and Subtitle) COMPARISON OF GERMANIUM-STAINLESS STEEL ELECTRODE CONFIGURATIONS FOR POSSIBLE UTILIZATION IN ELECTRIC DISCHARGE LASERS		5. TYPE OF REPORT & PERIOD COVERED MS Thesis
		6. PERFORMING ORG. REPORT NUMBER
7. AUTHOR(s) Roger J. Hoffman Lt USAF		8. CONTRACT OR GRANT NUMBER(s)
9. PERFORMING ORGANIZATION NAME AND ADDRESS Air Force Institute of Technology (AFIT/EN) Wright-Patterson AFB, Ohio 45433		10. PROGRAM ELEMENT, PROJECT, TASK AREA & WORK UNIT NUMBERS
11. CONTROLLING OFFICE NAME AND ADDRESS Electro-Optics Sources Group (AFAL/DHO) Air Force Avionics Laboratory Wright-Patterson AFB, Ohio 45433		12. REPORT DATE December 1979
14. MONITORING AGENCY NAME & ADDRESS (if different from Controlling Office)		13. NUMBER OF PAGES 108
		15. SECURITY CLASS. (of this report) Unclassified
15a. DECLASSIFICATION/DOWNGRADING SCHEDULE		
16. DISTRIBUTION STATEMENT (of this Report) Approved for public release; distribution unlimited.		
17. DISTRIBUTION STATEMENT (of the abstract entered in Block 20, if different from Report)		
18. SUPPLEMENTARY NOTES Approved for public release; IAW AFR 190-17 JOSEPH P. HIPPS, Major, USAF Director of Public Affairs		
19. KEY WORDS (Continue on reverse side if necessary and identify by block number) Gas Discharge Germanium Electrode HF Laser Resistive Electrodes		
20. ABSTRACT (Continue on reverse side if necessary and identify by block number) An HF laser cavity was designed and constructed in which four electrode combinations were tested. The electrodes consisted of two stainless steel Chang-profiled electrodes and two 50-Ω cm germanium electrodes. The four possible electrode combinations for anode and cathode were tested. Break-down, sustaining, and arcing voltages were recorded, for each combination, over a range of 25-200 pulses per second for the following gases with their respective pressure ranges: helium, 50-90 Torr; nitrogen, 5-30 Torr; sulfur-		

Unclassified

SECURITY CLASSIFICATION OF THIS PAGE(When Data Entered)

hexafluoride, 3-15 Torr. The use of germanium as a cathode material resulted in substantially greater suppression of arc formation than the use of stainless steel. Helium, which sustained arcs at 60 Torr and 100 pps with a stainless steel cathode-anode, was found to be arc-free at pressures up to 90 Torr with repetition rates as high as 200 pps using a germanium cathode. Similarly, sulfur-hexafluoride, which sustained arcing at 3 Torr and 150 pps with stainless steel electrodes was found to be arc-free at pressures over 13 Torr when germanium was used as a cathode. The use of germanium as both anode and cathode resulted in the highest suppression of arc formation.

Unclassified

SECURITY CLASSIFICATION OF THIS PAGE(When Data Entered)